Practical Challenges in the Method of Controlled Lagrangians

Konda Reddy Chevva

Dissertation submitted to the Faculty of the
Virginia Polytechnic Institute and State University
in partial fulfillment of the requirements for the degree of
Doctor of Philosophy
in
Engineering Science and Mechanics

Advisory Committee

Dr. Craig A. Woolsey, Chairman
Dr. Ali H. Nayfeh, Co-Chairman
Dr. Scott L. Hendricks
Dr. Daniel J. Inman
Dr. Ziyad N. Masoud

August 2005
Blacksburg

Keywords: Underactuated Systems, Energy Shaping Control, Method of Controlled Lagrangians,
Moving Mass Actuators.

Practical Challenges in the Method of Controlled Lagrangians

Konda Reddy Chevva

(Abstract)

The method of controlled Lagrangians is an energy shaping control technique for underactuated Lagrangian systems. Energy shaping control design methods are appealing as they retain the underlying nonlinear dynamics and can provide stability results that hold over larger domain than can be obtained using linear design and analysis. The objective of this dissertation is to identify the control challenges in applying the method of controlled Lagrangians to practical engineering problems and to suggest ways to enhance the closed-loop performance of the controller.

This dissertation describes a procedure for incorporating artificial gyroscopic forces in the method of controlled Lagrangians. Allowing these energy-conserving forces in the closed-loop system provides greater freedom in tuning closed-loop system performance and expands the class of eligible systems. In energy shaping control methods, physical dissipation terms that are neglected in the control design may enter the system in a way that can compromise stability. This is well illustrated through the "ball on a beam" example. The effect of physical dissipation on the closed-loop dynamics is studied in detail and conditions for stability in the presence of natural damping are discussed. The control technique is applied to the classic "inverted pendulum on a cart" system. A nonlinear controller is developed which asymptotically stabilizes the inverted equilibrium at a specific cart position for the conservative dynamic model. The region of attraction contains all states for which the pendulum is elevated above the horizontal plane. Conditions for asymptotic stability in the presence of linear damping are developed. The nonlinear controller is validated through experiments. Experimental cart damping is best modeled using static and Coulomb friction. Experiments show that static and Coulomb friction degrades the closed-loop performance and induces limit cycles. A Lyapunov-based switching controller is proposed and successfully implemented to suppress the limit cycle oscillations. The Lyapunov-based controller switches between

the energy shaping nonlinear controller, for states away from the equilibrium, and a well-tuned linear controller, for states close to the equilibrium.

The method of controlled Lagrangians is applied to vehicle systems with internal moving point mass actuators. Applications of moving mass actuators include certain spacecraft, atmospheric re-entry vehicles, and underwater vehicles. Control design using moving mass actuators is challenging; the system is often underactuated and multibody dynamic models are higher dimensional. We consider two examples to illustrate the application of controlled Lagrangian formulation. The first example is a spinning disk, a simplified, planar version of a spacecraft spin stabilization problem. The second example is a planar, streamlined underwater vehicle.

To my dear mother and father,
and my dear Poonu for their love and prayers.

Acknowledgments

I am indeed very fortunate to have Dr. Craig Woolsey as my research advisor. I thank him with all my heart for giving me a chance to work under his tutelage on an exciting and challenging research topic. I thank him for his invaluable guidance during my PhD studies and his strong belief in me. Dr. Woolsey is an excellent researcher and one of the finest teachers I have ever come across. He is a wonderful human being, very thoughtful and caring. My association with Dr. Woolsey has helped me grow both as a researcher and as an individual. It has been my pleasure to have him as a friend as well as a mentor. I am very certain that this is just the beginning of a long and fruitful association.

I express my sincere gratitude for Dr. Ali Nayfeh for advising me in the early stages of my graduate studies. Dr. Nayfeh has always been a source of inspiration for me. He has always been very supportive, kind and thoughtful. It is a honor for me to have worked with a researcher of the highest calibre like Dr. Nayfeh. His teachings and advice will always guide me in my research career.

I thank Dr. Scott Hendricks, Dr. Daniel Inman and Dr. Ziyad Masoud for serving on my committee. I thank them for taking the time off to read my dissertation and for their critical assessment of my research. Special thanks are due to Dr. Inman for helping me in my job search.

I thank Dr. Tony Bloch, Dr. Dong Eui Chang, Dr. Jerrold Marsden, Dr. Naomi Leonard and William Whitacre for being a part of my PhD research. I would like to specially thank Dr.

Marsden for his encouragement and support. Thanks are due to William Whitacre for his help with the experiments.

During my academic life at Virginia Tech, I have been fortunate enough to collaborate with some wonderful people on some very interesting research topics. I would like to thank Dr. Zafer Gurdal, Dr. Mostafa Abdalla, Dr. Waleed Faris, Dr. Xiaopeng Zhao and Dr. Harry Dankowicz for the collaborative efforts. A special word of thanks for Mostafa Abdalla for several stimulating discussions in areas as varied as science and music.

Dr. Naira Hovakimyan has always been a mentor and a friend. I thank her for all her advice and help for my career. I thank Dr. Rudra Pratap, Dr. Anindya Chatterjee and Dr. Andy Ruina for their friendship and support all through my graduate studies. I thank all my colleagues at the Nonlinear Systems Lab: Chris Nickell, Mike Morrow, Amy Linklater, Nate Lambeth, Jesse Whitfield, Amanda Young, Laszlo Techy, Nina Mahmoudian, Vahram Stepanyan, Jiang Wang and Jan Petrich, and at the Nonlinear Dynamics Group: Dr. Haider Arafat, Mohammed Daqaq, Greg Vogl, Imran Akhtar, Dr. Sameer Emam, Dr. Pramod Malatkar, Dr. Mohammed Younis and Dr. Eihab Rehman for their support and companionship. Special thanks are due to Sally Shrader for her friendship and help in administrative matters.

Graduate student life is not always books and research papers. A integral part of my life in Blacksburg was the Virginia Tech Table Tennis Club. I thank all my wonderful friends in and outside the club for their friendship and for making my stay in Blacksburg a most memorable one. I would like to thank Helen Castaneda for her love, friendship and moral support. And of course, the everlasting music of the Beatles and Vivaldi that accompanied me through the long hours of the night.

Most importantly, I express my deepest gratitude for the people closest to my heart and without whose support I would have never reached this point. My mother and father have waited patiently all these years to watch me accomplish something I had long dreamed of. Their love, sacrifice and prayers have been my greatest strength all these years. I thank them with all my heart for their

abiding faith in me and standing besides me through the toughest moments of my life. I thank my mother for holding back her tears all these years and wholeheartedly supporting me in my cause. I can tell that they feel extremely proud and that is my greatest happiness. I am forever grateful to Poonam for all her love, support, kindness and devotion. Poonam has always stood besides me through thick and thin and has been a source of my strength and moral support. I am looking forward to many wonderful years of togetherness with Poonam. Finally, I would like to thank the rest of my family for their support and love.

Contents

List of Figures

Mechanics is the paradise of the mathematical sciences,
because by means of it one comes to the fruits of mathematics.

Leonardo da Vinci

Chapter 1

Introduction

1.1 Motivation

Internally actuated systems have found applications in many ocean and space missions. Internally actuated systems are particularly useful in situations where the environment around a vehicle is very harsh. For instance, the temperature and pressure outside a hypersonic re-entry vehicle are very high for conventional external control devices. For example, for proposed missions to explore Venus, careful consideration must be given to the extreme heat and acidic atmosphere during actuator design. In long term ocean sensing missions, external actuators are exposed to corrosion and biological fouling. Actuators that are housed internally are isolated from the environment and less prone to physical damage and deterioration. For example, the autonomous underwater vehicle (AUV), Slocum [76], developed at the Webb Research Corporation[1], is a buoyancy driven underwater glider, used for ocean sampling, that uses moving masses for controlling the attitude.

In ocean applications, internal actuators provide control authority at low speeds where external control devices like fins and rudders are not effective. This might be useful, for instance, for scientists who use underwater vehicles to shoot pictures of deep-sea volcanic vents which requires

[1] www.webbresearch.com

the vehicle to hover. In addition, internal actuators do not add to the vehicle's hydrodynamic drag and do not stir up the surrounding environment.

Internally actuated systems are often underactuated. Underactuated systems are systems that have fewer control inputs than configuration variables. A system can be underactuated due to the following reasons:

1. *Design.* For example, the dynamics of some internally actuated systems are underactuated. In space applications, it is highly desirable that the control objective be met with fewer actuators, thereby reducing the weight.

2. *Actuator failure.* For example, a fully actuated system becomes underactuated if one of the actuators fails. Study of underactuated system control is key to understanding robustness to actuator failure. For critical applications like aircraft, robustness to actuator failure is extremely important.

Control of underactuated systems can be quite difficult. For a survey of control of general underactuated mechanical systems, see Spong [67] and Reyhanoglu et. al. [61]. Underactuated systems are often not even linearly controllable. Even for systems which are linearly controllable, it is often desirable to use nonlinear control techniques to obtain stability and control results that hold over a larger domain than can be obtained using linear design and analysis. Feedback linearization is a nonlinear control technique that seeks to transform a nonlinear control system into a linear control system through feedback transformations. Underactuated systems are not fully feedback linearizable. Recently developed methods of nonlinear control design, including backstepping and sliding mode control [40], are not directly applicable to many underactuated systems. Spong [68] showed that the actuated subsystem of a general underactuated system can be linearized using an invertible change of control, a procedure called *partial feedback linearization.* However, after partial linearization, the unactuated subsystem still remains a nonlinear system coupled with the linearized actuated subsystem and does not lead to much simplification. Olfati-Saber [53] presented a way

to decouple the actuated and unactuated subsystems that leads to some simplification in control design. More recently, hybrid and switching-based control methods have been used in the control of underactuated mechanical systems [7]. In spite of these advances, control of underactuated systems still poses a big challenge for control theorists.

A central theme in this dissertation is stabilization of equilibria of underactuated mechanical systems. Nonlinear control techniques exploit the underlying nonlinear dynamics for better control design and lead to stabilizing control laws valid over large regions of phase space. Many times, one can even cleverly use intrinsic system nonlinearities to aid stabilization. With the ultimate objective of improved vehicle control, it makes sense to consider only mechanical systems. Mechanical systems have an underlying geometric structure that can be exploited for nonlinear control design. This has motivated a great deal of research in geometric control theory. Energy-based geometric control methods retain a physical view of the system dynamics and yield Lyapunov functions that can be used for stability analysis. In energy shaping control techniques, feedback is used to modify the kinetic and potential energy of a mechanical system such that the closed-loop dynamic equations are also mechanical. Brockett [21] first introduced the idea of a mechanical control system. This led to a great deal of research in control of mechanical systems, especially on the Hamiltonian side. See, for example, the papers by van der Schaft [71, 72], Crouch and van der Schaft [25], Bloch, Krishnaprasad, Marsden and Sanchez [11] and Jalnapurkar and Marsden [38, 38]. The idea of shaping the potential energy through feedback was introduced by Takegaki and Arimoto [70]. The idea of shaping the kinetic energy through feedback was first introduced by Bloch, Krishnaprasad, Marsden and Sanchez [11].

Energy-based geometric control methods offer a promising approach to design nonlinear controllers for underactuated mechanical systems. In this dissertation, we consider underactuated Lagrangian mechanical systems: underactuated mechanical systems whose equations of motion are derived from a Lagrangian. The energy shaping control technique for Lagrangian systems is called the method of controlled Lagrangians. In this dissertation, we seek to identify the control challenges one faces when applying the method of controlled Lagrangians to practical engineering problems

and suggest ways to enhance the control technique.

1.2 Background

The method of controlled Lagrangians is a constructive technique for stabilizing underactuated Lagrangian mechanical systems. The method has its roots in the paper by Bloch, Krishnaprasad, Marsden and Sánchez [11], where it was shown that an internal rotor can be used to effectively shape the kinetic energy of a spacecraft in order to stabilize steady rotation about the intermediate principal axis of inertia. The method was systematically developed and formalized in a series of papers by Bloch, Leonard and Marsden [13, 14, 15, 16, 17]. As initially developed [13, 14, 17], the method of controlled Lagrangians provides a kinetic-shaping control design tool for a class of underactuated mechanical systems, which exhibit an abelian Lie group symmetry in the input directions. This class includes the spacecraft example described above and the classic inverted pendulum on a controlled cart. Bloch, Chang, Leonard and Marsden[10] and Bloch, Leonard and Marsden [15] introduced additional control freedom by allowing potential shaping and by relaxing the symmetry condition on the original and feedback-modified potential energy. Still more control freedom may be introduced by allowing for generalized gyroscopic forces in the closed-loop dynamics. The notion of gyroscopic control forces predates the method of controlled Lagrangians, appearing in the work of Wang and Krishnaprasad [74] and later in the developments of Bloch, Krishnaprasad, Marsden and Ratiu [12]. In related earlier work by Sánchez [26], Poisson control systems were introduced and studied. Controlled Lagrangians for nonholonomic systems has been addressed in [84, 85]

Concurrent with the development of the method of controlled Lagrangians, others have explored kinetic shaping in more general settings. A very reasonable question is: What are the general conditions under which a feedback-controlled, underactuated mechanical system is Lagrangian or Hamiltonian? That is, without imposing any *a priori* requirements on an underactuated mechanical system, when is it possible to choose feedback such that the closed-loop equations are Lagrangian

or Hamiltonian? This question was addressed by Auckly and Kapitanski [5], Auckly, Kapitanski and White [6] and Hamberg [30, 31] on the Lagrangian side and by Blankenstein et. al [8] and Ortega et. al. [55] on the Hamiltonian side. The question is one of feedback equivalence; one obtains conditions in the form of partial differential equations (PDEs).

In applying the method of controlled Lagrangians, one starts with a conservative Lagrangian system that has an equilibrium of interest. A feedback control law is derived such that the closed-loop system is mechanical and conditions on the control parameters are found for stability of the equilibrium. Feedback dissipation is used to asymptotically stabilize the equilibrium. After stabilization, external forces like physical dissipation are incorporated in the system and asymptotic stability in the presence of such external forces is examined. Physical dissipation effects that are neglected in the control design process may enter the system in a way that can compromise stability. One would naively expect that physical dissipation terms will help stability or, if not, that their effect could be cancelled using feedback dissipation. However, when the system is underactuated and the kinetic energy is shaped through feedback, physical damping terms do not necessarily enter as dissipation with respect to the closed-loop energy function. In many cases, even the linearized dynamics may not preserve stability after introduction of physical dissipation terms. One may lose stability if the control gains are not chosen carefully. This problem is well-illustrated by the cart-pendulum example in Woolsey et. al [83]. Even though the desired equilibrium is a strict minimum of the control-modified energy, simple Rayleigh dissipation makes the closed-loop system unstable.

The complications introduced by physical damping are not limited to the method of controlled Lagrangians. As observed in Reddy et. al. [60], the problem of physical dissipation is inherent to any control technique which modifies a system's kinetic energy through feedback, such as interconnection and damping assignment passivity based control (IDA-PBC) [55]. Working in the Hamiltonian setting, Gómez-Estern and van der Schaft [29] suggest procedures for recovering asymptotic stability in systems with feedback-modified kinetic energy. An essential requirement is that the system satisfies a dissipation condition involving the original and modified kinetic metrics and a matrix of damping coefficients. The cart-pendulum described in [83] fails to satisfy the dissipation condition.

Whether in the Lagrangian or Hamiltonian setting, it is paramount that one consider physical damping explicitly when implementing a kinetic-shaping control law. As an alternate to this type of controller re-design, one may attempt to address the issue of damping during the matching process, as in [6].

Gyroscopic forces are energy conserving forces and as such do not affect the closed-loop energy. However, they can be introduced in the closed-loop dynamics to gain additional freedom in the control synthesis. Chang [22] investigated the use of artificial gyroscopic forces to enhance the controlled Lagrangian design process in some depth. An example, involving stabilization of an inverted pendulum on a rotor arm, illustrated the utility of this idea. Chang et. al. [23] showed that the appearance of generalized gyroscopic forces in the controlled Lagrangian dynamics was related explicitly to a modification of the dynamic structure in the Hamiltonian setting. It was also shown in [23] that the most general formulation of the method of controlled Lagrangians, in which one places no prior restrictions on the class of eligible mechanical systems, is equivalent to the IDA-PBC technique described in [8] and [55].

While it is important and worthwhile to understand feedback equivalence of general Lagrangian and Hamiltonian systems, there are advantages in restricting one's view to a smaller class of systems. For example, the control design procedure defined in [17] is algorithmic and does not rely on case-by-case solution of a set of partial differential equations. We continue in this spirit and restrict the form of kinetic energy modifications to that described in [17]. We also allow forces due to a modified potential energy in the closed-loop dynamics, as in [10], as well as artificial gyroscopic forces. The approach strikes a physically motivated balance between the algorithmic simplicity of the method described in [17, 10] and the elegance and generality of [23].

One of the research goals is to apply the controlled Lagrangian technique to well motivated engineering problems. Vehicle systems with internal moving mass actuators (MMAs) form an important class of internally actuated systems. Examples include spacecrafts and underwater vehicles. Moving mass actuators occupy a small but important niche in the spectrum of actuators that are available for flight vehicle control. Because they can be housed inside a vehicle's chassis, MMAs are pro-

tected from the surrounding environment. Moreover, their effectiveness relies on action/reaction or on gravity rather than on relative fluid motion. As a result, these actuators can be used in environments or operating conditions where conventional actuators may be useless. Internal MMAs are used to control maneuverable atmospheric re-entry vehicles, for example, because they are protected from the high temperatures and forces that arise in hypersonic flight [34, 58]. MMAs have also been proposed for precision orbit control in spacecraft formations [62]. MMAs are also useful for controlling buoyancy-driven underwater gliders, a new class of long-endurance AUVs. In this application, because they are protected from corrosion and biological fouling, MMAs remain reliable actuators for deployments of months or even years [27, 43, 64, 77]. A classic problem in spacecraft attitude dynamics is stabilizing steady rotation about a principal axis of inertia. Assuming conservative dynamics, steady spin about the major axis is stable. This motion may be asymptotically stabilized using a "precession damper," a mass-spring-damper whose parameters are chosen to rapidly attenuate precessional motion [39]. To stabilize rotation about the minor or intermediate axis using a moving mass actuator, one must apply feedback. White and Robinett proposed actively modulated "principal axis misalignments" to stabilize minor axis rotation of a prolate, axisymmetric spacecraft [78]. The authors designed a linear state feedback control law to locally asymptotically stabilize the desired motion.

Control design using MMAs is challenging because the multibody dynamic models are relatively high-dimensional and often quite complicated. Because they are often underactuated, vehicles with MMAs are often not even linearly controllable. Even for systems which are linearly controllable, however, it is often desirable to obtain stability and control results that hold over a larger domain than can be obtained using linear design and analysis. New energy-based control design techniques applicable to underactuated mechanical systems provide a promising approach to control design for vehicles with internal actuators.

1.3 Objectives

The long term research goals are:

- Develop constructive energy shaping nonlinear control theory for underactuated Lagrangian mechanical systems. The approach is to use the geometric structure of the mechanical system and the underlying nonlinear dynamics to develop stabilizing control laws that are valid over large regions of phase space.
- Apply the resulting techniques to well motivated engineering problems like autonomous underwater vehicles using moving mass actuators.

The immediate goals that fall within the scope of this dissertation are:

- Investigate the use of artificial gyroscopic forces in the closed-loop system to enhance the controlled Lagrangian design process. This forms the discussion in Chapter 4.
- Apply the technique to a benchmark control problem. Carry out a detailed analysis of the effect of physical dissipation on closed-loop stability. Test the developed nonlinear controller experimentally and identify experimental control challenges, if any. Suggest methods to improve the closed-loop performance of the nonlinear controller. This forms the discussion in Chapter 5.
- Illustrate the applicability of the method of controlled Lagrangians to models that describe vehicle systems with internal MMAs. Formulate the dynamic equations for vehicle systems with internal MMAs. Suggest a general control design methodology based on the method of controlled Lagrangians. Illustrate the idea through simple examples. This forms the discussion in Chapter 6.

1.4 Contributions

The main contributions of the dissertation are:

- We modify the method of controlled Lagrangians, as presented in [17, 10], to include artificial gyroscopic forces in the closed-loop system. The introduction of gyroscopic forces allows additional freedom to tune the closed-loop system performance and expands the class of underactuated mechanical systems which can be stabilized using this technique. While the approach described here is less general than the formulation given in [23], it is more algorithmic.

- We illustrate through the "ball on a beam" example that when feedback is used to shape the kinetic energy in the Hamiltonian setting, introduction of physical damping can lead to a loss of stability.

- We apply the control design technique to the problem of stabilizing an inverted pendulum on a cart. We construct a control-modified energy such that the desired equilibrium is a minimum of the control-modified energy. We show that addition of feedback dissipation provides asymptotic stability within a region of attraction that contains all states for which the pendulum is inclined above the horizontal plane. We show that despite these results, generic physical damping makes the control-modified energy rate indefinite. In this case, we study spectral stability and determine system and control parameter values which ensure that the desired equilibrium is locally exponentially stable.

- We experimentally test the nonlinear controller. We observe that static and Coulomb friction in the cart direction degrades the energy shaping controller's local performance by inducing limit cycle oscillations. A well-designed linear state feedback control law, on the other hand, eliminates these oscillations. To recover the best features of both controllers, we propose and implement a Lyapunov based switching control law.

- We formulate the dynamic equations of motion for a class of vehicle systems with internal moving masses. In particular, we derive reduced Euler-Lagrange equations for a rigid body with n internal moving masses immersed in an ideal fluid. We derive sufficient matching conditions that are algebraic in nature and present an algorithm for matching and stabilization. We apply the technique to two systems with a single moving mass actuator: a spinning disk and a planar streamlined underwater vehicle.

1.5 Organization

This dissertation is organized as follows:

Chapter 2: We introduce some basic differential geometry that will be used throughout this dissertation. Important concepts related to differential manifolds and Lie groups are introduced. Since stabilization of equilibria is at the core of this dissertation, we present some stability results from control theory. The main purpose of this chapter is to fill any gaps the reader might have and to set the notation.

Chapter 3: We review the reduction process for Lagrangian systems with Lie group symmetries. We explain the role played by the "mechanical connection" in the reduction process. This chapter provides the setting for the formulation in Chapter 6.

Chapter 4: We introduce the method of controlled Lagrangians. We describe a way to include artificial gyroscopic forces in the closed-loop system and present a general way to "match" the open-loop and closed-loop equations.

Chapter 5: We apply the method of controlled Lagrangians to the classic inverted pendulum on a cart system and report experimental results.

Chapter 6: We apply the controlled Lagrangian formulation for developing nonlinear control laws for vehicle systems with internal moving mass actuators.

Chapter 7: We summarize the main results of the dissertation and present some open problems.

Chapter 2

Mathematical Preliminaries

Research in nonlinear control systems in the past few decades has shown rich connections between control theory and geometric mechanics. The constant need to push the performance envelope of a given control system has motivated researchers to look at a geometric approach to control theory. Differential geometry is becoming an integral part of modern nonlinear control theory. Although tools from differential geometry are being increasingly used in control theory, ideas and concepts from geometric mechanics are not yet familiar to a large part of the control community. The purpose of this chapter is to introduce the basic concepts from differential geometry that will be used throughout this dissertation. The discussion is kept as simple as possible without overwhelming the reader with a lot of abstraction and the ideas are conveyed graphically wherever possible. This chapter will also serve to set the notation. For a more comprehensive treatment of the subject, the reader is referred to Boothby [19], Crampin and Pirani [24], Kobayashi and Nomizu [41] and Spivak [66]. Applications of differential geometry to problems in physics and mechanics is not given much emphasis in the above references. For applications in the areas of physics and mechanics, see Abraham and Marsden [1], Abraham, Marsden and Ratiu [2], Arnold [4], Frankel [28], Isham [36], Marsden [45] and Marsden and Ratiu [46]. Murray, Li and Sastry [50] give a brief introduction to differential geometry (in an appendix) in the context of robotic systems. Also, Isidori [37] and

Nijmeijer and van der Schaft [52] give a very nice exposition of differential geometry in the light of nonlinear control systems. Application of differential geometry to the control of nonholonomic systems is addressed in Bloch [9]. Much of the discussion in this chapter is based on the texts by Bloch, Frankel, Isham and Murray, Li and Sastry. We give references to related topics whenever necessary. We hope that this chapter will fill any gaps the reader might have and be a guide to the literature for further reading.

In § 2.1, the important notions of topological spaces, differentiable manifolds, tangent and cotangent spaces are introduced. An important class of differentiable manifolds is Lie groups. Lie groups play an important role in systems with symmetry. We give a brief introduction to Lie groups in § 2.2. Fiber bundles provide the basic geometric structure for understanding many control problems. Section 2.3 introduces fiber bundles, namely principal fiber bundles. Since stabilization of equilibria is a central theme of this dissertation, we review some important results from stability theory in § 2.4.

2.1 Manifolds

Every engineer is familiar with differential and integral calculus in the context of Euclidean space $\mathbb{R}^n$, but sometimes it is necessary to apply calculus for problems involving *curved* spaces. Simply put, a manifold is a curved space that looks locally like an Euclidean space. A manifold is the most general setting for many problems in mechanics and control theory. For example, the most familiar manifold is, of course, the n-dimensional Euclidean space $\mathbb{R}^n$, the space of ordered n-tuples $(x^1,\ x^2, \ldots,\ x^n)$. The circle S^1 represents the configuration space for an inverted pendulum, whereas the sphere S^2 is the configuration space for a spherical pendulum. The configuration space of a free rigid body in rotation is $SO(3)$, the special orthogonal group. We discuss these examples in detail later. This section provides a basic exposition of differentiable manifolds and related topics. A detailed treatment can be found in Boothby [19]. A very accessible reference in this regard is Isham [36].

2.1.1 Topological Spaces and Related Concepts

This chapter is aimed at developing an intuitive feeling for manifolds without worrying much about topological details. However, some basic notions from point set topology are helpful. Here, we briefly review topological spaces and mappings between topological spaces. The reader is referred to Munkres [49] for more details.

The notion of "topology" allows us to talk about "continuous" functions and "neighborhoods" of points for spaces where the notion of distance might be lacking. A *topological space* is a set X together with a collection of subsets of X, called *open sets*, satisfying the following axioms:

1. The empty set and X are open sets.
2. The union of any collection of open sets is open.
3. The intersection of finitely many open sets is open.

The open sets define the "topology" on X. A different collection of open sets might define a different topology on X. For example, $\mathbb{R}^n$ is a topological space that is endowed with the notion of distance or a metric. Open sets in $\mathbb{R}^n$ are defined using "open balls". An *open ball* of radius ϵ centered at $\boldsymbol{a} \in \mathbb{R}^n$ is the set $B_{\boldsymbol{a}}(\epsilon) = \{\boldsymbol{x} \in \mathbb{R}^n \mid ||\boldsymbol{x} - \boldsymbol{a}|| < \epsilon\}$, where $||.||$ denotes the distance norm on $\mathbb{R}^n$. A set U in $\mathbb{R}^n$ is open if given any $\boldsymbol{a} \in U$ there is an open ball of some radius $r > 0$, centered at $\boldsymbol{a}$, that lies entirely in U. This collection of open sets defines the "usual" topology for $\mathbb{R}^n$.

A subset of X is *closed* if its complement is open. Any open set of X that contains a point $x \in X$ is called the *neighborhood* of x. Let $F : X \to Y$ be a map between topological spaces X and Y. We say that F is *continuous* if for every open set $V \subset Y$, the inverse image $F^{-1}V := \{x \in X \mid F(x) \in V\}$ is open in X. This reduces to the usual (ϵ, δ) definition if X and Y are Euclidean spaces. If $F : X \to Y$ is one to one and onto, then the inverse map $F^{-1} : Y \to X$ exists. If both F and F^{-1} are continuous, then F is called a homeomorphism and X and Y are homeomorphic spaces. A basis $\mathcal{B}$ is a collection of open sets of X such that every open set of X can be written as a union of

the open sets in $\mathcal{B}$. For example, the open balls in $\mathbb{R}^n$ are a basis for the usual topology in $\mathbb{R}^n$. A topological space is *connected* if it is not the union of a pair of disjoint, non-empty open sets. The technical definition of a manifold needs one more concept from topology, namely "Hausdorffness". A topological space X is *Hausdorff* if any two distinct points have disjoint neighborhoods. For example, every metric space is Hausdorff. If d is a metric and $d(x, y) = \epsilon > 0$ for a pair $x,\ y \in X$, then the sets $U_x := \{z \mid d(x, z) < \epsilon/2\}$ and $U_y := \{z \mid d(y, z) < \epsilon/2\}$ are disjoint neighborhoods.

2.1.2 Differentiable Manifolds

We are now in a position to define a differentiable manifold.

Definition 2.1.1 (Manifold) *An n-dimensional differentiable manifold M is a connected topological space (Hausdorff with a countable basis) with the following properties:*

1. *M is locally homeomorphic to $\mathbb{R}^n$ for some $n < \infty$. That is, around any point $p \in M$, there exists a neighborhood U and a homeomorphism $\phi : U \to B$, where B is an open ball of $\mathbb{R}^n$ as seen in Fig 2.1. The pair (U, ϕ) is called a coordinate chart.*

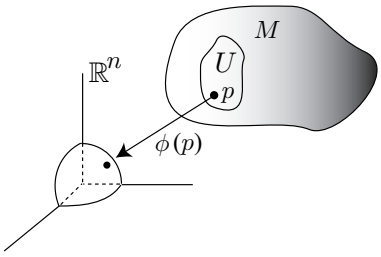

Figure 2.1: An n-dimensional manifold looks locally like an n-dimensional Euclidean space.

2. *If (U, ϕ) and (V, ψ) are any two coordinate charts, then the overlap map $\psi \circ \phi^{-1} : \phi(U \cap V) \to \psi(U \cap V)$ is differentiable. See Fig 2.2.*

The first property says that an n-dimensional manifold looks locally like an n-dimensional Euclidean space. The second property assigns the manifold a differential structure. We say that a manifold M

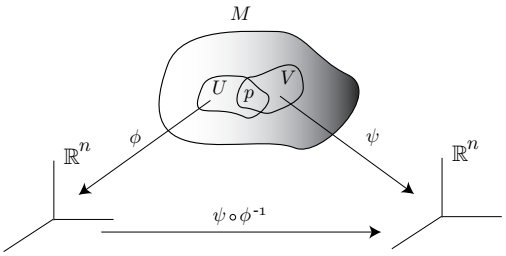

Figure 2.2: The overlap map $\psi \circ \phi^{-1} : \mathbb{R}^n \to \mathbb{R}^n$.

is C^k (resp. C^∞ or *smooth*) if the overlap maps $\psi \circ \phi^{-1} : \mathbb{R}^n \to \mathbb{R}^n$ are C^k (resp. C^∞ or *smooth*). The local coordinates of any point $p \in U \subset M$ are $(x^1(p),\ x^2(p), \ldots,\ x^n(p))$ (or simply $(x^1,\ x^2, \ldots,\ x^n)$), where the *coordinate functions* $x^i : U \to \mathbb{R}$ are defined as $x^i(p) := x^i,\ i = 1,\ 2, \ldots,\ n$.

Examples of Manifolds

- $\mathbb{R}^n$ is an n-dimensional manifold covered with a single coordinate system. Any open subset of $\mathbb{R}^n$ is also an n-dimensional manifold.

- The unit circle $S^1 = \{(x, y) \in \mathbb{R}^2 \mid x^2 + y^2 = 1\}$ is a 1-dimensional C^∞ manifold. S^1 is the configuration space for a planar pendulum where the angular position $\theta \in [0, 2\pi)$ is a coordinate.

- Let M be an m-dimensional manifold with local coordinates $(U; x^1,\ x^2, \ldots,\ x^m)$ and let N be an n-dimensional manifold with local coordinates $(V; y^1,\ y^2, \ldots,\ y^n)$. The product manifold is defined as $M \times N : \{(p, q) \mid p \in M \text{ and } q \in N\}$ where $(x^1,\ x^2, \ldots,\ x^m,\ y^1,\ y^2, \ldots,\ y^n)$ are local coordinates. As an example, $T^2 := S^1 \times S^1$ is a 2-dimensional torus with angular parameters θ^1 and θ^2 as coordinates. T^2 represents the configuration space for a planar double pendulum.

- Let $\mathcal{M}(n, \mathbb{R})$ denote the set of all real, $n \times n$ matrices. To every $\boldsymbol{A} \in \mathcal{M}(n, \mathbb{R})$, we can associate a point in $\mathbb{R}^{n^2}$ with coordinates $(A_{11},\ A_{12}, \ldots,\ A_{1n}, \ldots,\ A_{nn})$. Thus, topologically $\mathcal{M}(n, \mathbb{R})$ is an n^2-dimensional Euclidean space.

2.1.3 Mappings Between Manifolds

Let $F : M \to N$ be a map between the manifolds M and N, of dimensions m and n respectively. Let (U, ϕ) and (V, ψ) be coordinate charts on M and N respectively, as seen in Fig 2.3. The coordinate representation of F is

$$\bar{F} := \psi \circ F \circ \phi^{-1} : \mathbb{R}^m \to \mathbb{R}^n.$$

The map F is smooth if $\bar{F}$ is smooth for all choices of coordinate charts. In what follows, we shall usually omit the process of replacing a map $F : M \to N$ with its coordinate representation $\psi \circ F \circ \phi^{-1}$, thinking of F as directly expressible as a function of local coordinates $(x^1, x^2, \ldots, x^m)$.

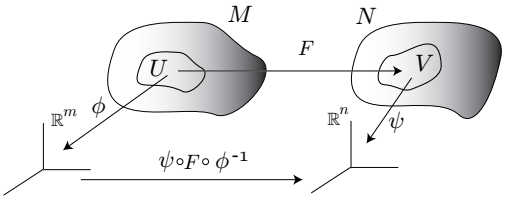

Figure 2.3: The local representation of the map $F : M \to N$.

2.1.4 Tangent Vectors and Tangent Spaces

The notion of a *tangent space* to a manifold is an important idea in differential geometry. The intuitive geometric idea one has is that of a tangent plane to a surface. For example, the tangent plane to an n-dimensional sphere, S^n, is given by

$$T_{\boldsymbol{x}} S^n := \{\boldsymbol{v} \in \mathbb{R}^{n+1} \mid \boldsymbol{x}^T \boldsymbol{v} = 0\},$$

where $\boldsymbol{x} \in S^n \subset \mathbb{R}^{n+1}$ is a point on the sphere (Fig 2.4).

The above representation involves embedding a manifold in a higher dimensional Euclidean space and then regarding the tangent space as a linear subspace of the Euclidean space. However, modern differential geometry tries to present ideas in a manner that is *intrinsic* to the manifold and not dependent on the embedding. In fact, the definition of a manifold made no reference to such an

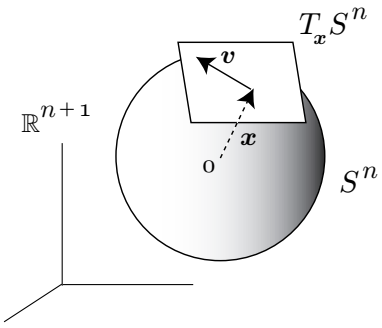

Figure 2.4: The tangent space for an n-dimensional sphere S^n.

embedding and so neither should the notion of a tangent space. In what follows, we give a geometric as well as an algebraic picture of a tangent vector.

The geometric definition stems from the idea of a tangent vector being tangent to a curve on the manifold. Note that a given curve lies on the manifold and not in the surrounding embedding. A *curve* on a manifold M is a smooth map σ from some open interval $(-\epsilon, \epsilon)$ of the real axis into M (Fig 2.5).

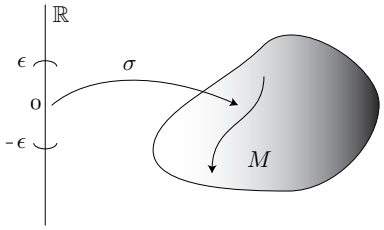

Figure 2.5: A curve on a manifold M.

Two curves σ_1 and σ_2 are tangent at a point p in M if,

1. $\sigma_1(0) = \sigma_2(0) = p$.
2. $\frac{d}{dt}x^i(\sigma_1(t))|_{t=0} = \frac{d}{dt}x^i(\sigma_2(t))|_{t=0}, \quad i = 1,\ 2, \ldots,\ n$, where $(x^1,\ x^2, \ldots,\ x^n)$ are local coordinates and $t \in (-\epsilon, \epsilon)$. That is, the two curves are tangent in the usual sense as curves in $\mathbb{R}^n$.

A tangent vector X_p at p is an equivalence class of curves in M where any two curves in the equivalence class are tangent at p and have "velocity" X_p (Fig 2.6).

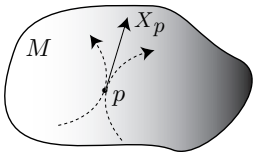

Figure 2.6: The tangent vector is an equivalence class of curves in M.

Let us see how the tangent vector can be regarded as a differential operator in the context of $\mathbb{R}^n$. Let $\boldsymbol{x}(t) = (x^1(t),\ x^2(t), \ldots,\ x^n(t))$ be a parameterized curve in $\mathbb{R}^n$. The tangent vector at any point $\boldsymbol{x}(0) = a$ is the usual velocity vector $\dot{\boldsymbol{x}} = (\dot{x}^1,\ \dot{x}^2, \ldots,\ \dot{x}^n)$ to the curve. Let $f : \mathbb{R}^n \to \mathbb{R}$ be a real valued function. We will use the Einstein summation convention throughout this dissertation. That is, in an expression involving indexed quantities, a repeated index implies summation over all possible values of the index; for example, $\alpha_i\beta^i := \sum_{i=1}^n \alpha_i\beta^i$. The derivative of f along the curve at a is

$$\left.\frac{df}{dt}\right|_{t=0} = \left.\frac{\partial f}{\partial x^i}\right|_a \dot{x}^i = \dot{x}^i \left.\frac{\partial}{\partial x^i}\right|_a (f) = X_a(f),$$

where $X_a = \dot{x}^i \left.\frac{\partial}{\partial x^i}\right|_a$ is the tangent vector expressed as a differential operator.

Thus, for any manifold M, the tangent vector can be thought of as the directional derivative of a function $f : M \to \mathbb{R}$ by defining

$$X_p(f) := \left.\frac{d}{dt}(f \circ \sigma)(t)\right|_{t=0}, \tag{2.1}$$

where σ is any curve in the equivalence class represented by X_p. Note that $f \circ \sigma : \mathbb{R} \to \mathbb{R}$. This motivates the algebraic definition of a tangent vector and the tangent space. Let $C^\infty(p)$ be the set of smooth, real valued functions defined in some neighborhood of $p \in M$.

Definition 2.1.2 (Derivation) *A derivation at a point $p \in M$ is a map $X_p : C^\infty(p) \to \mathbb{R}$ such that, for all $a,\ b \in \mathbb{R}$ and $f,\ g \in C^\infty(p)$,*

1. $X_p(af + bg) = aX_p(f) + bX_p(g)$ *(Linearity).*

2. $X_p(fg) = (X_p f)g(p) + f(p)(X_p g)$ *(Leibnitz rule).*

The space of all derivations can be given the structure of an n-dimensional real vector space by defining the operations:

$$(X_p + Y_p)f = X_p\ f + Y_p\ f$$

$$(aX_p)f = a(X_p f).$$

The *tangent space* T_pM at p to M is the set of all derivations at $p \in M$. From Eq. (2.1), we see that a tangent vector X_p is indeed a derivation. Let (U, ϕ) be a coordinate chart around $p \in M$ and $\boldsymbol{x} = (x^1,\ x^2, \ldots,\ x^n)$ be local coordinates. Equation (2.1) gives

$$\begin{aligned} X_p(f) &:= \frac{d}{dt}(f \circ \phi^{-1} \circ \phi \circ \sigma)(t)\Big|_{t=0} \\ &= \frac{\partial(f \circ \phi^{-1})}{\partial x^i}\Big|_{\phi(p)} \frac{dx^i}{dt}(0) \\ &= X^i \frac{\partial}{\partial x^i}(f), \end{aligned}$$

where X^i and $\frac{\partial}{\partial x^i}$ are defined as

$$X^i := X_p(x^i) = \frac{dx^i}{dt}(0) \quad \text{and} \quad \frac{\partial}{\partial x^i}(f) := \frac{\partial(f \circ \phi^{-1})}{\partial x^i}\Big|_{\phi(p)}.$$

Note, $f \circ \phi^{-1} : \mathbb{R}^n \to \mathbb{R}$ is the local representation of f.

The tangent vectors $\frac{\partial}{\partial x^i},\ i = 1,\ 2, \ldots,\ n$ form a basis for T_pM. Thus, any element $X_p \in T_pM$ is expressed in this basis as

$$X_p = X^i \frac{\partial}{\partial x^i},$$

where $X^i,\ i = 1,\ 2, \ldots,\ n$ are local coordinates of X_p.

The tangent bundle is defined as

$$TM := \bigcup_{p \in M} T_pM.$$

TM is a $2n$-dimensional manifold. A point in TM consists of the pair (p, X_p) where $p \in M$ and $X_p \in T_pM$. In some local coordinate system $(p, X_p) = (x^1,\ x^2, \ldots,\ x^n,\ X^1,\ X^2, \ldots,\ X^n)$. There is a natural *projection*,

$$\pi : TM \to M \qquad\qquad \pi(p, X_p) = p$$

that associates with every tangent vector X_p the point p at which it is tangent. In local coordinates

$$\pi(x^1,\ x^2, \ldots,\ x^n,\ X^1,\ X^2, \ldots,\ X^n) = (x^1,\ x^2, \ldots,\ x^n).$$

The inverse image $\pi^{-1}(p)$ is just the set of all vectors tangent at p, T_pM.

For example, in mechanics, the configuration of a dynamical system with n-degrees of freedom is described by a point in an n-dimensional manifold Q, called the *configuration space*. The coordinates of a point p are usually denoted by $\boldsymbol{q} = (q^1,\ q^2, \ldots,\ q^n)$, the *generalized coordinates*. The tangent vector at a point in the configuration space is thought of as the velocity vector whose components are $\dot{\boldsymbol{q}} = (\dot{q}^1,\ \dot{q}^2, \ldots,\ \dot{q}^n)$ with respect to the coordinates $\boldsymbol{q}$. These are *generalized velocities*. The tangent bundle TQ is the space of all generalized velocities. A point in TQ is the pair $(\boldsymbol{q}, \dot{\boldsymbol{q}}) = (q^1,\ q^2, \ldots,\ q^n,\ \dot{q}^1,\ \dot{q}^2, \ldots,\ \dot{q}^n)$. The tangent bundle TQ plays an important role in Lagrangian mechanics. The dynamics for a Lagrangian system evolves on TQ and the Lagrangian is a real valued function $L : TQ \to \mathbb{R}$.

Tangent Map

Let $F : M \to N$ be a smooth map between manifolds M and N of dimensions m and n respectively. The tangent map $F_{*p} : T_pM \to T_{F(p)}N$ is defined as

$$F_{*p}X_p(f) := X_p(f \circ F), \tag{2.2}$$

where $X_p \in T_pM$ and $f \in C^\infty(F(p))$ (Fig 2.7). The tangent map of F is also denoted by T_pF.

If $\bar{F}\ (= \phi^{-1} \circ F \circ \psi) : \mathbb{R}^m \to \mathbb{R}^n$ is the local representation of F, then locally the tangent map is given by the Jacobian of $\bar{F}$ evaluated at $\phi(p)$.

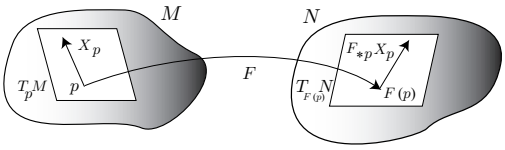

Figure 2.7: The tangent map F_{*p} of $F : M \to N$

2.1.5 Vector Fields

The tangent vectors were defined at a single point on the manifold. Now, we consider a field of tangent vectors in which a single tangent vector is assigned to every point of M.

Definition 2.1.3 (Vector Field) *A vector field X on a C^∞ manifold M is a smooth assignment of a tangent vector $X_p \in T_pM$ for each point $p \in M$, such that for all $f \in C^\infty(M)$, the function $Xf : M \to \mathbb{R}$ defined as*

$$(Xf)(p) := X_p(f)$$

is smooth.

Thus, the vector field can be regarded as the map $X : C^\infty(M) \to C^\infty(M), \quad f \mapsto X(f)$. The function $X(f)$ is called the *Lie derivative* of f along X.

The vector field X can be represented in local coordinates $\boldsymbol{x} = (x^1,\ x^2, \ldots,\ x^n)$ as

$$X(\boldsymbol{x}) = X^i(\boldsymbol{x})\frac{\partial}{\partial x^i},$$

where $X^i(\boldsymbol{x}),\ i = 1,\ 2, \ldots,\ n$ is a smooth function defined in some neighborhood of $\boldsymbol{x}$. In local coordinates, the Lie derivative is

$$Xf(p) := X_p(f) = \frac{\partial f}{\partial x^i}X^i(\boldsymbol{x}).$$

Let $\mathfrak{X}(M)$ denote the vector space of all smooth vector fields on M. Let $X,\ Y \in \mathfrak{X}(M)$. The *Lie bracket* of X and Y, $[X, Y]$, is a new vector field defined as

$$[X, Y]f = X(Yf) - Y(Xf). \tag{2.3}$$

A vector space V is a *Lie algebra* if there exists a bilinear operator $V \times V \to V$, denoted by $[.,.]$ satisfying,

1. Skew Symmetry: $[u, v] = -[v, u]$ for all $u, v \in V$
2. Jacobi Identity: $[[u, v], w] + [[w, u], v] + [[v, w], u] = 0$ for all $u, v, w \in V$

For example, the vector space $\mathfrak{X}(M)$ is an infinite dimensional Lie algebra with the Lie bracket (2.3) defining the bilinear operator. A subspace W of V is a *Lie subalgebra* if it is closed under the bracket operation.

2.1.6 Cotangent Vectors and Cotangent Spaces

Let E be an n-dimensional vector space and $\boldsymbol{e} = (\boldsymbol{e}_1,\ \boldsymbol{e}_2, \ldots,\ \boldsymbol{e}_n)$ be a basis for E. A vector $\boldsymbol{v} \in E$ has an expansion $\boldsymbol{v} = v^i \boldsymbol{e}_i$ where v^i are the components of $\boldsymbol{v}$ with respect to the basis $\boldsymbol{e}$. A *linear functional* on E is a real valued linear function $\alpha : E \to \mathbb{R}$. That is,

$$\alpha(a\,\boldsymbol{v} + b\,\boldsymbol{w}) = a\,\alpha(\boldsymbol{v}) + b\,\alpha(\boldsymbol{w})$$

for all $a,\ b \in \mathbb{R}$ and $\boldsymbol{v},\ \boldsymbol{w} \in E$. Using $\boldsymbol{v} = v^i \boldsymbol{e}_i$, we get

$$\alpha(\boldsymbol{v}) = \alpha_i v^i \quad \text{where} \quad \alpha_i := \alpha(\boldsymbol{e}_i).$$

Definition 2.1.4 (Dual Space of a Vector Space) *The set of all linear functionals on E forms an n-dimensional vector space E^* under the operations:*

$$\begin{aligned} (\alpha + \beta)\boldsymbol{v} &= \alpha(\boldsymbol{v}) + \beta(\boldsymbol{v}) \quad \alpha,\ \beta \in E^* \text{ and } \boldsymbol{v} \in E \\ (c\alpha)\boldsymbol{v} &= c\,\alpha(\boldsymbol{v}) \quad c \in \mathbb{R}. \end{aligned}$$

E^* is called the dual space of E.

The elements of E^* are called *covectors*. A dual basis $(\sigma^1,\ \sigma^2, \ldots,\ \sigma^n)$ is defined as $\sigma^i(\boldsymbol{e}_j) := \delta^i_j$. We have $\sigma^i(\boldsymbol{v}) = v^i$. That is, σ^i is the covector that reads off the i^{th} component of $\boldsymbol{v}$.

Let T_pM be the tangent space to a manifold M at p. T_pM has the structure of a vector space (set of all derivations X_p at p). The *cotangent space* T^*_pM is defined to be the dual space to T_pM at the point $p \in M$. T^*_pM is thus the set of all linear functionals $\omega_p : T_pM \to \mathbb{R}$. ω_p is called a *cotangent vector* or *1-form* or simply a *covector*. Cotangent vectors are examples of covariant tensors of rank 1. For a discussion on general tensors, see Appendix A. The natural pairing between cotangent and tangent vectors is often denoted as $\langle \omega_p, X_p \rangle$.

Let $f : M \to \mathbb{R}$ be a smooth function. The *differential* of f at p is the covector $df : T_pM \to \mathbb{R}$ defined as

$$\langle df, X_p \rangle := X_p(f).$$

In particular, consider the differential of a coordinate function, say x^i. We have,

$$\langle dx^i, X_p \rangle = X_p(x^i) = X^i.$$

Thus, the covectors $dx^1,\ dx^2, \ldots,\ dx^n$ form a basis for T^*_pM. Any cotangent vector ω_p can be locally expressed as

$$\omega_p = \omega_i\ dx^i,$$

and the natural pairing between ω_p and X_p is given by

$$\langle \omega_p, X_p \rangle = \omega_i X^i.$$

The *cotangent bundle* is defined as

$$T^*M = \bigcup_{p \in M} T^*_pM.$$

T^*M is a $2n$-dimensional manifold like the tangent bundle TM. The cotangent bundle plays an important role in Hamiltonian mechanics. If the configuration space for a Hamiltonian system is Q, the momentum phase space is the cotangent bundle T^*Q and the Hamiltonian is a real valued function $H : T^*Q \to \mathbb{R}$.

A vector field was defined as a smooth assignment of a tangent vector to each point on the manifold. Similarly, one can define a *field* of covectors on a manifold. A *covector field* ω on M is a smooth assignment of a covector ω_p to each $p \in M$. That is, given a vector field X, the function

$$\langle \omega, X \rangle(p) := \langle \omega_p, X_p \rangle$$

is smooth. In local coordinates $\omega(\boldsymbol{x}) = \omega_i(\boldsymbol{x})dx^i$. Given a smooth map $F : M \to N$, the tangent map F_{*p} of F takes tangent vectors at $p \in M$ to tangent vectors at $F(p) \in N$. Similarly, the *cotangent map* of F is the map $F_p^* : T^*_{F(p)}N \to T^*_pM$ defined as

$$\langle F_p^* \alpha, X_p \rangle := \langle \alpha, F_{*p} X_p \rangle$$

for all $\alpha \in T^*_{F(p)}N$ and $X_p \in T_pM$. Thus, F_p^* takes covectors at $F(p) \in N$ to covectors at $p \in M$. The local representation of a cotangent map is the *transpose* of the Jacobian matrix of F.

2.2 Lie Groups and Related Topics

Lie groups are of great importance in modern theoretical physics and dynamical systems. They form a very important class of differentiable manifolds. The configuration space of a given mechanical system is often a Lie group. For example, the configuration space of a free rigid body is the Lie group $SE(3)$, the special Euclidean group. This section discusses some important concepts in the study of Lie groups that will be used throughout the dissertation. The reader is referred to Warner [75] for a more detailed discussion on Lie groups. We begin by defining a *group*.

Definition 2.2.1 (Group) *A group G is a set of elements together with a binary operation "$\circ$", called the group "multiplication" satisfying*

1. *Closure. For all $g_1,\ g_2 \in G$, $g_1 \circ g_2 \in G$.*
2. *Associativity. $(g_1 \circ g_2) \circ g_3 = g_1 \circ (g_2 \circ g_3)$ for all $g_1,\ g_2$ and g_3 in G.*

3. *Existence of an identity. For all $g \in G$, there exists an identity element, $e \in G$, such that $e \circ g = g \circ e = g$.*

4. *Existence of an inverse. For all $g \in G$, there exists an inverse, $g^{-1} \in G$, such that $g^{-1} \circ g = g \circ g^{-1} = e$.*

For simplicity of notation, we refer to $g_1 \circ g_2$ as $g_1 g_2$. A group is *abelian* if the group multiplication commutes, that is, if $g_1 g_2 = g_2 g_1$ for all $g_1,\ g_2 \in G$.

Definition 2.2.2 (Lie Group) *A Lie group G is a set that is*

1. *A group in the usual algebraic sense.*

2. *A differential manifold such that the group multiplication and inversion are smooth operations.*

That is, the maps

$$\mu\ :\ G \times G \to G \qquad \text{and} \qquad \nu\ :\ G \to G$$
$$(g_1, g_2) \mapsto g_1 g_2 \qquad\qquad g \mapsto g^{-1}$$

are both smooth. In what follows, G will always denote a Lie group. A Lie group always has two families of diffeomorphisms[1], the left and right translations. The *left* and *right* translations of G by the element $g \in G$ are diffeomorphisms defined by

$$L_g\ :\ G \times G \to G \qquad \text{and} \qquad R_g\ :\ G \to G$$
$$h \mapsto gh \qquad\qquad h \mapsto hg$$

for every $h \in G$. If G is abelian, $L_g = R_g$.

Examples of Lie Groups

[1]Given two differentiable manifolds M and N, a bijective (one-to-one and onto) map $F : M \to N$ is called a diffeomorphism if both F and F^{-1} are smooth.

- The Euclidean space $\mathbb{R}^n$ is an abelian Lie group with addition as the group multiplication.
- The unit circle $S^1 \cong \{e^{i\theta} \mid 0 \leq \theta < 2\pi\}$ is a real, 1-dimensional Lie group with the group multiplication defined as complex multiplication.
- The general linear group $GL(n, \mathbb{R})$ is the set of all real, invertible $n \times n$ matrices,

  $$GL(n, \mathbb{R}) = \{\boldsymbol{A} \in \mathcal{M}(n, \mathbb{R}) \mid \mathrm{Det}(\boldsymbol{A}) \neq 0\},$$

  where $\mathcal{M}(n, \mathbb{R})$ denotes the set of all real, $n \times n$ matrices. $GL(n, \mathbb{R})$ is an n^2-dimensional Lie group with the group multiplication being matrix multiplication. The left and right translations are respectively left and right multiplication.
- The special orthogonal group is a subgroup of the general linear group defined as

  $$SO(n) = \{\boldsymbol{A} \in GL(n, \mathbb{R}) \mid \boldsymbol{A}\boldsymbol{A}^T = \mathbb{I},\ \mathrm{Det}(\boldsymbol{A}) \ = +1\},$$

  where $\mathbb{I}$ is the identity matrix. $SO(n)$ is a Lie group of dimension $\frac{n(n-1)}{2}$. A familiar example is $SO(3)$, the rotation group on $\mathbb{R}^3$, that represents the configuration space of a rigid body in rotational motion. The familiar Euler angles are one choice of coordinates for $SO(3)$. The special orthogonal group $SO(2)$ represents rotations in the plane. Any element $g \in SO(2)$ is given by

  $$g = \begin{pmatrix} \cos\theta & -\sin\theta \\ \sin\theta & \cos\theta \end{pmatrix},$$

  where θ is the angular coordinate.
- The special Euclidean group $SE(3)$ is the group of rigid body transformations (rotation and translation) on $\mathbb{R}^3$ defined as the set of mappings $g : \mathbb{R}^3 \to \mathbb{R}^3$,

  $$g(\boldsymbol{x}) = \boldsymbol{\mathcal{R}}\boldsymbol{x} + \boldsymbol{p},$$

  where $\boldsymbol{\mathcal{R}} \in SO(3)$ is the rotation matrix and $\boldsymbol{p} \in \mathbb{R}^3$. Any element $g \in SE(3)$ is written as $(\boldsymbol{p}, \boldsymbol{\mathcal{R}}) \in SE(3)$. If $g = (\bar{\boldsymbol{p}}, \bar{\boldsymbol{\mathcal{R}}})$ and $h = (\boldsymbol{p}, \boldsymbol{\mathcal{R}})$, then the left translation is defined as

  $$L_g(h) = gh = (\bar{\boldsymbol{\mathcal{R}}}\boldsymbol{\mathcal{R}}, \bar{\boldsymbol{\mathcal{R}}}\boldsymbol{p} + \bar{\boldsymbol{p}}).$$

Any element of $SE(3)$ can be identified with a 4×4 matrix of the form

$$g = \begin{pmatrix} \boldsymbol{\mathcal{R}} & \boldsymbol{p} \\ 0 & 1 \end{pmatrix}.$$

$SE(3)$ is a Lie group of dimension 6. Likewise, any element of $SE(2)$, the group of rigid body transformations in $\mathbb{R}^2$, can be identified with a 3×3 matrix of the form

$$g = \begin{pmatrix} \cos\theta & -\sin\theta & p_1 \\ \sin\theta & \cos\theta & p_2 \\ 0 & 0 & 1 \end{pmatrix}.$$

2.2.1 Lie Algebra of a Lie Group

Let X be a vector field on the Lie group G. The vector field X is *left invariant* if

$$(T_h L_g) X(h) = X(gh) \quad \forall \quad g,\ h \in G, \tag{2.4}$$

where $T_h L_g$ is the tangent map of L_g at $h \in G$. A *right invariant* vector field is defined analogously. Figure 2.8 shows the commutative diagram for a left invariant vector field. Let $\mathfrak{X}_L(G)$ denote the

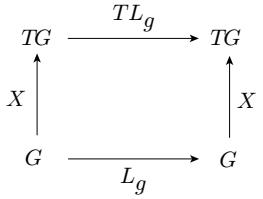

Figure 2.8: The commutative diagram for a left invariant vector field.

real vector space of all left invariant vector fields on G. If $X,\ Y$ are left invariant vector fields on G, that is, $X,\ Y \in \mathfrak{X}_L(G)$, then it follows that $[X,\ Y]$ is also left invariant, that is, $[X,\ Y] \in \mathfrak{X}_L(G)$ [36]. Thus, $\mathfrak{X}_L(G)$ is a Lie subalgebra of the Lie algebra $\mathfrak{X}(G)$ of all vector fields on G. $\mathfrak{X}_L(G)$ is called the *Lie algebra of* G.

Given a tangent vector ξ at the identity $e \in G$, one can left (resp. right) translate ξ to each point of G using the tangent map for L_g (resp. R_g). This yields a vector field X^ξ on G,

$$X^\xi(g) := (T_e L_g)\xi \quad (\text{ resp. } X^\xi(g) := (T_e R_g)\xi\ ). \tag{2.5}$$

If $(\xi_1,\ \xi_2, \ldots,\ \xi_n)$ is a basis for the tangent space at identity, T_eG, then we may left translate this basis to give n linearly independent vector fields,

$$(T_e L_g)\xi_1,\ (T_e L_g)\xi_2, \ldots,\ (T_e L_g)\xi_n,$$

on all of G. Recall that a vector field X on G is left invariant if it is invariant under all left translations. Indeed, (2.5) defines the unique left invariant vector field generated by $\xi = X(e)$. The tangent space at the identity T_eG is isomorphic[2] to $\mathfrak{X}_L(G)$ and dim T_eG = dim $\mathfrak{X}_L(G)$ [36]. If G is finite dimensional, so is $\mathfrak{X}_L(G)$. It is now possible to regard T_eG as the Lie algebra of G. The *Lie bracket* in T_eG is defined as

$$[\xi, \eta] := [X^\xi, X^\eta](e), \tag{2.6}$$

where $\xi,\ \eta \in T_eG$. The vector space T_eG with the above Lie algebra structure (2.6) constitutes the Lie algebra of G and is denoted by $\mathfrak{g}$. If $(e_1,\ e_2, \ldots,\ e_n)$ is a coordinate basis for $\mathfrak{g}$, then the *structure constants* C^a_{bc} of $\mathfrak{g}$ are defined as

$$[e_b, e_c] := C^a_{bc} e_a. \tag{2.7}$$

Any element $\xi \in \mathfrak{g}$ can be expressed in the chosen basis as $\xi = \xi^a e_a$.

Example of Lie Algebras

- Lie Algebra of the additive group $\mathbb{R}^n$: The identity element is $e = \mathbf{0}$ and the tangent space at identity is $T_e\mathbb{R}^n \cong \mathbb{R}^n$. For any $\xi \in T_e\mathbb{R}^n$, the left invariant vector field is the constant vector field, $X^\xi(\boldsymbol{x}) = \xi$, for all $\boldsymbol{x} \in \mathbb{R}^n$. Thus, the Lie algebra of $\mathbb{R}^n$ is $\mathbb{R}^n$ itself. Since the elements of the Lie algebra are constant vector fields, the Lie bracket is the trivial bracket, $[\xi, \eta] = 0$, for all $\xi,\ \eta \in \mathbb{R}^n$.

[2]Given two topological spaces X and $\hat{X}$, an isomorphism is a bijective map between the spaces that preserves the structure. X and $\hat{X}$ are said to be isomorphic and denoted as $X \cong \hat{X}$.

- The Lie algebra $\mathfrak{gl}(n,\mathbb{R})$ of the general linear group $GL(n,\mathbb{R})$ is the set of all $n \times n$, real matrices with the Lie bracket being matrix commutation, $[\boldsymbol{A},\boldsymbol{B}] = \boldsymbol{AB} - \boldsymbol{BA}$, for all $\boldsymbol{A},\ \boldsymbol{B} \in \mathfrak{gl}(n,\mathbb{R})$.

- The Lie algebra $\mathfrak{so}(3)$ of the special orthogonal group $SO(3)$ can be identified with the set of 3×3 skew symmetric matrices of the form

$$\hat{\boldsymbol{\omega}} = \begin{pmatrix} 0 & -\omega_3 & \omega_2 \\ \omega_3 & 0 & -\omega_1 \\ -\omega_2 & \omega_1 & 0 \end{pmatrix},$$

  where $\boldsymbol{\omega} = [\omega_1, \omega_2, \omega_3]^T \in \mathbb{R}^3$. The Lie bracket is defined as matrix commutation,

$$[\hat{\boldsymbol{\omega}}_1, \hat{\boldsymbol{\omega}}_2] = \hat{\boldsymbol{\omega}}_1\hat{\boldsymbol{\omega}}_2 - \hat{\boldsymbol{\omega}}_2\hat{\boldsymbol{\omega}}_1.$$

  The Lie algebra $\mathfrak{so}(2)$ of $SO(2)$ is given by the set of 2×2 skew symmetric matrices of the form

$$\hat{\boldsymbol{\omega}} = \begin{pmatrix} 0 & -\omega \\ \omega & 0 \end{pmatrix},$$

  where $\omega \in \mathbb{R}$ can be thought of as the angular speed.

- The Lie algebra $\mathfrak{se}(3)$ of the special Euclidean group $SE(3)$ can be identified with the set of all 4×4 matrices of the form

$$\hat{\xi} = \begin{pmatrix} \hat{\boldsymbol{\omega}} & \boldsymbol{v} \\ 0 & 0 \end{pmatrix},$$

  where $\boldsymbol{\omega},\ \boldsymbol{v} \in \mathbb{R}^3$. The Lie bracket is given by

$$[\hat{\xi}_1, \hat{\xi}_2] = \hat{\xi}_1\hat{\xi}_2 - \hat{\xi}_2\hat{\xi}_1.$$

  Similarly, the Lie algebra $\mathfrak{se}(2)$ of $SE(2)$ is represented by the set of 3×3 matrices of the form

$$\hat{\xi} = \begin{pmatrix} 0 & -\omega & v_1 \\ \omega & 0 & v_2 \\ 0 & 0 & 0 \end{pmatrix}.$$

2.2.2 Actions of Lie Groups

In almost all applications of group theory in theoretical mechanics, the groups arise as groups of transformations of some other space. We have already seen how Lie groups act on themselves through the left and right translations. More generally, let us consider the action of a Lie group G on a smooth manifold M.

A *left action* of G on M is a smooth map $\Phi : G \times M \to M$ such that,

$$\Phi(e, x) = x \quad \text{and} \quad \Phi(g, \Phi(h, x)) = \Phi(gh, x) \ \ \forall \ \ x \in M \ \ \text{and} \ \ g, h \in G.$$

The *right action* is defined in a similar manner. The action can be regarded as a map $\Phi_g : M \to M$ defined as $\Phi_g(x) := \Phi(g, x)$, $g \in G$ and $x \in M$. For convenience, $\Phi_g(x)$ is simply denoted as gx. The action is *free* if for all $x \in M$, $\{g \mid \Phi(g, x) = x\} = \{e\}$. Thus in a free action every point is moved away from itself by every element of G except e. Left and right translations are examples of free action. The action is *proper* is the mapping $\tilde{\Phi} : G \times M \to M \times M$ defined by,

$$\tilde{\Phi}(g, x) = (x, \Phi(g, x)),$$

is proper[3]. The *orbit* of x is the set of all points in M that can be reached from $x \in M$ through Φ,

$$\text{Orb}(x) = \{y \in M \mid y = \Phi(g, x)\}.$$

The orbits through any pair of points are either equal or disjoint. Thus, we have an equivalence relation on M in which two points are defined to be equivalent if and only if they lie on the same orbit. The set of equivalence classes is called the *orbit space* of the action on M and is denoted by M/G. This space carries a natural quotient topology. For more details about quotient spaces, see [49]. M/G is a smooth manifold if the action $\Phi : G \times M \to M$ is free and proper.

Examples of Group Actions

- The left and right translations, L_g and R_g respectively, are free actions of G on itself.

[3]In finite dimensions, this means that if $K \subset M \times M$ is compact, then $\tilde{\Phi}^{-1}(K)$ is compact.

- The *adjoint action of G on G* is the map $I_g : G \to G$ defined by $I_g(h) = R_{g^{-1}}(L_g\ h) = R_{g^{-1}}(gh) = ghg^{-1}$. I_g is an example of a left action. If G is abelian, I_g reduces to the identity on G. In this way, I_g reflects the non-commutativity of left and right actions.

- The *adjoint action of G on $\mathfrak{g}$*, $\mathrm{Ad} : G \times \mathfrak{g} \to \mathfrak{g}$ is obtained by differentiating I_g at e,

$$\mathrm{Ad}_g(\xi) = (T_e I_g)\xi = T_g R_{g^{-1}}(T_e L_g)\xi.$$

- If $M = G \times S$, then the left action of G on M is given by

$$\Phi_g(h, x) = (gh, x)$$

  for all $h \in G$ and $x \in S$.

- The *lifted action* is defined as the map,

$$T\Phi_g : TQ \to TQ \quad (q, \dot{q}) \mapsto (\Phi_g(q), T_q\Phi_g(\dot{q}))$$

  for all $g \in G$ and $\dot{q} \in T_qQ$, where $T_q\Phi_g$ is the tangent map of Φ_g evaluated at $q \in Q$.

2.2.3 The Exponential Map

A homomorphism of groups is a function $f : G \to H$ that preserves group multiplication, that is, $f(g_1g_2) = f(g_1)f(g_2)$ for all $g_1,\ g_2 \in G$. As an example, the usual exponential function $f(t) = e^t$ defines a homomorphism from the additive group of real numbers to the multiplicative group of positive real numbers since $e^{(s+t)} = e^s e^t$.

A *one-parameter subgroup* of G is a differentiable homomorphism

$$\phi : \mathbb{R} \to G \qquad t \mapsto \phi(t)$$

of the additive group of real numbers into G. Thus,

$$\phi(s + t) = \phi(s)\phi(t). \tag{2.8}$$

Differentiating both sides of (2.8) with respect to s and setting $s = 0$ gives

$$\phi'(t) = \phi(t)\phi'(0). \tag{2.9}$$

From (2.8), we get $\phi(0) = e \in G$ for any homomorphism and therefore $\phi'(0) = \xi \in T_eG$ (or $\mathfrak{g}$). Recall that the left translation of ξ yields a vector field $X^\xi(g) = (T_eL_g)\xi$. Thus, (2.9) implies that

$$\phi'(t) = X^\xi(\phi(t))$$

and therefore the one-parameter subgroup $\phi(t)$ is an integral curve of the vector field X^ξ. $\phi(t)$ is denoted as $\phi_\xi(t)$ in order to emphasize its relation to X^ξ.

The *exponential map* is the map $\exp : \mathfrak{g} \to G$, defined as

$$\exp(\xi) = \phi_\xi(1).$$

We claim that $\exp(t\xi) = \phi_\xi(t)$ (see [46] for a proof). Thus, the exponential map takes $t\xi \in \mathfrak{g},\ t \in \mathbb{R}$ into the one-parameter subgroup $\phi(t)$ of G, which is tangent to ξ at e.

As seen above, the exponential map generates a one-parameter subgroup of G. If G acts on M, then the action of each one-parameter subgroup of G produces a family of curves that fills M and hence a vector field on M that is tangent to this family everywhere. For every $\xi \in \mathfrak{g}$, the exponential map $\exp(t\xi)$ produces a flow,

$$\Phi^\xi : \mathbb{R} \times M \to M \qquad (t, x) \mapsto \Phi(\exp(t\xi), x).$$

The induced vector field given by

$$\xi_M(x) := \frac{d}{dt}\Phi(\exp(t\xi), x)|_{t=0}$$

is called the *infinitesimal generator* of the group action corresponding to ξ.

2.3 Principal Fiber Bundles

Fiber bundles provide the basic geometric setting for understanding many control problems. In this section, we introduce the basic ideas. Our intention is to provide the reader with an intuitive feel for

fiber bundles and related structures without worrying a lot about exact mathematical definitions. We will mainly be concerned with the study of principal fiber bundles. The reader is referred to Abraham, Marsden and Ratiu [2], Husemoller [33], Kobayashi and Nomizu [41], Schutz [63] and Steenrod [69] for a more comprehensive treatment of fiber bundles. For an introductory discussion on fiber bundles, the reader is referred to Bloch [9] and Isham [36]. We begin with the notion of a bundle.

A *bundle* is a triple (Q, π, M) where Q and M are topological spaces and $\pi : Q \to M$ is a continuous map. Q and M are called the *total space* and *base space* respectively. π is called the *projection map.* The inverse image $\pi^{-1}(x),\ x \in M$ is called the *fiber* over x. If for all x, $\pi^{-1}(x)$ is homeomorphic to a common space F, then F is called the *fiber* of the bundle and the bundle is called a *fiber bundle.* Often, the total space Q is referred to as the "bundle", though strictly, this refers to the triple (Q, π, M).

A simple example of a fiber bundle is the product bundle over M represented by the triple $(M \times F, \pi, M)$ (Fig 2.9). Here, the product space $M \times F$ is the total space, M is the base space and F is the fiber over M. A *vector bundle* is a bundle in which the fiber is a vector space. As an example, the product space $M \times \mathbb{R}^n$ is a vector bundle over the base space M. The tangent bundle TM and cotangent bundle T^*M are familiar examples of vector bundles.

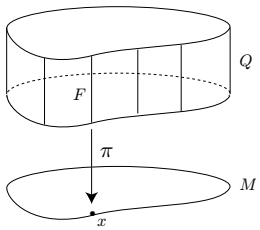

Figure 2.9: The product bundle is an example of a fiber bundle.

Many problems in mechanics involve action of a Lie group G on the configuration space Q. Lie groups describe position and orientation and as such arise naturally in the study of locomotion. A principal fiber bundle is a bundle in which the fiber is a Lie group. More precisely, suppose G has a

left action on Q. Furthermore, let the action be free and proper. We have seen that the action of G on Q induces a quotient space. Let $M = Q/G$ denote the quotient space of Q under the G-induced equivalence relation and let $\pi : Q \to M$ be the canonical projection.

A *principal fiber bundle* is a bundle $(Q,\ \pi,\ M = Q/G)$ such that Q is locally trivial or a product space, that is, given a point $x \in M$ and a neighborhood U of x, $\pi^{-1}(U)$ is homeomorphic to $G \times U$.

The fibers are orbits of the G-action on Q with each orbit being homeomorphic to G. G is called the *structure group* of the bundle. Often, the configuration space Q can be written globally as a product space $Q = G \times M$. A *trivial* principal fiber bundle is the product bundle $(G \times M, \pi, M)$ under the group action $\Phi_h(g, x) := (hg, x)$ for all $h \in G$ and $(g, x) \in G \times M$. As an example, the configuration space for the classic "inverted pendulum on a cart" system $Q = G \times M = \mathbb{R} \times S^1$ is a trivial principal fiber bundle. The trivial principal fiber bundle has two canonical projections, namely, $\pi : Q \to M :\ (g, x) \mapsto x$ and $\pi' : Q \to G :\ (g, x) \mapsto g$.

2.4 Stability Theory: Some Results

Consider a dynamical system whose dynamics evolve on an n-dimensional smooth manifold M according to the following differential equation:

$$\dot{x} = X(x),\ x \in M, \tag{2.10}$$

where X is a given vector field. A point $x_e \in M$ is an *equilibrium point* if $X(x_e) = 0$. An equilibrium point is stable if trajectories starting near x_e stay close to x_e for all times. More precisely,

Definition 2.4.1 (Stability, Asymptotic Stability and Instability) *An equilibrium point x_e of the dynamical system (2.10) is*

1. *stable if for every $\epsilon > 0$, there exists a δ such that any trajectory satisfying $||x(0) - x_e|| \leq \delta$ also satisfies $||x(t) - x_e|| \leq \epsilon$ for all $t \geq 0$, where $\|.\|$ is a norm on M.*

2. *asymptotically stable if it is stable and* $x(t) \to x_e$ *as* $t \to \infty$.

3. *unstable if it is not stable.*

The stability of an equilibrium can be studied using Lyapunov's *indirect* and *direct* methods. The well-known indirect method involves examining the eigenvalues or the spectrum of the linearization of X at x_e.

Theorem 2.4.2 (Lyanponov's Indirect Method) *An equilibrium* x_e *of the dynamical system (2.10) is*

1. *asymptotically stable if all the eigenvalues lie in the open left half of the complex plane.*

2. *unstable if any of the eigenvalues lies in the open right half of the complex plane.*

For a proof of the above theorem, see [40]. In many cases, linear analysis is not sufficient to prove nonlinear stability. For example, all the eigenvalues of a canonical Hamiltonian system are distributed symmetrically in the complex plane under reflection about the real and the imaginary axis. Thus, any eigenvalue is either located at the origin or is a member of a real conjugate pair, a purely imaginary conjugate pair, or a symmetric quartet of eigenvalues. Therefore, linear analysis can predict instability but cannot prove stability for Hamiltonian systems.

Lyapunov's direct method involves finding an energy-like function V called the *Lyapunov function*, that is positive definite and whose time rate is negative semidefinite.

Theorem 2.4.3 (Lyapunov's Direct Method) *Suppose there exists a function* $V(x)$ *that has a strict minimum value, say zero, in a neighborhood* D *of* x_e,

$$V(x_e) = 0 \quad \textit{and} \quad V(x) > 0 \ \forall \ x \in D - \{x_e\}.$$

The equilibrium is stable if

$$\dot{V}(x) \leq 0 \ \forall \ x \in D.$$

The equilibrium is asymptotically stable if

$$\dot{V}(x) < 0 \ \forall \ x \in D - \{x_e\}.$$

See [40] for a proof. A big hurdle in using the above theorem is construction of V. There is no general systematic procedure to find V. If the system is mechanical, then energy of the system is a good candidate. When $\dot{V}$ is negative semidefinite, *LaSalle's invariance* principle can be used to prove asymptotic stability. A set Ω is *invariant* with respect to the dynamics (2.10) if $x(0) \in \Omega \Rightarrow x(t) \in \Omega \ \forall \ t \in \mathbb{R}$. The set Ω is *positively invariant* if $x(0) \in \Omega \Rightarrow x(t) \in \Omega \ \forall \ t \geq 0$.

Theorem 2.4.4 (LaSalle's Invariance Principle) *Let $\Omega \subset D$ be a compact set that is positively invariant with respect to the dynamics (2.10). Let $E = \{x \in \Omega \mid \dot{V}(x) = 0\}$ and let $\mathcal{M}$ be the largest invariant set contained in E. Then all trajectories starting in Ω approach $\mathcal{M}$ as $t \to \infty$.*

Corollary 2.4.5 *If $\mathcal{M} = \{x_e\}$ then the equilibrium is asymptotically stable.*

For a proof of LaSalle's invariance principle, see [40].

The basic goals of control systems fall in two parts. One goal is to drive the system from one point in the state space to another point and the other is to stabilize the system about a given equilibrium. In this dissertation, we will be mainly concerned with the second objective, that is, stabilization of equilibria.

Chapter 3

Reduction of Lagrangian Systems with Symmetry

This chapter gives a quick introduction to reduction of Lagrangian systems with Lie group symmetries. By symmetry, we mean the invariance of a certain quantity, the Lagrangian in our case, under the action of a Lie group. The discussion in this chapter is adapted from Bloch [9], Ostrowskii [56], Marsden and Ratiu [46] and Marsden and Scheurle [47, 48]. Ideas presented here will be applied for developing energy shaping control laws for vehicle systems with internal moving mass actuators in Chapter 6.

Reduction theory for mechanical systems with symmetry has its roots in the classical works of Euler, Lagrange, Routh, Poincaré and others. In this dissertation, we shall be concerned with rotational and translational symmetries. The reduction process involves removing the symmetries and reducing the dynamics to a lower dimensional space. This leads to a simplified set of dynamic equations. Reduction theory dates back to Routh who studied reduction for Lagrangian systems with abelian group symmetry. Besides Routh reduction, another early and fundamental reduction is that of Euler-Poincaré reduction that occurs when the configuration space Q is a Lie group G. The Euler-Poincaré reduction was originally developed by Lagrange [42] and Poincaré [59]. The

reader is referred to [46] for a detailed exposition of Lagrangian reduction for both the Routh and Euler-Poincaré reduction. Marsden and Scheurle [47, 48] gave an intrinsic formulation of Routh reduction for the non-abelian case as well as the general formulation of Euler-Poincaré equations in terms of variational principles. They presented the general form for the reduced Euler-Lagrange equations, referred as Lagrange-Poincaré equations. The Lagrange-Poincaré equations reduce to Euler-Poincaré equations when $Q = G$ and to the classical Routhian reduction when G is abelian.

In Section § 3.1, we present the Euler-Lagrange equations for an unconstrained Lagrangian systems. For a mechanical system, the Euler-Lagrange equations can be presented in a matrix form. The exact notion of symmetry for a Lagrangian system is presented in Section § 3.2. The classic inverted pendulum on a cart system is used to illustrate the idea of a G-invariant Lagrangian. The reduction process involves identifying symmetries in a system and decomposing the tangent space according to the symmetries. A "connection" provides a way to decompose the tangent space into complementary spaces and plays a central role in the reduction process. Section § 3.3 introduces the notion of a connection on a principal fiber bundle. For mechanical systems with symmetry, the kinetic energy metric can be used to define a connection. Section § 3.4 defines the mechanical connection and related concepts. Finally, in Section § 3.5 we discuss the general structure of the reduced Euler-Lagrange equations.

3.1 Review of Lagrangian Mechanics

In this section, we briefly review Lagrangian mechanics. Suppose that we have a configuration manifold Q of dimension n and a tangent bundle TQ. Let the coordinates of any point $q \in Q$ be $(q^1,\ q^2, \ldots,\ q^i, \ldots,\ q^n)$. The *Lagrangian* is a real valued function $L(q^i, \dot{q}^i) : TQ \to \mathbb{R}$. Any admissible trajectory $(q^1(t),\ q^2(t), \ldots,\ q^i(t), \ldots,\ q^n(t))$ satisfies *Hamilton's principle of least action*,

$$\delta \int_a^b L(q^i, \dot{q}^i)dt = 0, \tag{3.1}$$

where δ is the variation of the path with end points a and b. The boundary conditions are assumed

fixed, $\delta q^i(a) = \delta q^i(b) = 0$. Integrating (3.1) by parts and using the boundary conditions, we get

$$\int \left[\frac{\partial L}{\partial q^i} - \frac{d}{dt}\frac{\partial L}{\partial \dot{q}^i} \right] \delta q^i dt = 0. \tag{3.2}$$

Since (3.2) has to hold for all variations, it follows

$$\frac{d}{dt}\frac{\partial L}{\partial \dot{q}^i} - \frac{\partial L}{\partial q^i} = 0 \quad i = 1,\ 2, \ldots,\ n. \tag{3.3}$$

Equations (3.3) are called the *Euler-Lagrange* equations. Let $\mathcal{E}$ represent the *Euler-Lagrange operator* defined as follows: given a Lagrangian L and a generalized coordinate q^i,

$$\mathcal{E}_{q^i}(L) = \frac{d}{dt}\frac{\partial L}{\partial \dot{q}^i} - \frac{\partial L}{\partial q^i}\ .$$

A *Riemannian metric* on a differentiable manifold M is a positive definite inner product $\ll .\ ,\ . \gg$ on each tangent space T_pM defined as

$$\ll \boldsymbol{v}, \boldsymbol{w} \gg\ := g(\boldsymbol{v}, \boldsymbol{w}) = g_{ij} v^i w^j, \quad g_{ij} = g_{ji},$$

where $\boldsymbol{v}, \boldsymbol{w} \in T_pM$ and g_{ij} is the ij^{th} component of the metric tensor g. The tensor g is a covariant tensor of rank 2. A manifold with a Riemannian metric is called a *Riemannian manifold*. The Riemannian metric $\ll .\ ,\ . \gg$ is often denoted by $g(.\ ,\ .)$. For mechanical systems, g represents the kinetic energy metric.

A Lagrangian is called *simple* if it has the following form:

$$L = \text{kinetic energy} - \text{potential energy} = \frac{1}{2} g_{ij}(\boldsymbol{q}) \dot{q}^i \dot{q}^j - V(\boldsymbol{q}).$$

where $\boldsymbol{q} = [q^1,\ q^2, \ldots,\ q^n]^T$ is the state vector. The Euler-Lagrange equations for a simple Lagrangian are

$$\mathcal{E}_{\boldsymbol{q}}(L) = \boldsymbol{M}(\boldsymbol{q})\ddot{\boldsymbol{q}} + \boldsymbol{C}(\boldsymbol{q}, \dot{\boldsymbol{q}})\dot{\boldsymbol{q}} + \frac{\partial V}{\partial \boldsymbol{q}} = 0, \tag{3.4}$$

where $\boldsymbol{M}$, the *mass matrix* is the matrix representation of the Riemannian metric g, $\boldsymbol{C}$ is the "Coriolis and centripetal" matrix defined as

$$C_{ij}(\boldsymbol{q}, \dot{\boldsymbol{q}}) = \Gamma_{ijk}\dot{q}^k = \frac{1}{2}\left(\frac{\partial M_{ij}}{\partial q^k} + \frac{\partial M_{ik}}{\partial q^j} - \frac{\partial M_{kj}}{\partial q^i} \right) \dot{q}^k,$$

where M_{ij} is the ij^{th} component of the mass matrix $\boldsymbol{M}$ and Γ_{ijk} is the "Christoffel symbol of the first kind" associated with $\boldsymbol{M}$. It can be shown that $\dot{\boldsymbol{M}} - 2\boldsymbol{C}$ is skew-symmetric [50]. In the presence of external forces, the Euler-Lagrange equations take the form

$$\mathcal{E}_{\boldsymbol{q}}(L) = \boldsymbol{F}(\boldsymbol{q}, \dot{\boldsymbol{q}}) + \boldsymbol{u},$$

where $\boldsymbol{F} : TQ \to \mathbb{R}^n$ is the external force and $\boldsymbol{u} : U \to \mathbb{R}^m,\ m \leq n$ is any applied control force, where U is some appropriate domain of $\boldsymbol{u}$. When $\boldsymbol{u} : TQ \to \mathbb{R}^m$, the system is a *closed-loop* Lagrangian system. When $\boldsymbol{u} : t \in \mathbb{R} \to \mathbb{R}^m$, the system is an *open-loop* Lagrangian system. When $m < n$, the system is *underactuated*. In coordinate form,

$$\begin{aligned} \frac{d}{dt}\frac{\partial L}{\partial \dot{q}^i} - \frac{\partial L}{\partial q^i} &= F_i \quad i = 1,\ 2, \ldots,\ n - m \\ \frac{d}{dt}\frac{\partial L}{\partial \dot{q}^j} - \frac{\partial L}{\partial q^j} &= F_j + u_j \quad j = n - m + 1,\ n - m + 2, \ldots,\ n. \end{aligned} \tag{3.5}$$

For closed-loop and simple Lagrangian systems, the Euler-Lagrange equations with external forces take the form,

$$\boldsymbol{M}(\boldsymbol{q})\ddot{\boldsymbol{q}} + \boldsymbol{C}(\boldsymbol{q}, \dot{\boldsymbol{q}})\dot{\boldsymbol{q}} + \frac{\partial V}{\partial \boldsymbol{q}} = \boldsymbol{F}(\boldsymbol{q}, \dot{\boldsymbol{q}}) + \boldsymbol{G}\,\boldsymbol{u}(\boldsymbol{q}, \dot{\boldsymbol{q}}), \tag{3.6}$$

where $\boldsymbol{G}$ is assumed to be a constant matrix of rank m. The external forces may include *dissipative* and *gyroscopic* forces. We discuss the nature of dissipative and gyroscopic forces in Chapter 4.

3.2 Symmetry and Invariances

Consider a mechanical system with an n-dimensional configuration manifold Q acted upon by a Lie group G. When we talk about a mechanical system with a Lie group symmetry, we imply invariance of the Lagrangian L under the action of G. Without any loss of generality, we will only consider invariance under the left action of G. For unconstrained and holonomically constrained systems, the invariance of L is a sufficient condition for the existence of a conservation law. This leads to reduced-dimensional dynamics. However, in the presence of nonholonomic constraints, the conservation laws may no longer hold. In order to appropriately represent the nonholonomic constraints [9],

one needs to consider the invariance of vector fields and one-forms. In this dissertation, we only consider systems with holonomic constraints.

Definition 3.2.1 (G-Invariant Lagrangian) *A Lagrangian $L : TQ \to \mathbb{R}$ is G-invariant if*

$$L(\Phi_g(q), T_q\Phi_g(\boldsymbol{v}_q)) = L(q, \boldsymbol{v}_q)$$

for all $g \in G$, $\boldsymbol{v}_q \in T_qQ$.

3.2.1 Example: Inverted Pendulum on a Cart System

The inverted pendulum on a cart system is shown in Fig. 3.1. The configuration space $Q = G \times M = \mathbb{R} \times S^1$ is a trivial principal fiber bundle. The coordinates of any point $q \in Q$ are $(s, \phi) \in \mathbb{R} \times S^1$, where s is the cart displacement and ϕ is the angular position of the pendulum from the vertical. The tangent vector $\boldsymbol{v}_q \in T_qQ$ is the velocity vector $(\dot{s}, \dot{\phi}) \in \mathbb{R}^2$.

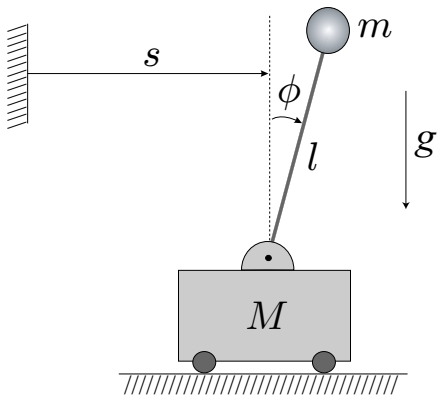

Figure 3.1: Inverted pendulum on a cart system

The action of $G = \mathbb{R}$ on Q represents translation along the cart direction. In particular,

$$\Phi_a(s, \phi) = (s + a, \phi)$$

for all $a \in \mathbb{R}$. The tangent map $T_q\Phi_a$ is simply the identity matrix

$$T_q\Phi_a = \begin{pmatrix} 1 & 0 \\ 0 & 1 \end{pmatrix}.$$

Thus $T_q\Phi_a(\dot{s}, \dot{\phi}) = (\dot{s}, \dot{\phi})$. The Lagrangian L for the cart-pendulum system is

$$\begin{aligned} L(s, \phi, \dot{s}, \dot{\phi}) &= \text{kinetic energy} - \text{potential energy} \\ &= \frac{1}{2} \begin{pmatrix} \dot{s} \\ \dot{\phi} \end{pmatrix}^T \begin{pmatrix} M+m & ml\cos\phi \\ ml\cos\phi & ml^2 \end{pmatrix} \begin{pmatrix} \dot{s} \\ \dot{\phi} \end{pmatrix} - mgl\cos\phi, \end{aligned}$$

where M is the cart mass, m is the pendulum mass, l is the pendulum length and g is the gravitational constant. We have

$$L(\Phi_a(s, \phi), T_q\Phi_a(\dot{s}, \dot{\phi})) = L(s + a, \phi, \dot{s}, \dot{\phi}) = L(s, \phi, \dot{s}, \dot{\phi})$$

as L does not depend on the cart position s, which is called a cyclic coordinate. Then, the corresponding conjugate momentum

$$p_s = \frac{\partial L}{\partial \dot{s}}$$

is a conserved quantity.

3.3 Connections on Principal Fiber Bundles

Symmetries in a Lagrangian system lead to a simplified set of dynamic equations. For unconstrained Lagrangian systems, the process of "reduction" involves identifying Lie group symmetries and splitting the dynamics according to these symmetries. The configuration of vehicle systems with internal actuators can be written as $q = (g, x) \in Q = G \times M$, where $g \in G$, the *group* variables, describe the position and orientation of the vehicle and $x \in M$, the *shape* variables, describe the internal degrees of freedom. An example is a satellite with internal rotors. Many problems in locomotion involve manipulating motion in the group directions using controls in the shape directions. For example, internal rotors can be used to stabilize the attitude of the satellite. We

therefore seek a splitting of the dynamics that highlights the structure of the shape space. The system is then reduced to the lower dimensional shape space in which the group directions have been "modded" out. One begins by defining two subspaces: one that contains the group directions, the *vertical* subspace, and one that appropriately reflects the interaction between group and shape motions, the *horizontal* subspace. A *connection* is a mathematical construction that allows us to define the horizontal subspace given the vertical subspace.

The setting is a principal fiber bundle (Q, π, M), where $M = Q/G$ is the shape space and $\pi : Q \to M$ is the projection map. The fibers in a principal fiber bundle are the group orbits. There is a natural way of defining the *vertical* space as the set of all vectors tangent to the group orbits.

Definition 3.3.1 *The vertical space is a subspace of T_qQ defined as*

$$V_qQ := \{\boldsymbol{v}_q \in T_qQ \mid \boldsymbol{v}_q \in \ker\, T_q\pi\},$$

where $T_q\pi$ is the tangent map induced by π. Vectors in V_qQ are said to be vertical.

For a trivial principal fiber bundle $Q = G \times M$, the vertical vectors are of the form $(\boldsymbol{v}_g, 0)$, for $\boldsymbol{v}_g \in T_{\pi'(q)}G$ where $\pi' : Q \to G$.

Example

For the cart-pendulum system studied in § 3.2.1, $Q = G \times M = \mathbb{R} \times S^1$. The projection maps, π and π', are

$$\pi(s, \phi) = \phi, \qquad \pi'(s, \phi) = s.$$

The tangent map $T_q\pi$ is

$$T_q\pi = [0 \;\; 1] \;\; \text{so that} \;\; T_q\pi(\boldsymbol{v}_q) = \phi.$$

Clearly, the kernel of $T_q\pi$ is the set of all vectors of the form $(a, 0)$. For the cart-pendulum system, the group orbits represent translations along the cart directions. The vertical vectors, $(a, 0)$, are indeed tangent to group orbits. ■

We need a way to construct vectors that point away from the fibers. That is, elements in T_qQ that will complement the vertical vectors. This complementary space is called the *horizontal* space. For a general principal fiber bundle there is no canonical way to define the horizontal space. Depending upon the problem one may have a different choice of horizontal space. For a trivial principal bundle, we can define the horizontal space as the set of vectors tangent to the shape space M, that is, vectors of the form $(0, \boldsymbol{v}_x)$ where $\boldsymbol{v}_x \in T_{\pi(q)}M$. For mechanical systems, the horizontal vectors can be chosen so that they are metric orthogonal to the vertical vectors. As we shall see in § 3.4, this is exactly how the horizontal space is defined for the cart-pendulum system. However, for systems with constraints, the above choices are not necessarily the most appropriate ones. A *connection* provides a way to define the horizontal space that appropriately reflects the interaction between group and shape motions.

Definition 3.3.2 (Connection [41]) *A connection is an assignment of a horizontal subspace H_qQ of T_qQ, for each point $q \in Q$ such that*

1. $T_qQ = V_qQ \oplus H_qQ$,
2. $T_q\Phi_g(H_qQ) = H_{gq}Q$ *for all* $g \in G$,
3. H_qQ *depends smoothly on* q,

Property (1) implies that any tangent vector $\boldsymbol{v}_q \in T_qQ$ can be uniquely decomposed into a sum of vertical and horizontal components lying in V_qQ and H_qQ. We will denote these components by Ver $\boldsymbol{v}_q$ and Hor $\boldsymbol{v}_q$ respectively. That is,

$$\boldsymbol{v}_q = \text{Ver } \boldsymbol{v}_q + \text{Hor } \boldsymbol{v}_q.$$

Property (2) implies that H_qQ is invariant under the left action of G on Q. Note that $\Phi_g(q) := gq$ denotes the left action of G on Q.

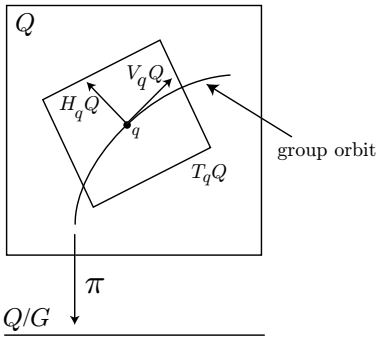

Figure 3.2: Decomposition of T_qQ into vertical and horizontal subspaces.

An alternate way of defining the connection is by introducing a *connection one-form*. Recall that the exponential map $\exp : \mathfrak{g} \to G,\ \xi \mapsto \exp(t\xi)$ induces a vector field ξ_Q defined as

$$\xi_Q(q) := \frac{d}{dt}\Phi(\exp(t\xi), q)|_{t=0}.$$

Thus, given any vertical vector $\boldsymbol{w}_q \in V_qQ$, there is a unique Lie algebra element, $\xi \in \mathfrak{g}$, such that ξ generates $\boldsymbol{w}_q$. That is,

$$\boldsymbol{w}_q = \xi_Q(q).$$

Definition 3.3.3 (Principal Connection One-Form) *A principal connection one-form $\mathcal{A}$ is a Lie algebra valued one-form on Q that satisfies the following:*

1. $\mathcal{A}(\xi_Q(q)) = \xi$ *for all* $\xi \in \mathfrak{g}$ *and* $q \in Q$,
2. $\mathcal{A}(T_q\Phi_q(\boldsymbol{v}_q)) = \mathrm{Ad}_q\ \mathcal{A}(\boldsymbol{v}_q)$ *for all* $\boldsymbol{v}_q \in T_qQ$ *and* $g \in G$, *where* Ad *denotes the adjoint action of* G *on* $\mathfrak{g}$, *and*
3. $\boldsymbol{h}_q \in H_qQ$ *if and only if* $\mathcal{A}(\boldsymbol{h}_q) = 0$.

Thus, $\mathcal{A}$ takes any vector $\boldsymbol{v}_q \in T_qQ$ and gives the Lie algebra element ξ corresponding to the vertical component Ver $\boldsymbol{v}_q$. That is, $\mathcal{A}(\boldsymbol{v}_q) = \xi$. As before, we have the following decomposition,

$\boldsymbol{v}_q = \text{Ver } \boldsymbol{v}_q + \text{Hor } \boldsymbol{v}_q$, where

$$\text{Ver } \boldsymbol{v}_q = \mathcal{A}(\boldsymbol{v}_q)_Q(q) \quad \text{and} \quad \text{Hor } \boldsymbol{v}_q = \boldsymbol{v}_q - \mathcal{A}(\boldsymbol{v}_q)_Q(q).$$

3.4 Momentum Map and Mechanical Connection

The reduction process for unconstrained systems with symmetries involves three primary elements: momentum map, locked inertia tensor and connection one-form. The momentum map represents in a geometric way conserved quantities associated with symmetries, such as linear and angular momentum that correspond to translational and rotational invariances.

Assume that we have a configuration manifold Q. Let G be a Lie group that acts on Q and let $\mathfrak{g}$ be the Lie algebra of G. Let $L : TQ \to \mathbb{R}$ be a G-invariant Lagrangian. Also, assume that we have a metric $\ll \ , \ \gg$ on Q that is invariant under the group action. The *momentum map* is a map $\mathbf{J} : TQ \to \mathfrak{g}^*$ defined as

$$\langle \mathbf{J}(\boldsymbol{v}_q), \xi \rangle \ := \ \ll \boldsymbol{v}_q, \xi_Q(q) \gg, \tag{3.7}$$

for all $\xi \in \mathfrak{g}$ and $\boldsymbol{v}_q \in T_qQ$. Note that $\mathfrak{g}^*$ denotes the dual of $\mathfrak{g}$ and $< \ . \ , \ . >$ denotes the natural pairing between $\mathfrak{g}$ and $\mathfrak{g}^*$. Noether's theorem is a conservation law for systems with Lie group symmetries.

Theorem 3.4.1 (Noether) *Given a G-invariant Lagrangian L, the momentum map $\mathbf{J}$ is conserved along trajectories of a system whose dynamics are given by the Euler-Lagrange equations.*

For a proof of Noether's theorem, see [9]. Mechanical systems possess a metric that corresponds to the kinetic energy of the system. The existence of such a metric allows one to define a connection one-form for systems with symmetries, called the *mechanical connection*. The notion of a mechanical connection was introduced by Smale [65]. The mechanical connection is related to the momentum map through the *locked inertia tensor*. The locked inertia tensor is a map $\boldsymbol{I}(q) : \mathfrak{g} \to \mathfrak{g}^*$ defined as

$$\langle \boldsymbol{I}(q) \ \xi, \eta \rangle \ := \ \ll \xi_Q(q), \eta_Q(q) \gg, \tag{3.8}$$

for all $\xi,\ \eta \in \mathfrak{g}$. The mechanical connection on the principal bundle $(Q, \pi, Q/G)$ is a map $\mathcal{A} : TQ \to \mathfrak{g}$ given by

$$\mathcal{A}(\boldsymbol{v}_q) := \boldsymbol{I}^{-1}(q)\mathbf{J}(\boldsymbol{v}_q). \tag{3.9}$$

Coordinate Formulas for $\mathbf{J}$, $\boldsymbol{I}$ and $\mathcal{A}$

Let $e_a,\ a = 1,\ 2, \ldots,\ m$ be a basis for $\mathfrak{g}$. Locally, any $\xi \in \mathfrak{g}$ can be expressed as $\xi = \xi^a e_a$. The infinitesimal generator of the action of G on Q has a local representation,

$$\xi_Q(q) = K_a^i \xi^a \frac{\partial}{\partial q^i} \tag{3.10}$$

relative to coordinates $q^i,\ i = 1,\ 2, \ldots,\ n$ of Q. K_a^i are called *action coefficients*. For a trivial principal fiber bundle, we have $\xi_Q(q) = (T_e R_g \xi, 0) \in T_q Q$. That is, for a trivial principal fiber bundle, the infinitesimal generator is simply the Lie algebra element pushed forward through the right action on G. This gives the $n \times m$ matrix

$$[K_a^i] = \begin{pmatrix} [T_e R_g]_{m\times m} \\ 0_{(n-m)\times m} \end{pmatrix},$$

where $[T_e R_g]$ is the local matrix representation for the tangent map $T_e R_g$.

Let $\sigma^a,\ a = 1,\ 2, \ldots,\ m$ be a basis for $\mathfrak{g}^*$. Then, locally $\mathbf{J}(\boldsymbol{v}_q) = J_a \sigma^a$. Thus,

$$J_a \xi^a = \ \ll \boldsymbol{v}_q, \xi_Q(q) \gg \ = g_{ij} v^j K_a^i \xi^a,$$

where g_{ij}'s are components of the kinetic energy metric g. Using (3.7), we have the local representation for the momentum map,

$$J_a = g_{ij} v^j K_a^i = \frac{\partial L}{\partial \dot{q}^i} K_a^i, \tag{3.11}$$

where $\frac{\partial L}{\partial \dot{q}^i} = g_{ij} v^j$.

In local coordinates,

$$\langle \boldsymbol{I}\ \xi, \eta \rangle = I_{ab} \xi^a \eta^b = \ \ll \xi_Q(q), \eta_Q(q) \gg \ = g_{ij} K_a^i K_b^j \xi^a \eta^b.$$

The local form of a locked inertia tensor, therefore, is

$$I_{ab} = g_{ij} K_a^i K_b^j. \tag{3.12}$$

Locally, let the mechanical connection be $\mathcal{A}(\boldsymbol{v}_q) = \mathcal{A}^a e_a$. Using (3.9) and (3.11), we have

$$\mathcal{A}^a = I^{ab} J_b = I^{ab} g_{ij} K_b^i v^j, \tag{3.13}$$

where I^{ab} is the coordinate representation for $\boldsymbol{I}^{-1}$. The components of $\mathcal{A}$, the *connection coefficients*, are defined as

$$\mathcal{A}_j^a = I^{ab} g_{ij} K_b^i$$

so that $\mathcal{A}^a = \mathcal{A}_j^a v^j$. In particular, using (3.10), we get

$$\mathcal{A}(\xi_Q(q)) = (I^{ab} g_{ij} K_b^i K_c^j \xi^c)\ e_a = (I^{ab} I_{bc} \xi^c)\ e_a = (\delta_c^a \xi^c)\ e_a = \xi^a\ e_a.$$

That is, $\mathcal{A}(\xi_Q(q)) = \xi$. The horizontal space is defined as

$$H_q Q = \{\boldsymbol{v}_q \in T_q Q \mid \mathcal{A}(\boldsymbol{v}_q) = 0\}.$$

Since $\mathcal{A}(\boldsymbol{v}_q) := \boldsymbol{I}^{-1}(q)\mathbf{J}(\boldsymbol{v}_q)$, we have $\boldsymbol{v}_q \in H_q Q$ if and only if $\mathbf{J}(\boldsymbol{v}_q) = 0$. That is,

$$\mathbf{J}(\text{Hor } \boldsymbol{v}_q) = g_{ij} K_a^i h^j = 0, \tag{3.14}$$

where Hor $\boldsymbol{v}_q = h^j \frac{\partial}{\partial q^j}$. A vertical vector is given by Ver $\boldsymbol{v}_q = \xi_Q(q) = K_a^i \xi^a\ \frac{\partial}{\partial q^i}$. We have,

$$g(\text{Ver } \boldsymbol{v}_q, \text{Hor } \boldsymbol{v}_q) = g_{ij} K_a^i \xi^a h^j = (g_{ij} K_a^i h^j) \xi^a.$$

It follows from (3.14) that $g(\text{Ver } \boldsymbol{v}_q, \text{Hor } \boldsymbol{v}_q) = 0$. That is, a mechanical connection splits the tangent space such that the horizontal vectors are metric orthogonal to vertical vectors.

Example: Inverted Pendulum on a Cart

We revisit the uncontrolled inverted pendulum-on-a-cart system of § 3.2.1 to illustrate the concepts of momentum map, locked inertia tensor and mechanical connection. Recall that the configuration

manifold for the pendulum cart system is a trivial principal fiber bundle $Q = G \times M = \mathbb{R} \times S^1$. A point on the manifold has coordinates $q = (s, \phi)$, where s is the cart position and ϕ is the pendulum angle. A tangent vector is simply the velocity vector $\boldsymbol{v}_q = (\dot{s}, \dot{\phi})$. The Lie algebra $\mathfrak{g}(= T_eG)$ of G is the real line $\mathbb{R}$. Since we are working with a trivial bundle, the infinitesimal generator is

$$\xi_Q(s, \phi) = (T_eR_g\xi, 0),$$

where $\xi \in \mathfrak{g} = \mathbb{R}$. The right action of G on itself is $R_g(s) = s + g$ for all $g \in \mathbb{R}$. The tangent map is $T_eR_g = 1$. The matrix of action coefficients, therefore, is

$$[K^i] = \begin{pmatrix} T_eR_g \\ 0 \end{pmatrix} = \begin{pmatrix} 1 \\ 0 \end{pmatrix}.$$

The momentum map for the pendulum-cart system is

$$J = \frac{\partial L}{\partial \dot{q}^i} K^i = \begin{pmatrix} \frac{\partial L}{\partial \dot{s}} & \frac{\partial L}{\partial \dot{\phi}} \end{pmatrix} \begin{pmatrix} 1 \\ 0 \end{pmatrix} = \frac{\partial L}{\partial \dot{s}} = (M + m)\dot{s} + ml \cos\phi \ \dot{\phi}.$$

Noether's theorem gives the conservation of J along the trajectories. Equivalently, since s is a cyclic coordinate, the momentum conjugate to s, $\partial L/\partial \dot{s}$, is conserved. In this example, the symmetry group G was abelian. For non-abelian symmetry groups, the conservation law is not so intuitive. For the cart-pendulum system, the locked inertia tensor is given by

$$\boldsymbol{I} = g_{ij} K^i K^j = \begin{pmatrix} 1 & 0 \end{pmatrix} \begin{pmatrix} M + m & ml\cos\phi \\ ml\cos\phi & ml^2 \end{pmatrix} \begin{pmatrix} 1 \\ 0 \end{pmatrix} = M + m.$$

Physically, it represents the inertia of the system when the pendulum is not moving relative to the mass; the pendulum is "locked" in one position relative to the cart. The mechanical connection is

$$\mathcal{A}(\boldsymbol{v}_q) = \boldsymbol{I}^{-1} J = \dot{s} + \frac{ml\cos\phi}{M + m} \ \dot{\phi},$$

where the term $(\frac{ml\cos\phi}{M+m})$ is recognized as the connection coefficient. The vertical and horizontal components of $\boldsymbol{v}_q = (\dot{s}, \dot{\phi})$ are given by

$$\text{Ver } \boldsymbol{v}_q = \mathcal{A}(\boldsymbol{v}_q)_Q(q) = (\mathcal{A}(\boldsymbol{v}_q), 0) = (\dot{s} + \frac{ml\cos\phi}{M + m} \ \dot{\phi}, \ 0), \text{ and} \tag{3.15}$$

$$\text{Hor } \boldsymbol{v}_q = \boldsymbol{v}_q - \text{Ver } \boldsymbol{v}_q = (-\frac{ml\cos\phi}{M + m} \ \dot{\phi}, \ \dot{\phi}) \tag{3.16}$$

respectively. The group orbit and the vertical/horizontal decomposition for the cart-pendulum system is illustrated in Fig. 3.3.

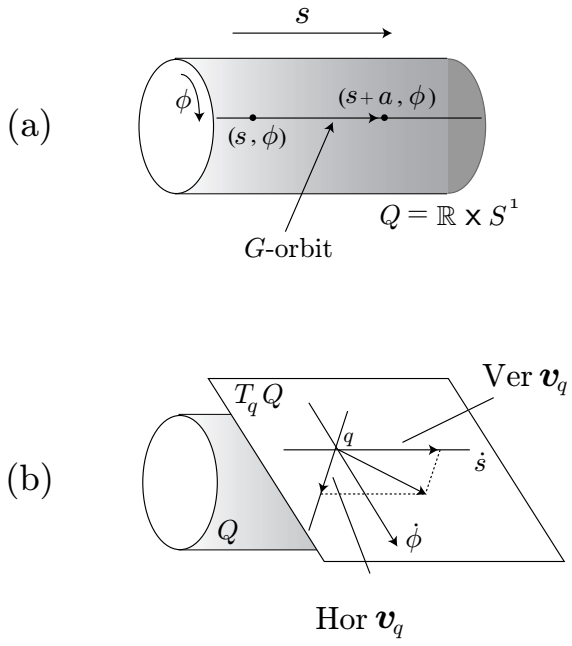

Figure 3.3: (a) The configuration space for the cart-pendulum is the cylinder $Q = \mathbb{R} \times S^1$. (b) Splitting of T_qQ into vertical and horizontal subspaces for the cart-pendulum system.

The kinetic energy for the cart-pendulum system can be written as

$$\begin{aligned}
\frac{1}{2}g(\boldsymbol{v}_q, \boldsymbol{v}_q) &= \frac{1}{2}\left[(M+m)\dot{s}^2 + 2ml\cos\phi\dot{s}\dot{\phi} + ml^2\dot{\phi}^2\right] \\
&= \frac{1}{2}\left[(M+m)(\dot{s} + \frac{ml\cos\phi}{M+m}\dot{\phi})^2 - \frac{(ml\cos\phi)^2}{M+m}\dot{\phi}^2 + ml^2\dot{\phi}^2\right] \\
&= \frac{1}{2}(M+m)(\dot{s} + \frac{ml\cos\phi}{M+m}\dot{\phi})^2 + \\
&\quad \frac{1}{2}\left[(M+m)(\frac{ml\cos\phi}{M+m}\dot{\phi})^2 - 2ml\cos\phi\left(\frac{ml\cos\phi\dot{\phi}}{M+m}\right)\dot{\phi} + ml^2\dot{\phi}^2\right].
\end{aligned}$$

If we define Ver $\boldsymbol{v}_q$ and Hor $\boldsymbol{v}_q$ as in (3.15) and (3.16), we get

$$\frac{1}{2}g(\boldsymbol{v}_q, \boldsymbol{v}_q) = \frac{1}{2}g(\text{Ver } \boldsymbol{v}_q, \text{Ver } \boldsymbol{v}_q) + \frac{1}{2}g(\text{Hor } \boldsymbol{v}_q, \text{Hor } \boldsymbol{v}_q).$$

Thus, essentially the vertical/horizontal decomposition can be regarded as a "block diagonalization" of the kinetic energy. This also suggests a way of shaping the kinetic energy. Choosing a different horizontal space (and therefore a new vertical space) and modifying the metric acting on the new vertical and horizontal vectors leads to a new kinetic energy.

3.5 Reduced Euler-Lagrange Equations

We start with a principal fiber bundle $(Q, \pi, Q/G)$, where Q represents the configuration manifold and G is a Lie group that acts on Q. Let $\mathfrak{g}$ denote the Lie algebra of G. Suppose that the Lagrangian $L : TQ \to \mathbb{R}$ is G-invariant. Let $\mathcal{A}$ denote the principal connection one-form on $(Q, \pi, Q/G)$. The connection splits the tangent space T_qQ into vertical and horizontal spaces. This splitting is used to break up the Euler-Lagrange equations on Q. Invariance of L allows us to drop L to TQ/G to obtain a reduced Lagrangian $l : TQ/G \to \mathbb{R}$. Let x^α denote the coordinates for the shape space $S = Q/G$ and ξ^a be the coordinates for the Lie algebra $\mathfrak{g}$ with respect to some chosen basis.

If we had a trivial fiber bundle, that is, $Q = S \times G$, then we could choose a trivial principal connection such that $TQ = TS \oplus TG$. This implies $TQ/G \cong TS \oplus \mathfrak{g}$. However, the principal fiber bundle may not always admit a trivial connection. More generally, the connection $\mathcal{A}$ is used to define the vertical and horizontal vectors as

$$\text{Ver } \boldsymbol{v}_q = (\xi^a + \mathcal{A}^a_\alpha \dot{x}^\alpha, 0), \text{ and Hor } \boldsymbol{v}_q = (-\mathcal{A}^a_\alpha \dot{x}^\alpha, \dot{x}^\alpha)$$

respectively, where $\mathcal{A}^a_\alpha$ are the connection coefficients. In case of a trivial connection, $\mathcal{A}^a_\alpha = 0$ so that

$$\text{Ver } \boldsymbol{v}_q = (\xi^a, 0), \text{ and Hor } \boldsymbol{v}_q = (0, \dot{x}^\alpha).$$

The following theorem gives the form for the reduced Euler-Lagrange equations. See [48] for a proof.

Theorem 3.5.1 (Lagrange-Poincaré Equations) *A curve $(q^i, \dot{q}^i) \in TQ$ satisfies the Euler-Lagrange equations if and only if the induced curve in TQ/G with coordinates $(x^\alpha, \dot{x}^\alpha, \Omega^a)$ in some*

local trivialization satisfies the Lagrange-Poincaré equations given by:

$$\begin{aligned} \frac{d}{dt}\frac{\partial l}{\partial \dot{x}^\alpha} - \frac{\partial l}{\partial x^\alpha} &= \frac{\partial l}{\partial \Omega^a}(B^a_{\alpha\beta}\dot{x}^\beta + \mathcal{E}^a_{\alpha d}\Omega^d), \\ \frac{d}{dt}\frac{\partial l}{\partial \Omega^b} &= \frac{\partial l}{\partial \Omega^a}(\mathcal{E}^a_{b\alpha}\dot{x}^\alpha + C^a_{db}\Omega^d). \end{aligned} \tag{3.17}$$

In the above equations, $B^a_{\alpha\beta}$ are the curvature coefficients defined as

$$B^a_{\alpha\beta} = \left(\frac{\partial \mathcal{A}^a_\alpha}{\partial x^\beta} - \frac{\partial \mathcal{A}^a_\beta}{\partial x^\alpha}\right),$$

$$\mathcal{E}^a_{\alpha d} = C^a_{bd}\mathcal{A}^b_\alpha, \text{ and } \mathcal{E}^a_{b\alpha} = -\mathcal{E}^a_{\alpha b},$$

where C^a_{db} are the structure constants of the Lie algebra $\mathfrak{g}$ defined in § 2.2.1. In case of mechanical systems, it is possible to write down an explicit form for the above reduced Euler-Lagrange equations (for example, see Ostrowski [56, 57]).

If one uses a trivial connection, as would be the case for a trivial principal bundle, the Lagrange-Poincaré equations reduce to the *Hamel equations*. Setting the connection coefficients $\mathcal{A}^a_\alpha = 0$ and $\Omega^a = \xi^a$, we get the Hamel equations:

$$\begin{aligned} \frac{d}{dt}\frac{\partial l}{\partial \dot{x}^\alpha} - \frac{\partial l}{\partial x^\alpha} &= 0, \\ \frac{d}{dt}\frac{\partial l}{\partial \xi^b} &= \frac{\partial l}{\partial \xi^a}C^a_{db}\xi^d. \end{aligned} \tag{3.18}$$

Let $\mathrm{ad}_\xi : \mathfrak{g} \to \mathfrak{g}$ be the linear map defined as

$$\mathrm{ad}_\xi(\eta) := [\xi, \eta],$$

where $\xi, \eta \in \mathfrak{g}$ and $[\xi, \eta]$ denotes the Lie bracket on $\mathfrak{g}$. The algebraic dual of ad_ξ is the map $\mathrm{ad}^*_\xi : \mathfrak{g}^* \to \mathfrak{g}^*$ defined as

$$\left\langle \mathrm{ad}^*_\xi(\alpha), \eta \right\rangle := \left\langle \alpha, \mathrm{ad}_\xi(\eta) \right\rangle,$$

where $\alpha \in \mathfrak{g}^*$. The Hamel equations are expressed in the above notation as

$$\begin{aligned} \frac{d}{dt}\frac{\partial l}{\partial \dot{x}} - \frac{\partial l}{\partial x} &= 0, \\ \frac{d}{dt}\frac{\partial l}{\partial \xi} &= \mathrm{ad}^*_\xi \frac{\partial l}{\partial \xi}. \end{aligned} \tag{3.19}$$

When G is abelian, invariance of the Lagrangian under the group action is equivalent to the Lagrangian being independent of the group variable. Thus, the group variables are cyclic coordinates and the corresponding conjugate momenta are conserved. Recall the cart-pendulum example where the group variable, the cart position s, was a cyclic coordinate. In this case, the familiar *Routhian* plays the role of the reduced Lagrangian l. Specifically, when one drops the Euler-Lagrange equations to the quotient space associated with the symmetry, and when the momentum map is constrained to have a specific value (that is, the cyclic coordinates and their velocities are eliminated using the value of the momentum map), then the resulting equations are in the Euler-Lagrange form with respect to the Routhian. The reader is referred to [48] and [56] for more details.

The *Euler-Poincaré* equations are a special case of the more general Hamel equations that result when $Q = G$. Let $L : TG \to \mathbb{R}$ be a G-invariant Lagrangian and $l : TG/G \cong \mathfrak{g} \to \mathbb{R}$ denote its restriction to the identity. The reduced Euler-Lagrange equations, called Euler-Poincaré in this case, are given by

$$\frac{d}{dt}\frac{\partial l}{\partial \xi} = \mathrm{ad}^*_\xi \frac{\partial l}{\partial \xi}, \tag{3.20}$$

where $\xi \in \mathfrak{g}$ and $\frac{\partial l}{\partial \xi} \in \mathfrak{g}^*$. One can see that the above equations are essentially the second part of Hamel equations (3.19). As an example, we show that the dynamic equations for a free rigid body in rotational motion are Euler-Poincaré.

Example: Rotational Dynamics of a Free Rigid Body

As an example, we derive the reduced Euler-Lagrange equations for a free rigid body $\mathcal{B}$ in rotation shown in Fig. 3.4. More details about the example can be found in Marsden and Ratiu [46]. The reference frame $\Sigma_{\text{inertial}} = \{\boldsymbol{i}_1, \boldsymbol{i}_2, \boldsymbol{i}_3\}$ is fixed in space and the reference frame $\Sigma_{\text{body}} = \{\boldsymbol{b}_1, \boldsymbol{b}_2, \boldsymbol{b}_3\}$ is fixed in the body. Both reference frames are located at the center of mass O_{cm} of the rigid body. The orientation of a free rigid body is represented by the rotation matrix $\boldsymbol{\mathcal{R}} \in SO(3)$, the special orthogonal group in $\mathbb{R}^3$. The matrix $\boldsymbol{\mathcal{R}}$ maps vectors expressed in the body reference frame to those in the inertial reference frame. Let $\boldsymbol{x}_s \in \mathbb{R}^3$ be any point in the rigid body expressed in the

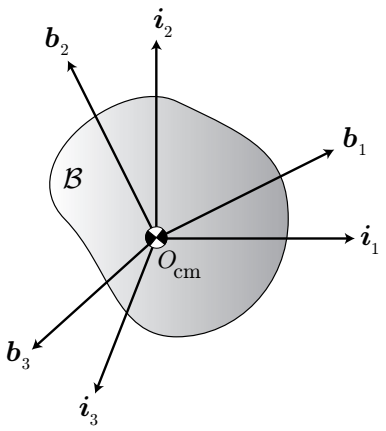

Figure 3.4: A free rigid body in rotation.

inertial frame and let $\boldsymbol{x}_b \in \mathbb{R}^3$ be the same point expressed in the body frame. We have

$$\boldsymbol{x}_s = \boldsymbol{\mathcal{R}}\boldsymbol{x}_b.$$

The inertial velocity of the point is

$$\boldsymbol{v}_s = \frac{d\boldsymbol{x}_s}{dt} = \dot{\boldsymbol{\mathcal{R}}}\boldsymbol{x}_b.$$

Since $\boldsymbol{\mathcal{R}}$ is orthogonal, we have

$$\boldsymbol{\mathcal{R}}\boldsymbol{\mathcal{R}}^T = \boldsymbol{\mathcal{R}}^T\boldsymbol{\mathcal{R}} = \mathbb{I},$$

where $\mathbb{I}$ is the identity matrix. Differentiating $\boldsymbol{\mathcal{R}}\boldsymbol{\mathcal{R}}^T = \mathbb{I}$ and $\boldsymbol{\mathcal{R}}^T\boldsymbol{\mathcal{R}} = \mathbb{I}$ with respect to t gives that both $\dot{\boldsymbol{\mathcal{R}}}\boldsymbol{\mathcal{R}}^{-1}$ and $\boldsymbol{\mathcal{R}}^{-1}\dot{\boldsymbol{\mathcal{R}}}$ are skew-symmetric. Let $\hat{\boldsymbol{a}}$ denote the skew-symmetric matrix associated with $\boldsymbol{a} \in \mathbb{R}^3$ and defined as

$$\hat{\boldsymbol{a}}\boldsymbol{b} := \boldsymbol{a} \times \boldsymbol{b},$$

where $\boldsymbol{b} \in \mathbb{R}^3$ and "$\times$" denotes the usual cross-product. If we denote body angular velocity by $\boldsymbol{\omega}$, then we have

$$\hat{\boldsymbol{\omega}} = \boldsymbol{\mathcal{R}}^{-1}\dot{\boldsymbol{\mathcal{R}}}.$$

The Lagrangian $L : TSO(3) \to \mathbb{R}$ is the kinetic energy of the system given by

$$\begin{aligned} L(\boldsymbol{\mathcal{R}}, \dot{\boldsymbol{\mathcal{R}}}) &= \frac{1}{2}\int_{\mathcal{B}} ||\dot{\boldsymbol{\mathcal{R}}}\boldsymbol{x}_b||^2 \, dm \\ &= \frac{1}{2}\int_{\mathcal{B}} (\boldsymbol{\mathcal{R}}\hat{\boldsymbol{\omega}}\boldsymbol{x}_b)^T (\boldsymbol{\mathcal{R}}\hat{\boldsymbol{\omega}}\boldsymbol{x}_b) \, dm \\ &= \frac{1}{2}\int_{\mathcal{B}} [\boldsymbol{\mathcal{R}}(-\hat{\boldsymbol{x}}_b\boldsymbol{\omega})]^T [\boldsymbol{\mathcal{R}}(-\hat{\boldsymbol{x}}_b\boldsymbol{\omega})] \, dm \\ &= \frac{1}{2}\boldsymbol{\omega}^T \int_{\mathcal{B}} (-\hat{\boldsymbol{x}}_b\hat{\boldsymbol{x}}_b) \, dm \, \boldsymbol{\omega} \\ &= \frac{1}{2}\boldsymbol{\omega}^T \boldsymbol{I}\boldsymbol{\omega}, \end{aligned}$$

where dm is an infinitesimal mass element located at $\boldsymbol{x}_b$ and $\boldsymbol{I}$ is the inertial tensor. Let us show that L is invariant under the left action of $SO(3)$ on itself. In particular, we want to show the invariance under the lifted action. The left action of $SO(3)$ on itself is defined as

$$\Phi_{\bar{\boldsymbol{\mathcal{R}}}}(\boldsymbol{\mathcal{R}}) = \bar{\boldsymbol{\mathcal{R}}}\boldsymbol{\mathcal{R}}$$

for all $\bar{\boldsymbol{\mathcal{R}}} \in SO(3)$ and the corresponding tangent map is

$$T_{\boldsymbol{\mathcal{R}}}\Phi_{\bar{\boldsymbol{\mathcal{R}}}}(\dot{\boldsymbol{\mathcal{R}}}) = \bar{\boldsymbol{\mathcal{R}}}\dot{\boldsymbol{\mathcal{R}}}.$$

The Lagrangian under the lifted action of $SO(3)$ is

$$\begin{aligned} L(\Phi_{\bar{\boldsymbol{\mathcal{R}}}}(\boldsymbol{\mathcal{R}}), T_{\boldsymbol{\mathcal{R}}}\Phi_{\bar{\boldsymbol{\mathcal{R}}}}(\dot{\boldsymbol{\mathcal{R}}})) &= L(\bar{\boldsymbol{\mathcal{R}}}\boldsymbol{\mathcal{R}}, \bar{\boldsymbol{\mathcal{R}}}\dot{\boldsymbol{\mathcal{R}}}) \\ &= \frac{1}{2}\int_{\mathcal{B}} ||\bar{\boldsymbol{\mathcal{R}}}\dot{\boldsymbol{\mathcal{R}}}\boldsymbol{x}_b||^2 \, dm(\boldsymbol{x}_b) \\ &= \frac{1}{2}\int_{\mathcal{B}} ||\dot{\boldsymbol{\mathcal{R}}}\boldsymbol{x}_b||^2 \, dm(\boldsymbol{x}_b) = L(\boldsymbol{\mathcal{R}}, \dot{\boldsymbol{\mathcal{R}}}) \end{aligned} \tag{3.21}$$

since $\bar{\boldsymbol{\mathcal{R}}}^T = \bar{\boldsymbol{\mathcal{R}}}^{-1}$. Therefore, the Lagrangian is G-invariant. The invariance of L suggests that we can drop L to $TSO(3)/SO(3) \cong \mathfrak{so}(3)$ to obtain the reduced Lagrangian $l : \mathfrak{so}(3) \to \mathbb{R}$,

$$l(\boldsymbol{\omega}) = \frac{1}{2}\boldsymbol{\omega}^T \boldsymbol{I}\boldsymbol{\omega}, \tag{3.22}$$

where $\mathfrak{so}(3)$ is identified with $\mathbb{R}^3$. The reduced dynamics are given by the Euler-Poincaré equations (3.20)

$$\frac{d}{dt}\frac{\partial l}{\partial \boldsymbol{\omega}} = \mathrm{ad}^*_{\boldsymbol{\omega}} \frac{\partial l}{\partial \boldsymbol{\omega}}, \tag{3.23}$$

where $\frac{\partial l}{\partial \boldsymbol{\omega}} \in \mathfrak{so}(3)^* \cong \mathbb{R}^3$. It can be shown that [46, 79]

$$\mathrm{ad}^*_{\boldsymbol{\omega}} \frac{\partial l}{\partial \boldsymbol{\omega}} = \frac{\partial l}{\partial \boldsymbol{\omega}} \times \boldsymbol{\omega}. \tag{3.24}$$

Using (3.22) and (3.24) in (3.23), we get the familiar looking *Euler* equations for the rigid body,

$$\frac{d}{dt}\boldsymbol{I}\boldsymbol{\omega} = \boldsymbol{I}\boldsymbol{\omega} \times \boldsymbol{\omega}. \tag{3.25}$$

■

Chapter 4

Controlled Lagrangians with Gyroscopic Forcing and Dissipation

> "*All happy families (linear systems) are alike. Every unhappy family (nonlinear system) is unhappy (nonlinear) in its own way*"
>
> *- A control theorist's view of Leo Tolstoy.*

In this chapter, we introduce the method of controlled Lagrangians. The method of controlled Lagrangians is a technique for stabilizing underactuated mechanical systems. As initially presented [13, 14, 17], the method provides a kinetic-shaping algorithm for systems with symmetries in the input directions. Later work introduced additional control freedom by allowing potential shaping as well as kinetic shaping [10, 15]. In this dissertation, we completely relax the symmetry requirement and allow for generalized gyroscopic forces in the closed-loop equations [22, 23]. This provides more extra freedom in matching and stabilization. In all of these cases, the modified kinetic energy is restricted to a certain form, one which is inspired by observations from geometric mechanics.

Other papers describe more general conditions under which a feedback-controlled, underactuated mechanical system is Lagrangian [5, 6, 30] or Hamiltonian [8]. The equivalence of the Lagrangian and Hamiltonian views was established in [23] for the most general case, where there are no prior restrictions on the form of the closed-loop dynamics. There are advantages, however, in restricting one's view to a smaller class of systems. The control design problem may be simplified, for example, by assuming a certain structural form for the closed-loop kinetic energy.

The outline of the chapter is as follows: In § 4.1, we introduce dissipative and gyroscopic forces. The effect of dissipative and gyroscopic forces on system stability is examined. Section 4.2 reviews the method of controlled Lagrangians. We introduce the idea of shaping the energy through feedback with a simple example. Kinetic energy shaping for a class of systems with symmetry is explained. General matching conditions between the open-loop and closed-loop systems are derived and the effect of physical dissipation on closed-loop stability is studied in detail. In § 4.3, we study the "ball on a beam" system and illustrate the potentially detrimental effect of physical damping for a system controlled by kinetic shaping in the Hamiltonian setting. We conclude in § 4.4 by summarizing the matching and stabilization procedure.

4.1 Dissipative and Gyroscopic Forces

In Section § 3.1, we saw that the closed-loop Euler-Lagrange equations for a simple Lagrangian mechanical system can be written in matrix form as

$$\boldsymbol{M}(\boldsymbol{q})\ddot{\boldsymbol{q}} + \boldsymbol{C}(\boldsymbol{q},\dot{\boldsymbol{q}})\dot{\boldsymbol{q}} + \frac{\partial V}{\partial \boldsymbol{q}} = \boldsymbol{F}(\boldsymbol{q},\dot{\boldsymbol{q}}) + \boldsymbol{G}\boldsymbol{u}, \tag{4.1}$$

where $\boldsymbol{q} = (q^1,\ q^2, \ldots,\ q^n)^T$ is the vector of generalized coordinates, $\boldsymbol{M}$ is the mass matrix, $\boldsymbol{C}$ is the Coriolis and centripetal matrix, $\partial V/\partial \boldsymbol{q}$ is the vector of partial derivatives of the potential V with respect to the coordinates q^i, $\boldsymbol{F}$ is the vector of external forces, $\boldsymbol{u}$ is the vector of control inputs and $\boldsymbol{G}$ is a $n \times m$ constant matrix of rank m. In this dissertation, we shall primarily be concerned with two types of external forces: *dissipative* and *gyroscopic*.

Dissipative Forces

Physically, a dissipative force $\boldsymbol{F}_{\text{diss}}(\boldsymbol{q}, \dot{\boldsymbol{q}})$ is a force that decreases the system energy. That is,

$$\langle \dot{\boldsymbol{q}}, \boldsymbol{F}_{\text{diss}}(\boldsymbol{q}, \dot{\boldsymbol{q}}) \rangle \leq 0$$

for all $(\boldsymbol{q}, \dot{\boldsymbol{q}}) \in TQ$. Often, the dissipative force can be expressed as

$$\boldsymbol{F}_{\text{diss}}(\boldsymbol{q}, \dot{\boldsymbol{q}}) = -\boldsymbol{R}(\boldsymbol{q}, \dot{\boldsymbol{q}})\dot{\boldsymbol{q}}, \tag{4.2}$$

where $\boldsymbol{R}^T = \boldsymbol{R} > 0$ is the dissipation matrix. For simple Lagrangian systems, the energy of the system is the kinetic energy plus the potential,

$$E(\boldsymbol{q}, \dot{\boldsymbol{q}}) = \frac{1}{2}\dot{\boldsymbol{q}}^T \boldsymbol{M}\dot{\boldsymbol{q}} + V(\boldsymbol{q}). \tag{4.3}$$

If all the external forces are dissipative in nature ($\boldsymbol{u} = 0$), then the energy rate is

$$\dot{E}(\boldsymbol{q}, \dot{\boldsymbol{q}}) = \dot{\boldsymbol{q}}^T \boldsymbol{F}_{\text{diss}}(\boldsymbol{q}, \dot{\boldsymbol{q}}) = -\dot{\boldsymbol{q}}^T \boldsymbol{R}\, \dot{\boldsymbol{q}} \leq 0. \tag{4.4}$$

If the equilibrium is a minimum of the energy E, then stability follows from Lyapunov's direct method (see Thm. 2.4.3). LaSalle's invariance principle (Thm. 2.4.4) can be used to prove asymptotic stability.

Gyroscopic Forces

In a mechanical system, gyroscopic forces arise from couplings between modes of vibration. Gyroscopic forces are special because they conserve energy. Formally, a gyroscopic force is given as

$$\boldsymbol{F}_{\text{gyr}}(\boldsymbol{q}, \dot{\boldsymbol{q}}) = \boldsymbol{\mathcal{S}}(\boldsymbol{q}, \dot{\boldsymbol{q}})\dot{\boldsymbol{q}}, \tag{4.5}$$

where $\boldsymbol{\mathcal{S}}$ is a skew-symmetric matrix; that is, $\boldsymbol{\mathcal{S}}^T = -\boldsymbol{\mathcal{S}}$. If the external forces are gyroscopic ($\boldsymbol{u} = 0$), then the energy rate for a simple Lagrangian system is

$$\dot{E} = \dot{\boldsymbol{q}}^T \boldsymbol{F}_{\text{gyr}}(\boldsymbol{q}, \dot{\boldsymbol{q}}) = -\dot{\boldsymbol{q}}^T \boldsymbol{\mathcal{S}}\dot{\boldsymbol{q}} = 0, \tag{4.6}$$

which follows from the skew-symmetry of $\boldsymbol{\mathcal{S}}$.

4.2 Method of Controlled Lagrangians: An Introduction

This section introduces the method of controlled Lagrangians. The method of controlled Lagrangians is an energy shaping control technique for underactuated Lagrangian systems. One begins with a simple Lagrangian system, $L = K - V$, where K is the uncontrolled kinetic energy and V is the uncontrolled potential energy. The method of controlled Lagrangians tries to seek a feedback control such that the closed-loop equations derive from a new Lagrangian, called the *controlled Lagrangian*, $L_c = K_c - V_c$, where K_c and V_c are feedback-modified kinetic and potential energies, respectively. The conditions under which the open-loop and closed-loop equations are equivalent are referred to as "matching" conditions. Modification of kinetic energy is called *kinetic shaping* and that of potential energy is termed *potential shaping*. Before we provide details about the technique, we illustrate the idea of *energy shaping* through a simple example.

4.2.1 Energy Shaping: The Central Idea

Consider a mechanical system whose Lagrangian is given by

$$L(x, \dot{x}) = K(\dot{x}) - V(x) = \frac{1}{2}\dot{x}^2 - \frac{1}{2}\beta x^2,$$

where $(x, \dot{x}) \in T\mathbb{R} = \mathbb{R} \times \mathbb{R}$ and $\beta < 0$. The above system represents *balance type systems*, for example, an inverted pendulum. The energy of the system is

$$E(x, \dot{x}) = \frac{1}{2}\dot{x}^2 + \frac{1}{2}\beta x^2.$$

The equilibrium $(x, \dot{x}) = (0, 0)$ is a saddle [51] and thus unstable. It is a minimum of the kinetic energy but a maximum of the potential energy. With a control input u, the equations of motion are

$$\ddot{x} + \beta x = u. \tag{4.7}$$

The objective is to stabilize the equilibrium by shaping the energy. Suppose we chose a control u such that the closed-loop equations derive from the controlled Lagrangian

$$L_c = \frac{1}{2}\dot{x}^2 - \frac{1}{2}\tilde{\beta}x^2,$$

where $\tilde{\beta} > 0$. The closed-loop energy or the *controlled energy* is

$$E_c = \frac{1}{2}\dot{x}^2 + \frac{1}{2}\tilde{\beta}x^2.$$

The equilibrium is a minimum of this new energy and $\dot{E}_c = 0$. Thus, E_c serves as a *Lyapunov* function to prove stability. The closed-loop equations are

$$\ddot{x} + \tilde{\beta}x = 0. \tag{4.8}$$

Comparing (4.7) and (4.8), we have

$$u = (\beta - \tilde{\beta})x. \tag{4.9}$$

Adding feedback dissipation will make the equilibrium asymptotically stable. In the above procedure, we modified the potential energy through feedback. Similarly, one can modify the kinetic energy through feedback by applying the spring-like force (4.9). Suppose this time, the closed-loop equations derive from a different controlled Lagrangian,

$$L_c = \frac{1}{2}\alpha\dot{x}^2 - \frac{1}{2}\beta x^2.$$

The controlled energy is

$$E_c = \frac{1}{2}\alpha\dot{x}^2 + \frac{1}{2}\beta x^2.$$

Choosing $\alpha < 0$ makes the equilibrium a maximum of E_c. In this case, $\dot{E}_c = 0$ too and the equilibrium is stable. The closed-loop equations are

$$\alpha\ddot{x} + \beta x = 0. \tag{4.10}$$

Comparing (4.7) and (4.10), we have

$$u = (\beta - \frac{\beta}{\alpha})x,$$

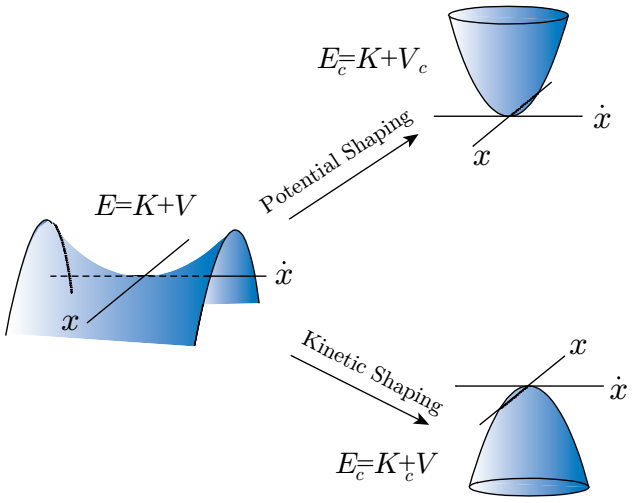

Figure 4.1: The basic idea underlying energy shaping control.

which is the same as the potential shaping control (4.9) if we set $\tilde{\beta} = \beta/\alpha$. However, this time we shaped the kinetic energy. The energy shaping idea is illustrated in Fig. 4.1. The above example was a fully actuated system and stabilization could be achieved either by potential or kinetic shaping. However, for underactuated systems, it might not be possible to achieve stabilization through potential shaping only. To see this, consider the "inverted pendulum on a cart" system described in § 3.2.1. The Lagrangian for the cart-pendulum system is

$$L(\boldsymbol{q}, \dot{\boldsymbol{q}}) = \frac{1}{2}\dot{\boldsymbol{q}}^T \boldsymbol{M}(\boldsymbol{q})\dot{\boldsymbol{q}} - V(\boldsymbol{q}), \tag{4.11}$$

where

$$\boldsymbol{q} = \begin{pmatrix} \phi \\ s \end{pmatrix}, \quad \boldsymbol{M}(\phi) = \begin{pmatrix} ml^2 & ml\cos\phi \\ ml\cos\phi & M+m \end{pmatrix}, \quad V(\phi) = mgl\cos\phi.$$

Assume that a control u is applied only in the cart direction. This makes the system underactuated. Note that $\boldsymbol{M}$ is a positive definite matrix and V is a negative definite function. The open-loop equations for the controlled cart-pendulum system are

$$\begin{pmatrix} ml^2 & ml\cos\phi \\ ml\cos\phi & M+m \end{pmatrix} \begin{pmatrix} \ddot{\phi} \\ \ddot{s} \end{pmatrix} + \begin{pmatrix} ml\dot{s}\dot{\phi}\sin\phi - mgl\sin\phi \\ 0 \end{pmatrix} = \begin{pmatrix} 0 \\ u \end{pmatrix}. \tag{4.12}$$

The uncontrolled equations of motions ($u = 0$) are invariant with respect to s. We wish to stabilize the unstable relative equilibrium $(\phi, \dot{\phi}, \dot{s}) = (0, 0, 0)$. Suppose there exists a stabilizing control law u that only shapes the potential energy of the system and preserves the symmetry. The closed-loop equations are, thus, derived from the controlled Lagrangian

$$L_c(\boldsymbol{q}, \dot{\boldsymbol{q}}) = \frac{1}{2}\dot{\boldsymbol{q}}^T \boldsymbol{M}(\phi)\dot{\boldsymbol{q}} - V_c(\phi),$$

where $V_c(\phi)$, the control-modified potential energy, is a positive definite function. The closed-loop equations are

$$\begin{pmatrix} ml^2 & ml\cos\phi \\ ml\cos\phi & M+m \end{pmatrix} \begin{pmatrix} \ddot{\phi} \\ \ddot{s} \end{pmatrix} + \begin{pmatrix} ml\dot{s}\dot{\phi}\sin\phi + \frac{\partial V_c}{\partial \phi} \\ 0 \end{pmatrix} = \begin{pmatrix} 0 \\ 0 \end{pmatrix}. \tag{4.13}$$

Using (4.12) and (4.13) and comparing the equation for ϕ, we get

$$\frac{\partial V_c}{\partial \phi} = -mgl\sin\phi \Rightarrow V_c = V + \text{constant}.$$

Thus, V_c has the same definiteness as V. This shows that potential shaping alone might not lead to a stabilizing control law. However, for the cart-pendulum example, stabilization can be achieved using kinetic shaping only. In [17], a stabilizing control law u is obtained such that the closed-loop equations are derived from the controlled Lagrangian

$$L_c(\boldsymbol{q}, \dot{\boldsymbol{q}}) = \frac{1}{2}\dot{\boldsymbol{q}}^T \boldsymbol{M}_c(\phi)\dot{\boldsymbol{q}} - V(\phi),$$

where

$$\boldsymbol{M}_c(\phi;\kappa) = \begin{pmatrix} ml^2 + \frac{(ml)^2\kappa}{M+m}(\kappa + 2\cos^2\phi - 1) & (\kappa+1)ml\cos\phi \\ (\kappa+1)ml\cos\phi & M+m \end{pmatrix}$$

is the control-modified kinetic energy metric and $\kappa > \frac{M}{m} > 0$ is a control parameter. Note that the closed-loop equations preserve the symmetry with respect to s.

4.2.2 The Controlled Lagrangian Formulation

In this section, we describe the mathematical details for the method of controlled Lagrangians. Much of the discussion in this chapter is based on Woolsey et. al [83]. We start with a simple

Lagrangian system with symmetry in the input directions. We then modify both the kinetic energy and potential energy to produce a new controlled Lagrangian. We also allow for generalized gyroscopic forces in the closed-loop system to provide additional freedom in "matching" the open-loop and closed-loop equations. Moreover, we do not require the closed-loop equations to preserve symmetry. The controlled Lagrangian together with the gyroscopic forces describe the dynamics of the controlled closed-loop system.

The Setting

Suppose we have a mechanical system with a configuration manifold Q and that an abelian Lie group G acts freely and properly on Q. The action of G on Q induces a quotient space, $S = Q/G$, called shape space. The fiber bundle is a principal fiber bundle (Q, π, S). The goal of kinetic shaping is to control the variables lying in the shape space S using controls that act directly on the variables in G. This approach differs from the idea of locomotion via shape change, where one controls the shape variables in order to effect group motions; see [9], for example.

Assume that the kinetic energy $K : TQ \to \mathbb{R}$ is invariant under the given action of G on Q. The modification of L involves changing the metric tensor $g(\cdot, \cdot)$ that defines the kinetic energy $K = \frac{1}{2} g(\dot{q}, \dot{q})$. Define local coordinates x^α for S and θ^a for G. (In examples, the latter coordinates are often cyclic; hence the notation θ^a.) The kinetic energy may be written as

$$K = \frac{1}{2} g_{\alpha\beta} \dot{x}^\alpha \dot{x}^\beta + g_{\alpha b} \dot{x}^\alpha \dot{\theta}^b + \frac{1}{2} g_{ab} \dot{\theta}^a \dot{\theta}^b,$$

where $g_{\alpha\beta}, g_{\alpha b}$, and g_{ab} are the local components of $g(\cdot, \cdot)$.

As seen is § 3.4, the mechanical connection $\mathcal{A}$ can be used to split the tangent space $T_q Q$ into vertical and horizontal spaces. That is, for each tangent vector $\boldsymbol{v}_q$ at a point $q \in Q$, we can write a unique decomposition

$$\boldsymbol{v}_q = \operatorname{Ver} \boldsymbol{v}_q + \operatorname{Hor} \boldsymbol{v}_q,$$

such that the vertical part is tangent to the orbit of the G-action and the horizontal part is the

metric orthogonal to the vertical part. The vertical component is uniquely defined by requiring that

$$g(\boldsymbol{v}_q, \boldsymbol{w}_q) = g(\mathrm{Hor}\,\boldsymbol{v}_q, \mathrm{Hor}\,\boldsymbol{w}_q) + g(\mathrm{Ver}\,\boldsymbol{v}_q, \mathrm{Ver}\,\boldsymbol{w}_q). \tag{4.14}$$

for every $\boldsymbol{v}_q, \boldsymbol{w}_q \in T_qQ$. Let the pair $(\dot{x}^\alpha, \dot{\theta}^a)$ represent the local expression for velocity $\boldsymbol{v}_q$. In terms of the mechanical connection $\mathcal{A}$, the vertical and horizontal vectors are given by (see § 3.4)

$$\mathrm{Ver}\,\boldsymbol{v}_q = \mathcal{A}(\boldsymbol{v}_q)_Q(q) = (0, \mathcal{A}(\boldsymbol{v}_q)) = (0, \dot{\theta}^a + \mathcal{A}^a_\alpha \dot{x}^\alpha) \tag{4.15}$$

$$\mathrm{Hor}\,\boldsymbol{v}_q = \boldsymbol{v}_q - \mathrm{Ver}\,\boldsymbol{v}_q = (\dot{x}^\alpha, -\mathcal{A}^a_\alpha \dot{x}^\alpha), \tag{4.16}$$

where $\mathcal{A}^a_\alpha$ are the connection coefficients.

Requirement (4.14) may be thought of as a block diagonalization procedure or "completing the square" by rewriting the kinetic energy in the form

$$K = \frac{1}{2}(g_{\alpha\beta} - g_{\alpha a} g^{ab} g_{b\beta})\dot{x}^\alpha \dot{x}^\beta + \frac{1}{2} g_{ab}(\dot{\theta}^a + g^{ac} g_{c\alpha}\dot{x}^\alpha)(\dot{\theta}^b + g^{bd} g_{d\beta}\dot{x}^\beta). \tag{4.17}$$

(Note: If $[g_{ab}]$ represents the matrix form of the tensor g_{ab} then $\left[g^{ab}\right]$ is the matrix inverse of $[g_{ab}]$.) Then

$$\mathrm{Ver}\,\boldsymbol{v}_q = (0, \dot{\theta}^a + g^{ab} g_{\alpha b}\dot{x}^\alpha) \tag{4.18}$$

$$\mathrm{Hor}\,\boldsymbol{v}_q = (\dot{x}^\alpha, -g^{ab} g_{\alpha b}\dot{x}^\alpha). \tag{4.19}$$

Comparing (4.15)-(4.16) with (4.18)-(4.19), the connection coefficients are simply

$$\mathcal{A}^a_\alpha = g^{ab} g_{\alpha b}. \tag{4.20}$$

Note that $g^{ab} g_{\alpha b}\dot{x}^\alpha$ appears as a "velocity shift" in the expressions (4.18) and (4.19).

The Controlled Lagrangian

An essential feature of the controlled Lagrangian is the feedback-modified kinetic energy. The modification consists of three ingredients:

- a different choice of horizontal space, denoted Hor_τ,
- a change $g \to g_\sigma$ of the metric acting on horizontal vectors, and
- a change $g \to g_\rho$ of the metric acting on vertical vectors.

The first ingredient above can be thought of as a shift in the mechanical connection. Let τ be a Lie algebra-valued, G-equivariant *horizontal* one-form on Q; that is, a one-form with values in the Lie algebra $\mathfrak{g}$ of G that annihilates vertical vectors[1]. The ***τ-horizontal space*** at $q \in Q$ consists of tangent vectors to Q at q of the form $\mathrm{Hor}_\tau \boldsymbol{v}_q = \mathrm{Hor}\, \boldsymbol{v}_q - \tau(\boldsymbol{v}_q)_Q(q)$, which also defines the ***τ-horizontal projection*** $\boldsymbol{v}_q \mapsto \mathrm{Hor}_\tau \boldsymbol{v}_q$. The ***$\tau$-vertical projection*** operator is defined by $\mathrm{Ver}_\tau \boldsymbol{v}_q = \mathrm{Ver}\, \boldsymbol{v}_q + \tau(\boldsymbol{v}_q)_Q(q)$. The left half of Figure 4.2 depicts the role of $\mathcal{A}$ in the original decomposition; the right half depicts the analogous role of τ in defining the new decomposition.

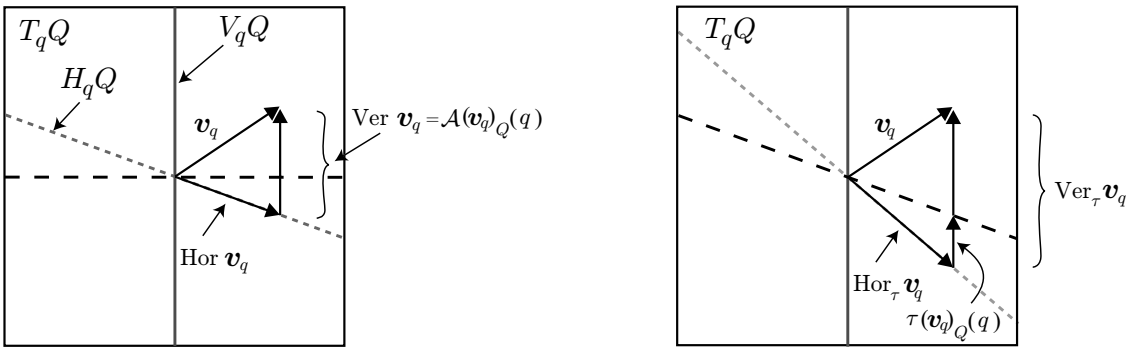

Figure 4.2: Original (left) and modified (right) decompositions of T_qQ.

Given τ, g_σ, and g_ρ, define the control-modified kinetic energy

$$K_{\tau,\sigma,\rho}(\boldsymbol{v}_q) = \frac{1}{2}\left[g_\sigma\left(\mathrm{Hor}_\tau \boldsymbol{v}_q, \mathrm{Hor}_\tau \boldsymbol{v}_q\right) + g_\rho\left(\mathrm{Ver}_\tau \boldsymbol{v}_q, \mathrm{Ver}_\tau \boldsymbol{v}_q\right)\right].$$

[1]One of the basic requirements of a connection is that, when applied to an infinitesimal generator of the group $\xi_Q(q)$ at any point $q \in Q$, one recovers the Lie algebra element ξ. For this condition to be maintained when τ is added to $\mathcal{A}$, the one-form τ must be horizontal; this means that it should vanish when applied to vertical vectors which are vectors of the form $\xi_Q(q)$.

Assume that $g = g_\sigma$ on H_qQ and that H_qQ and V_qQ are orthogonal for g_σ. Then, as shown in [17],

$$K_{\tau,\sigma,\rho}(\boldsymbol{v}_q) = K(\boldsymbol{v}_q + \tau(\boldsymbol{v}_q)_Q(q)) + \frac{1}{2} g_\sigma \left(\tau(\boldsymbol{v}_q)_Q(q), \tau(\boldsymbol{v}_q)_Q(q)\right) + \frac{1}{2} \left(g_\rho - g\right) \left(\mathrm{Ver}_\tau \, \boldsymbol{v}_q, \mathrm{Ver}_\tau \, \boldsymbol{v}_q\right). \quad (4.21)$$

The controlled Lagrangian is

$$L_{\tau,\sigma,\rho}(\boldsymbol{v}_q) = K_{\tau,\sigma,\rho}(\boldsymbol{v}_q) - \Big(V(q) + \tilde{V}(q)\Big)$$

where $\tilde{V}(q)$ is an artificial potential function which modifies the effective potential energy in the closed-loop system. We define $V'(q) = V(q) + \tilde{V}(q)$ to be the complete, control-modified potential energy. Then, using (4.21),

$$\begin{aligned} L_{\tau,\sigma,\rho}(\boldsymbol{v}_q) &= K(\boldsymbol{v}_q + \tau(\boldsymbol{v}_q)_Q(q)) + \frac{1}{2} g_\sigma \left(\tau(\boldsymbol{v}_q)_Q(q), \tau(\boldsymbol{v}_q)_Q(q)\right) \\ &\quad + \frac{1}{2} \left(g_\rho - g\right) \left(\mathrm{Ver}_\tau \, \boldsymbol{v}_q, \mathrm{Ver}_\tau \, \boldsymbol{v}_q\right) - V'(q). \end{aligned} \quad (4.22)$$

The goal is to determine conditions on the original kinetic energy, on the energy modification parameters (τ, g_σ, and g_ρ), and on the potential functions V and $\tilde{V}$ such that a particular choice of feedback yields closed-loop equations which are Euler-Lagrange equations for $L_{\tau,\sigma,\rho}$. These conditions are referred to as "matching" conditions. They ensure that no inputs are necessary in uncontrolled directions in order to effect the desired closed-loop dynamics. In examples, the matching conditions often leave freedom in the control parameters which can be used to satisfy conditions for stability.

We can write the horizontal one form in coordinates as $\tau = \tau_\alpha^a dx^\alpha$. Thus,

$$\tau(\boldsymbol{v}_q)_Q(q) = (0, \tau(\boldsymbol{v}_q)) = (0, \tau_\alpha^a \dot{x}^\alpha),$$

which gives

$$\mathrm{Ver}_\tau \, \boldsymbol{v}_q = (0, \dot{\theta}^a + g^{ab} g_{\alpha b} \dot{x}^\alpha + \tau_\alpha^a \dot{x}^\alpha) \quad (4.23)$$

$$\mathrm{Hor}_\tau \, \boldsymbol{v}_q = (\dot{x}^\alpha, -g^{ab} g_{\alpha b} \dot{x}^\alpha - \tau_\alpha^a \dot{x}^\alpha). \quad (4.24)$$

Also, let σ_{ab} and ρ_{ab} represent the "ab" components of g_σ and g_ρ, respectively. Then, in coordinates, the controlled Lagrangian becomes

$$\begin{aligned} L_{\tau,\sigma,\rho}(x^\alpha,\theta^a,\dot{x}^\alpha,\dot{\theta}^a) &= L(x^\alpha,\theta^a,\dot{x}^\alpha,\dot{\theta}^a+\tau^a_\alpha\dot{x}^\alpha)+\frac{1}{2}\sigma_{ab}\tau^a_\alpha\tau^b_\beta\dot{x}^\alpha\dot{x}^\beta \\ &\quad+\frac{1}{2}(\rho_{ab}-g_{ab})\left(\dot{\theta}^a+(g^{ac}g_{c\alpha}+\tau^a_\alpha)\dot{x}^\alpha\right)\left(\dot{\theta}^b+(g^{bd}g_{d\beta}+\tau^b_\beta)\dot{x}^\beta\right) \\ &\quad-\tilde{V}(x^\alpha,\theta^a) \\ &=\frac{1}{2}(g_{\tau,\sigma,\rho})_{\alpha\beta}\dot{x}^\alpha\dot{x}^\beta+(g_{\tau,\sigma,\rho})_{\alpha b}\dot{x}^\alpha\dot{\theta}^b+\frac{1}{2}(g_{\tau,\sigma,\rho})_{ab}\dot{\theta}^a\dot{\theta}^b-V'(x^\alpha,\theta^a). \end{aligned} \tag{4.25}$$

Equation (4.25) introduces the coordinate form of the modified kinetic energy metric $g_{\tau,\sigma,\rho}$. Let

$$B_{\alpha\beta}=g_{\alpha\beta}-g_{\alpha a}g^{ab}g_{b\beta} \tag{4.26}$$

and let

$$A_{\alpha\beta}=B_{\alpha\beta}+\tau^c_\alpha\sigma_{cd}\tau^d_\beta. \tag{4.27}$$

It is readily shown that

$$\begin{aligned} (g_{\tau,\sigma,\rho})_{\alpha\beta} &= A_{\alpha\beta}+(\mathcal{A}^c_\alpha+\tau^c_\alpha)\rho_{cd}(\mathcal{A}^d_\beta+\tau^d_\beta) \\ (g_{\tau,\sigma,\rho})_{\alpha b} &= (\mathcal{A}^c_\alpha+\tau^c_\alpha)\rho_{cb} \\ (g_{\tau,\sigma,\rho})_{ab} &= \rho_{ab}, \end{aligned} \tag{4.28}$$

As may be seen from equation (4.17), $B_{\alpha\beta}$ represents the original horizontal kinetic energy metric. Noting that

$$L_{\tau,\sigma,\rho}=\frac{1}{2}A_{\alpha\beta}\dot{x}^\alpha\dot{x}^\beta+\frac{1}{2}\rho_{ab}\left(\dot{\theta}^a+(\mathcal{A}^a_\alpha+\tau^a_\alpha)\dot{x}^\alpha\right)\left(\dot{\theta}^b+(\mathcal{A}^b_\beta+\tau^b_\beta)\dot{x}^\beta\right)-V'(x^\alpha,\theta^a), \tag{4.29}$$

one sees that $A_{\alpha\beta}$ plays an analogous role as the "τ-horizontal" kinetic energy metric [17].

In the matching process, the terms σ_{ab}, ρ_{ab}, and τ^a_α provide freedom to ensure that no inputs are required in uncontrolled directions. The artificial potential energy term $\tilde{V}(x^\alpha,\theta^a)$ provides more freedom. Still more freedom is introduced by allowing energy-conserving gyroscopic forces in the closed-loop system. After the requirements for matching are satisfied, the modified energy can be used to derive criteria for closed-loop stability. Any remaining freedom in the control parameters can then be used to satisfy these criteria and to tune controller performance.

4.2.3 Matching Conditions

Assume that the Euler-Lagrange equations hold for a mechanical system with Lagrangian

$$L(x^\alpha, \theta^a, \dot{x}^\alpha, \dot{\theta}^a) = \frac{1}{2} g_{\alpha\beta} \dot{x}^\alpha \dot{x}^\beta + g_{\alpha b} \dot{x}^\alpha \dot{\theta}^b + \frac{1}{2} g_{ab} \dot{\theta}^a \dot{\theta}^b - V(x^\alpha, \theta^a). \tag{4.30}$$

The control effort u_a enters in the θ^a direction so that the open-loop equations of motion are

$$\begin{aligned} \frac{d}{dt}\frac{\partial L}{\partial \dot{x}^\alpha} - \frac{\partial L}{\partial x^\alpha} &= 0 \\ \frac{d}{dt}\frac{\partial L}{\partial \dot{\theta}^a} - \frac{\partial L}{\partial \theta^a} &= u_a. \end{aligned} \tag{4.31}$$

Suppose we wish to stabilize an unstable equilibrium

$$(x^\alpha, \theta^a, \dot{x}^\alpha, \dot{\theta}^a)_e = (x_e^\alpha, \theta_e^a, 0, 0) \tag{4.32}$$

for the uncontrolled system (4.31).[2] The method of controlled Lagrangians provides, under certain conditions, a control law u_a for which the closed-loop equations are Lagrangian with respect to a modified Lagrangian $L_{\tau,\sigma,\rho}(x^\alpha, \theta^a, \dot{x}^\alpha, \dot{\theta}^a)$. In prior treatments, the closed-loop Euler-Lagrange equations included no gyroscopic forces. More generally, one may seek conditions under which

$$\begin{aligned} \frac{d}{dt}\frac{\partial L_{\tau,\sigma,\rho}}{\partial \dot{x}^\alpha} - \frac{\partial L_{\tau,\sigma,\rho}}{\partial x^\alpha} &= \mathcal{S}_{\alpha\beta}\dot{x}^\beta + \mathcal{S}_{\alpha b}\dot{\theta}^b \\ \frac{d}{dt}\frac{\partial L_{\tau,\sigma,\rho}}{\partial \dot{\theta}^a} - \frac{\partial L_{\tau,\sigma,\rho}}{\partial \theta^a} &= \mathcal{S}_{a\beta}\dot{x}^\beta + \mathcal{S}_{ab}\dot{\theta}^b, \end{aligned} \tag{4.33}$$

where

$$\boldsymbol{\mathcal{S}} = -\boldsymbol{\mathcal{S}}^T = \begin{pmatrix} [\mathcal{S}_{\alpha\beta}] & [\mathcal{S}_{\alpha b}] \\ [\mathcal{S}_{a\beta}] & [\mathcal{S}_{ab}] \end{pmatrix}. \tag{4.34}$$

The components of $\boldsymbol{\mathcal{S}}$ depend on both the configuration and the velocity. Skew-symmetry of $\boldsymbol{\mathcal{S}}$ ensures that the control-modified energy corresponding to $L_{\tau,\sigma,\rho}$ is conserved; the corresponding generalized forces are referred to as "gyroscopic". The conditions under which equations (4.33) hold

[2] As described in [17], in cases where θ^a is cyclic, one may instead stabilize steady motions of the form $(x^\alpha, \dot{x}^\alpha, \dot{\theta}^a)_e = (x_e^\alpha, 0, \dot{\theta}_e^a)$. Alternatively, one may use feedback to break the symmetry and stabilize to a specific equilibrium configuration.

are the "matching conditions." These conditions ensure that equations (4.33) require no control authority in unactuated directions.

The matching conditions are derived by comparing equations (4.31) and (4.33) and then choosing the control u_a and the energy modification parameters τ, g_σ, and g_ρ so that (4.33) holds. Define the local matrix forms of g and $g_{\tau,\sigma,\rho}$ as follows,

$$\boldsymbol{M} = \begin{pmatrix} [g_{\alpha\beta}] & [g_{\alpha b}] \\ [g_{a\beta}] & [g_{ab}] \end{pmatrix} \quad \text{and} \quad \boldsymbol{M}_{\tau,\sigma,\rho} = \begin{pmatrix} [(g_{\tau,\sigma,\rho})_{\alpha\beta}] & [(g_{\tau,\sigma,\rho})_{\alpha b}] \\ [(g_{\tau,\sigma,\rho})_{a\beta}] & [(g_{\tau,\sigma,\rho})_{ab}] \end{pmatrix}.$$

Also, define the state vector

$$\boldsymbol{q} = \left[q^k\right] = \begin{pmatrix} [x^\alpha] \\ [\theta^a] \end{pmatrix}.$$

Thus $\boldsymbol{q}$ is an $(r+n)$-vector where r is the dimension of $[x^\alpha]$ and n is the dimension of $[\theta^a]$. The open-loop (4.31) and closed-loop equations (4.33) may be written respectively as

$$\begin{pmatrix} [\mathcal{E}_{x^\alpha}(L)] \\ [\mathcal{E}_{\theta^a}(L)] \end{pmatrix} = \boldsymbol{M}\ddot{\boldsymbol{q}} + \boldsymbol{C}\dot{\boldsymbol{q}} + \begin{pmatrix} [V_{,\alpha}] \\ [V_{,a}] \end{pmatrix} = \begin{pmatrix} \boldsymbol{0} \\ [u_a] \end{pmatrix}, \quad \text{and} \tag{4.35}$$

$$\begin{pmatrix} [\mathcal{E}_{x^\alpha}(L_{\tau,\sigma,\rho})] \\ [\mathcal{E}_{\theta^a}(L_{\tau,\sigma,\rho})] \end{pmatrix} = \boldsymbol{M}_{\boldsymbol{\tau,\sigma,\rho}}\ddot{\boldsymbol{q}} + \boldsymbol{C}_{\boldsymbol{\tau,\sigma,\rho}}\dot{\boldsymbol{q}} + \begin{pmatrix} [V'_{,\alpha}] \\ [V'_{,a}] \end{pmatrix} = \boldsymbol{\mathcal{S}}\dot{\boldsymbol{q}}. \tag{4.36}$$

Here, $\boldsymbol{C}_{\tau,\sigma,\rho}$ is the Coriolis and centripetal matrix corresponding to $\boldsymbol{M}_{\tau,\sigma,\rho}$. By convention, commas in subscripts denote partial differentiation. For example, $V_{,a}$ is the partial derivative of V with respect θ^a. Solving for $\ddot{\boldsymbol{q}}$ in (4.35) and substituting into the desired closed-loop equations (4.36) gives

$$\boldsymbol{M}_{\tau,\sigma,\rho}\,\boldsymbol{M}^{-1}\left\{-\boldsymbol{C}\dot{\boldsymbol{q}} + \begin{pmatrix} [-V_{,\alpha}] \\ [-V_{,a} + u_a] \end{pmatrix}\right\} + \boldsymbol{C}_{\tau,\sigma,\rho}\dot{\boldsymbol{q}} + \begin{pmatrix} [V'_{,\alpha}] \\ [V'_{,a}] \end{pmatrix} = \boldsymbol{\mathcal{S}}\dot{\boldsymbol{q}}. \tag{4.37}$$

To find the matching conditions, we partition the input into two components,

$$u_a = u_a^{\mathrm{k/g}}(x^\alpha, \theta^a, \dot{x}^\alpha, \dot{\theta}^a) + u_a^{\mathrm{p}}(x^\alpha, \theta^a), \tag{4.38}$$

and match velocity-dependent and velocity-independent terms separately. The first term $u_a^{\mathrm{k/g}}$ shapes the closed-loop kinetic energy and introduces gyroscopic forces into the closed-loop Euler-Lagrange equations. The second term u_a^{p} shapes the closed-loop potential energy.

Velocity-dependent terms. Referring to equations (4.37), we must find the velocity-dependent component of the control law $\left(u_a^{\mathrm{k/g}}\right)$ and conditions on the system and control parameters such that

$$\boldsymbol{M}_{\tau,\sigma,\rho}\boldsymbol{M}^{-1}\left(\begin{pmatrix}\mathbf{0}\\ \left[u_a^{\mathrm{k/g}}\right]\end{pmatrix}-\boldsymbol{C}\dot{\boldsymbol{q}}\right)+\boldsymbol{C}_{\tau,\sigma,\rho}\dot{\boldsymbol{q}}=\boldsymbol{\mathcal{S}}\dot{\boldsymbol{q}}. \tag{4.39}$$

Motivated by the form of the terms in (4.39), we let

$$\begin{pmatrix}\mathbf{0}\\ \left[u_a^{\mathrm{k/g}}\right]\end{pmatrix}=\boldsymbol{U}(x^\alpha,\theta^a,\dot{x}^\alpha,\dot{\theta}^a)\dot{\boldsymbol{q}} \tag{4.40}$$

where

$$\boldsymbol{U}=\begin{pmatrix}\mathbf{0} & \mathbf{0}\\ [U_{a\beta}] & [U_{ab}]\end{pmatrix}. \tag{4.41}$$

Substituting in equation (4.39), we require

$$\left[\boldsymbol{M}_{\tau,\sigma,\rho}\boldsymbol{M}^{-1}\left(\boldsymbol{U}-\boldsymbol{C}\right)+\boldsymbol{C}_{\tau,\sigma,\rho}-\boldsymbol{\mathcal{S}}\right]\dot{\boldsymbol{q}}=\mathbf{0}$$

for all $\dot{\boldsymbol{q}}\in T_qQ$. Recognizing that $\boldsymbol{C}$ and $\boldsymbol{C}_{\tau,\sigma,\rho}$ are linear in velocity, these are n equations which are quadratic in the components of velocity; these equations provide the necessary and sufficient conditions for matching as well as the functional form of the velocity-dependent control term $u_a^{\mathrm{k/g}}$.

More modest conditions, which are sufficient for matching, are obtained by assuming that $\boldsymbol{U}$ and $\boldsymbol{\mathcal{S}}$ are also linear in velocity and requiring that

$$\boldsymbol{M}_{\tau,\sigma,\rho}\boldsymbol{M}^{-1}\left(\boldsymbol{U}-\boldsymbol{C}\right)+\boldsymbol{C}_{\tau,\sigma,\rho}=\boldsymbol{\mathcal{S}}.$$

By skew symmetry of $\boldsymbol{\mathcal{S}}$, we need

$$\left(\boldsymbol{M}_{\tau,\sigma,\rho}\boldsymbol{M}^{-1}\left(\boldsymbol{U}-\boldsymbol{C}\right)+\boldsymbol{C}_{\tau,\sigma,\rho}\right)+\left(\left(\boldsymbol{U}^T-\boldsymbol{C}^T\right)\left(\boldsymbol{M}_{\tau,\sigma,\rho}\boldsymbol{M}^{-1}\right)^T+\boldsymbol{C}_{\tau,\sigma,\rho}^T\right)=\mathbf{0}. \tag{4.42}$$

Recalling that $\dot{\boldsymbol{M}}_{\tau,\sigma,\rho} - 2\boldsymbol{C}_{\tau,\sigma,\rho}$ is skew symmetric, we may rewrite equation (4.42) as

$$\boldsymbol{M}_{\tau,\sigma,\rho}\boldsymbol{M}^{-1}\left(\boldsymbol{U}-\boldsymbol{C}\right) + \left(\boldsymbol{U}^T - \boldsymbol{C}^T\right)\left(\boldsymbol{M}_{\tau,\sigma,\rho}\boldsymbol{M}^{-1}\right)^T + \dot{\boldsymbol{M}}_{\tau,\sigma,\rho} = \boldsymbol{0}. \tag{4.43}$$

For convenience, define

$$\boldsymbol{\mathcal{M}} = \begin{pmatrix} \left[\mathcal{M}_\alpha^\beta\right] & \left[\mathcal{M}_\alpha^b\right] \\ \left[\mathcal{M}_a^\beta\right] & \left[\mathcal{M}_a^b\right] \end{pmatrix} = \boldsymbol{M}_{\tau,\sigma,\rho}\boldsymbol{M}^{-1}.$$

Also, let tilde denote a component of a transposed matrix; for example, $\left[\tilde{\mathcal{M}}_\alpha^b\right]$ represents the upper right block of $\boldsymbol{\mathcal{M}}^T$. Equation (4.43) implies that

$$0 = (-\mathcal{M}_\alpha^\gamma C_{\gamma\beta} + \mathcal{M}_\alpha^c(U_{c\beta} - C_{c\beta})) + \left(-\tilde{C}_{\alpha\gamma}\tilde{\mathcal{M}}_\beta^\gamma + (\tilde{U}_{\alpha c} - \tilde{C}_{\alpha c})\tilde{\mathcal{M}}_\beta^c\right) + (\dot{\boldsymbol{M}}_{\tau,\sigma,\rho})_{\alpha\beta} \tag{4.44}$$

$$0 = (-\mathcal{M}_\alpha^\gamma C_{\gamma b} + \mathcal{M}_\alpha^c(U_{cb} - C_{cb})) + \left(-\tilde{C}_{\alpha\gamma}\tilde{\mathcal{M}}_b^\gamma + (\tilde{U}_{\alpha c} - \tilde{C}_{\alpha c})\tilde{\mathcal{M}}_b^c\right) + (\dot{\boldsymbol{M}}_{\tau,\sigma,\rho})_{\alpha b} \tag{4.45}$$

$$0 = (-\mathcal{M}_a^\gamma C_{\gamma\beta} + \mathcal{M}_a^c(U_{c\beta} - C_{c\beta})) + \left(-\tilde{C}_{a\gamma}\tilde{\mathcal{M}}_\beta^\gamma + (\tilde{U}_{ac} - \tilde{C}_{ac})\tilde{\mathcal{M}}_\beta^c\right) + (\dot{\boldsymbol{M}}_{\tau,\sigma,\rho})_{a\beta} \tag{4.46}$$

$$0 = (-\mathcal{M}_a^\gamma C_{\gamma b} + \mathcal{M}_a^c(U_{cb} - C_{cb})) + \left(-\tilde{C}_{a\gamma}\tilde{\mathcal{M}}_b^\gamma + (\tilde{U}_{ac} - \tilde{C}_{ac})\tilde{\mathcal{M}}_b^c\right) + (\dot{\boldsymbol{M}}_{\tau,\sigma,\rho})_{ab} \tag{4.47}$$

Solving equation (4.47) for U_{ab}, one finds that it is linear in velocity, since all other terms in (4.47) are linear in velocity. Substituting the solution for U_{ab} into equation (4.45) or (4.46), one obtains the solution for $U_{a\beta}$, which is also linear in velocity. Substituting the control terms U_{ab} and $U_{a\beta}$ into equation (4.44) gives the final conditions for matching. Since each term in (4.44) is linear in velocity, and the identity must hold for any velocity, there are $\frac{1}{2}r(r+1)$ independent equations which are linear in velocity. Since $\dot{x}^\alpha$ and $\dot{\theta}^a$ are independent, each of these $\frac{1}{2}r(r+1)$ equations can be decomposed into $r+n$ independent equations. In all, there are $\frac{1}{2}r(r+1)(r+n)$ partial differential equations. These equations involve the $n(n+r+1)$ unspecified functions τ_α^a, σ_{ab}, and ρ_{ab}, and their first partial derivatives. Matching involves using freedom available in τ_α^a, σ_{ab}, and ρ_{ab} to solve these equations. Ideally, some parametric freedom will remain after the velocity-dependent matching problem has been solved. If so, this freedom can be exploited in later analysis to help obtain conditions for closed-loop stability.

Note, in the procedure described above, that the components of $\boldsymbol{\mathcal{S}}$ do not appear explicitly in

the matching process; $\boldsymbol{\mathcal{S}}$ is a product of the procedure, to be computed after matching has been achieved.

Velocity-independent terms. Since the terms in (4.37) involving the potential energy V are independent of velocity, we require that

$$\boldsymbol{M}_{\tau,\sigma,\rho}\boldsymbol{M}^{-1}\begin{pmatrix}[-V_{,\alpha}]\\ [-V_{,a}+u_a^{\mathrm{p}}]\end{pmatrix}+\begin{pmatrix}[V'_{,\alpha}]\\ [V'_{,a}]\end{pmatrix}=\begin{pmatrix}\mathbf{0}\\ \mathbf{0}\end{pmatrix}. \tag{4.48}$$

Written explicitly in terms of the component matrices

$$\begin{aligned}
&\boldsymbol{M}_{\tau,\sigma,\rho}\boldsymbol{M}^{-1}\\
&=\begin{pmatrix}\left[A_{\alpha\gamma}+(\mathcal{A}^d_\alpha+\tau^d_\alpha)\rho_{de}(\mathcal{A}^e_\gamma+\tau^e_\gamma)\right] & \left[(\mathcal{A}^d_\alpha+\tau^d_\alpha)\rho_{dc}\right]\\ \left[\rho_{ad}(\mathcal{A}^d_\gamma+\tau^d_\gamma)\right] & [\rho_{ac}]\end{pmatrix}\circ\begin{pmatrix}\left[B^{\gamma\beta}\right] & -\left[B^{\gamma\delta}\mathcal{A}^b_\delta\right]\\ -\left[\mathcal{A}^c_\delta B^{\delta\beta}\right] & \left[g^{cb}+\mathcal{A}^c_\delta B^{\delta\nu}\mathcal{A}^b_\nu\right]\end{pmatrix}\\
&=\begin{pmatrix}\left[A_{\alpha\gamma}B^{\gamma\beta}+(\mathcal{A}^d_\alpha+\tau^d_\alpha)\rho_{de}\tau^e_\gamma B^{\gamma\beta}\right] & \left[-A_{\alpha\gamma}B^{\gamma\delta}\mathcal{A}^b_\delta+(\mathcal{A}^c_\alpha+\tau^c_\alpha)\rho_{cd}D^{cb}\right]\\ \left[\rho_{ac}\tau^c_\gamma B^{\gamma\beta}\right] & \left[\rho_{ac}D^{cb}\right]\end{pmatrix}
\end{aligned} \tag{4.49}$$

where

$$D^{ab}=g^{ab}-\tau^a_\gamma B^{\gamma\delta}\mathcal{A}^b_\delta. \tag{4.50}$$

Substituting (4.49) into (4.48), one obtains two equations. The second equation of (4.48) requires that

$$0=\rho_{ac}\tau^c_\gamma B^{\gamma\beta}\left(-V_{,\beta}\right)+\rho_{ac}D^{cb}\left(u^{\mathrm{p}}_b-V_{,b}\right)+V'_{,a}. \tag{4.51}$$

Solving (4.51) for the control law gives

$$u^{\mathrm{p}}_a=V_{,a}+D_{ac}\left(\tau^c_\gamma B^{\gamma\beta}V_{,\beta}-\rho^{cb}V'_{,b}\right) \tag{4.52}$$

The problem remains to find a condition such that the first equation in (4.48) holds under the control law (4.52). As shown in Appendix B, the appropriate "potential matching condition" is the following partial differential equation for $V'(x^\alpha,\theta^a)$:

$$\begin{aligned}
0=\left(V'_{,\alpha}-V_{,\alpha}\right)&-\left(\tau^c_\alpha\sigma_{cd}g^{de}+\mathcal{A}^e_\alpha\right)D_{ef}\tau^f_\gamma B^{\gamma\beta}V_{,\beta}\\
&+\left(\left(\tau^c_\alpha\sigma_{cd}g^{de}+\mathcal{A}^e_\alpha\right)D_{ef}\rho^{fb}-\tau^c_\alpha\sigma_{cd}\rho^{db}-\mathcal{A}^b_\alpha-\tau^b_\alpha\right)V'_{,b}.
\end{aligned} \tag{4.53}$$

Remark 4.2.1 *If the potential energy remains unaltered by feedback ($V' = V$) and is independent of θ^a, then condition (4.53) is satisfied by choosing*

$$\tau_\alpha^a = -\sigma^{ac} g_{c\alpha}.$$

If the potential energy is not modified in the uncontrolled directions ($V'_{,\alpha} = V_{,\alpha}$), then condition (4.53) is satisfied by choosing

$$\tau_\alpha^a = -\sigma^{ac} g_{c\alpha} \qquad \text{and} \qquad \sigma^{ab} + \rho^{ab} = g^{ab}.$$

This choice of τ_α^a is common to several previous matching results, including the "first matching theorem" of [17], the "Euler-Poincaré matching conditions" of [18], and the "general matching conditions" stated in [16]. The choice of ρ_{ab} is common to the "Euler-Poincaré matching conditions" and the "general matching conditions" of [16] where the problem of stabilizing the rotary inverted pendulum was considered. In all these previous cases, the choices were made to satisfy matching conditions for kinetic energy shaping rather than potential energy shaping. Because the term $\boldsymbol{M}_{\tau,\sigma,\rho}\boldsymbol{M}^{-1}$ appears in the kinetic shaping identity (4.39) and the potential shaping identity (4.48) in precisely the same way, it is not surprising that conditions developed for kinetic energy shaping also arise when shaping the potential energy.

4.2.4 The General Strategy

The general procedure to achieve stabilization is outlined below.

1. Start with a mechanical system with a Lagrangian of the form $L = K - V$, where K is the kinetic energy and V is the potential energy, and a symmetry group G.
2. Write down the equations of motion for the uncontrolled system.
3. Introduce τ, g_ρ and g_σ to determine the control-modified kinetic energy $K_{\tau,\sigma,\rho}$ (4.21).
4. Define $V'(q) = V(q) + \tilde{V}(q)$ to be the control-modified potential energy to get the controlled Lagrangian $L_{\tau,\sigma,\rho} = K_{\tau,\sigma,\rho} - V'$.

5. Write down the equations of motion corresponding to the controlled Lagrangian and introduce the gyroscopic force matrix $\boldsymbol{\mathcal{S}}$ in the closed-loop equations.

6. Choose $\tau,\ g_\sigma,\ g_\rho$ so that the open-loop Euler-Lagrange equations (4.31) "match" with the Euler-Lagrange equations corresponding to the $L_{\tau,\sigma,\rho}$ (4.33) using the general kinetic and potential energy matching conditions. Determine the feedback control law u_a by finding the kinetic and potential shaping components, $u_a^{\mathrm{k/g}}$ and u_a^{p} respectively.

7. After the matching process, use the controlled energy $E_{\tau,\sigma,\rho}$ to determine conditions for closed-loop stability. Any freedom in the control parameters can be used to determine the stability conditions and tune the controller performance.

4.2.5 Stability in Presence of Physical Dissipation

To determine how dissipation, either natural or artificial, affects the closed-loop system (4.33), consider a more general version of the open-loop equations (4.31):

$$\begin{aligned} \frac{d}{dt}\frac{\partial L}{\partial \dot{x}^\alpha} - \frac{\partial L}{\partial x^\alpha} &= F_\alpha \\ \frac{d}{dt}\frac{\partial L}{\partial \dot{\theta}^a} - \frac{\partial L}{\partial \theta^a} &= u_a + F_a. \end{aligned} \tag{4.54}$$

The term F_α represents generalized forces which are inherent to the system, such as friction. The term F_a represents some combination of natural forces within the system and user-defined control forces applied to it. With u_a determined according to the procedure described in Section 4.2.3, we consider stability of the equilibrium (4.32), where it is assumed that $F_\alpha = F_a = 0$ at the equilibrium. (See [23] for a general discussion of external forces in controlled Lagrangian and controlled Hamiltonian systems.)

We assume that the control-modified energy $E_{\tau,\sigma,\rho}$ is a Lyapunov function in the conservative setting. That is, the energy and structure shaping control law $u_a = u_a^{\mathrm{k/g}} + u_a^{\mathrm{p}}$ stabilizes the system about a minimum or a maximum of $E_{\tau,\sigma,\rho}$. Under this choice of feedback, the closed-loop dynamics

with the external forces become

$$\begin{pmatrix} [\mathcal{E}_{x^\alpha}(L_{\tau,\sigma,\rho})] \\ [\mathcal{E}_{\theta^a}(L_{\tau,\sigma,\rho})] \end{pmatrix} = \boldsymbol{\mathcal{S}}\dot{\boldsymbol{q}} + \boldsymbol{M}_{\tau,\sigma,\rho}\,\boldsymbol{M}^{-1} \begin{pmatrix} [F_\alpha] \\ [F_a] \end{pmatrix}.$$

Referring to equation (4.49) for $\boldsymbol{M}_{\tau,\sigma,\rho}\boldsymbol{M}^{-1}$, the control-modified energy satisfies

$$\frac{d}{dt}E_{\tau,\sigma,\rho} = \dot{\boldsymbol{q}}^T \boldsymbol{M}_{\tau,\sigma,\rho}\,\boldsymbol{M}^{-1} \begin{pmatrix} [F_\alpha] \\ [F_a] \end{pmatrix} \tag{4.55}$$

$$= \dot{x}^\alpha A_{\alpha\gamma} B^{\gamma\beta}\left(F_\beta - \mathcal{A}^b_\beta F_b\right) + \left(\dot{\theta}^a + \dot{x}^\alpha\left(\mathcal{A}^a_\alpha + \tau^a_\alpha\right)\right)\rho_{ac}\left(D^{cb}F_b + \tau^c_\gamma B^{\gamma\beta}F_\beta\right). \tag{4.56}$$

The desired equilibrium will remain stable in the presence of damping if $\dot{E}_{\tau,\sigma,\rho}$ is semidefinite with opposite sign to $E_{\tau,\sigma,\rho}$.

Remark 4.2.2 ***Feedback dissipation with no physical damping.*** *Suppose that $F_\alpha = 0$ and that F_a can be specified as a dissipative feedback control law. Then*

$$\frac{d}{dt}E_{\tau,\sigma,\rho} = \left(D^{ab}\rho_{bc}\left(\dot{\theta}^c + \left(\mathcal{A}^c_\alpha + \tau^c_\alpha\right)\dot{x}^\alpha\right) - \mathcal{A}^a_\alpha B^{\alpha\beta}A_{\beta\gamma}\dot{x}^\gamma\right)F_a.$$

Therefore, choosing

$$F_a = u^{\text{diss}}_a = k^{\text{diss}}_{ab}\left(D^{bc}\rho_{cd}\left(\dot{\theta}^d + \left(\mathcal{A}^d_\alpha + \tau^d_\alpha\right)\dot{x}^\alpha\right) - \mathcal{A}^d_\alpha B^{\alpha\beta}A_{\beta\gamma}\dot{x}^\gamma\right) \tag{4.57}$$

makes $\dot{E}_{\tau,\sigma,\rho}$ quadratic. The modified energy rate can clearly be made either positive or negative semidefinite, as desired, by choosing k^{diss}_{ab} appropriately. For example, if $E_{\tau,\sigma,\rho}$ is positive definite at the desired equilibrium, one may choose k^{diss}_{ab} negative definite so that $\dot{E}_{\tau,\sigma,\rho}$ will be negative semidefinite. The equilibrium thus remains stable and asymptotic stability may be assessed using LaSalle's invariance principle.

When the system is subject to physical damping, asymptotic stabilization is more subtle. Consider the simplest case of linear damping

$$\begin{pmatrix} [F_\alpha] \\ [F_a] \end{pmatrix} = -\boldsymbol{R}\dot{\boldsymbol{q}}, \tag{4.58}$$

where $\boldsymbol{R}$ is a constant dissipation matrix.

$$\begin{aligned}\frac{d}{dt}E_{\tau,\sigma,\rho} &= -\dot{\boldsymbol{q}}^T \boldsymbol{M}_{\tau,\sigma,\rho}\, \boldsymbol{M}^{-1}\, \boldsymbol{R}\dot{\boldsymbol{q}} \\ &= -\frac{1}{2}\dot{\boldsymbol{q}}^T \left(\boldsymbol{M}_{\tau,\sigma,\rho}\, \boldsymbol{M}^{-1}\, \boldsymbol{R} + \boldsymbol{R}^T\, \boldsymbol{M}^{-1}\, \boldsymbol{M}_{\tau,\sigma,\rho}\right) \dot{\boldsymbol{q}}\end{aligned}$$

If $\boldsymbol{M}_{\tau,\sigma,\rho}$, $\boldsymbol{M}$, and the symmetric part of $\boldsymbol{R}$ are all positive definite, one might expect that

$$\boldsymbol{M}_{\tau,\sigma,\rho}\, \boldsymbol{M}^{-1}\, \boldsymbol{R} + \boldsymbol{R}^T\, \boldsymbol{M}^{-1}\, \boldsymbol{M}_{\tau,\sigma,\rho} > 0 \tag{4.59}$$

and therefore that $\dot{E}_{\tau,\sigma,\rho} \leq 0$. In general, this is *not* the case. Thus, one must take special care when considering the effect of linear damping in systems controlled using kinetic energy shaping feedback. The "inverted pendulum on a cart" example described in Chapter 5 illustrates this issue. The importance of physical damping in general controlled Lagrangian systems is acknowledged in [5]. The issue is also discussed, for special classes of controlled Lagrangian systems, in [82] and [81].

The problem of physical dissipation is not unique to the method of controlled Lagrangians, but arises whenever the kinetic energy metric is modified through feedback, as seen by the example in the following section. As observed in [29], the problem can be understood as a lack of passivity in the closed-loop system. Taking $E_{\tau,\sigma,\rho}$ as the natural storage function, and referring to (4.55), one sees that the passive output for the closed-loop system is $\boldsymbol{M}^{-1}\boldsymbol{M}_{\tau,\sigma,\rho}\dot{\boldsymbol{q}}$. The dissipative forces (4.58) depend on the open-loop passive output $\dot{\boldsymbol{q}}$ rather than the closed-loop passive output. Observing that $\dot{E}_{\tau,\sigma,\rho}$ fails to be negative semidefinite under these damping forces is equivalent to observing that the theorem of passivity does not apply.

4.3 Physical dissipation in the Hamiltonian Setting: "Ball on a beam" example

An alternative control design approach in the Hamiltonian framework, similar in spirit to the method of controlled Lagrangians, is interconnection and damping assignment, passivity based control (IDA-PBC) [54, 73]. In [55] the authors apply the IDA-PBC technique to stabilize a ball

on a servo-actuated beam. Through energy-shaping feedback, the desired equilibrium is made a minimum of a control-modified energy. Although the authors do not consider physical damping in the dynamic model, one might expect that physical damping would decrease the control-modified energy, enhancing closed-loop stability. This is not necessarily true as we show here.

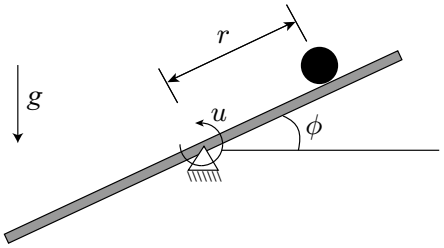

Figure 4.3: The ball on a beam system

The well known "ball on a beam" system is shown in Fig. 4.3 where the control u is applied in the ϕ direction. The control objective is to stabilize the ball at the center with the beam horizontal. The equations of motion, in the absence of physical damping and neglecting rotational inertia of the ball, are

$$\begin{aligned} \ddot{r} + g\sin\phi - r\dot{\phi}^2 &= 0 \\ (ML^2 + r^2)\ddot{\phi} + 2r\dot{r}\dot{\phi} + g\, r\cos\phi &= u, \end{aligned} \tag{4.60}$$

where $M = \frac{m_2}{12m_1}$, m_1 and m_2 being the masses of the ball and beam, respectively, and L is the length of the beam. If we assume Rayleigh dissipation, then the equations in (4.60) take the form

$$\begin{aligned} \ddot{r} + g\sin\phi - r\dot{\phi}^2 + c_1\dot{r} &= 0 \\ (ML^2 + r^2)\ddot{\phi} + 2r\dot{r}\dot{\phi} + g\, r\cos\phi + c_2\dot{\phi} &= u, \end{aligned} \tag{4.61}$$

where c_1 and c_2 are the damping coefficients in the uncontrolled (r) and controlled (ϕ) directions respectively. We introduce nondimensional variables,

$$\hat{r} = \frac{r}{L}; \quad \tau = \omega t; \quad \beta_1 = \frac{c_1}{\omega}; \quad \beta_2 = \frac{c_2}{\omega L^2}; \quad \hat{u} = \frac{u}{gL},$$

where $\omega = \sqrt{g/L}$. The nondimensionalized equations of motion are

$$\begin{aligned} \ddot{r} + \sin\phi - r\dot{\phi}^2 + \beta_1 \dot{r} &= 0 \\ (M + r^2)\ddot{\phi} + 2r\dot{r}\dot{\phi} + r\cos\phi + \beta_2\dot{\phi} &= u, \end{aligned} \tag{4.62}$$

where the derivatives are with respect to τ and the hat over the variables is dropped for convenience. The stabilizing control law for the conservative system ($\beta_1 = \beta_2 = 0$) as presented in [55] is

$$u = u_{\rm es} + u_{\rm di}, \tag{4.63}$$

where the energy shaping control $u_{\rm es}$ and the damping injection $u_{\rm di}$ are given by

$$\begin{aligned} u_{\rm es} &= \frac{r}{\sqrt{2}(1+r^2)}(-\sqrt{1+r^2}\dot{r}^2 + \sqrt{2}(1+r^2)\dot{r}\dot{\phi} + (1+r^2)^{3/2}\dot{\phi}^2) \\ &+ r\cos\phi - \sqrt{2(1+r^2)}\sin\phi - k_{\rm es}\sqrt{\frac{1+r^2}{2}}(\phi - \frac{1}{\sqrt{2}}\text{arcsinh}(r)) \\ u_{\rm di} &= \frac{k_{\rm di}}{1+r^2}(\dot{r} - \sqrt{\frac{2}{1+r^2}}(1+r^2)\dot{\phi}), \end{aligned} \tag{4.64}$$

where $k_{\rm es} > 0$ and $k_{\rm di} > 0$ are the stabilizing control gains. Next, we carry out a spectral analysis to show that addition of physical damping can destabilize the system.

Spectral Analysis

We linearize the equations in (4.62) about the equilibrium $(r, \dot{r}, \phi, \dot{\phi}) = (0, 0, 0, 0)$ to obtain

$$\dot{\boldsymbol{q}} = \boldsymbol{A}\boldsymbol{q}, \tag{4.65}$$

where $\boldsymbol{q} = [r,\ \dot{r},\ \phi,\ \dot{\phi}]^T$ is the state vector and

$$\boldsymbol{A} = \begin{bmatrix} 0 & 1 & 0 & 0 \\ 0 & -\beta_1 & -1 & 0 \\ 0 & 0 & 0 & 1 \\ \frac{k_{\rm es}}{2} & k_{\rm di} & -\frac{2+k_{\rm es}}{\sqrt{2}} & -\sqrt{2}\,k_{\rm di} - \beta_2 \end{bmatrix}. \tag{4.66}$$

The eigenvalues, s, of $\boldsymbol{A}$ satisfy the following fourth-order polynomial

$$s^4 + p_3 s^3 + p_2 s^2 + p_1 s + p_0 = 0, \tag{4.67}$$

where the coefficients are

$$\begin{aligned} p_0 &\equiv \frac{k_{\rm es}}{2}, \\ p_1 &\equiv k_{\rm di} + \frac{(2+k_{\rm es})\beta_1}{\sqrt{2}}, \\ p_2 &\equiv \frac{2+k_{\rm es}}{\sqrt{2}} + \sqrt{2}k_{\rm di}\beta_1 + \beta_1\beta_2, \\ p_3 &\equiv \sqrt{2}k_{\rm di} + \beta_1 + \beta_2. \end{aligned} \tag{4.68}$$

Necessary conditions for all eigenvalues to have negative real parts are

$$p_0 > 0, \quad p_1 > 0, \quad p_2 > 0, \quad \text{and} \quad p_3 > 0. \tag{4.69}$$

Since $k_{\rm es},\ k_{\rm di},\ \beta_1,\ \beta_2 > 0$, the above necessary conditions are satisfied. Routh's criterion gives the other necessary conditions for exponential stability,

$$\begin{aligned} \delta \equiv p_2 p_3 - p_1 &> 0 \\ \delta_1 \equiv \delta\, p_1 - p_3^2\, p_0 &> 0. \end{aligned} \tag{4.70}$$

Equations (4.68) give

$$\begin{aligned} \delta &= 2k_{\rm di}^2\beta_1 + \frac{2+k_{\rm es}}{\sqrt{2}}\beta_2 + \beta_1\beta_2(\beta_1+\beta_2) + k_{\rm di}(1 + k_{\rm es} + \sqrt{2}\beta_1(\beta_1+2\beta_2)) \\ \delta_1 &= \delta\, k_{\rm di} + \frac{(2+k_{\rm es})\beta_1}{\sqrt{2}} - \frac{k_{\rm es}}{2}(\sqrt{2}k_{\rm di} + \beta_1 + \beta_2)^2. \end{aligned} \tag{4.71}$$

It is clear that $\delta > 0$. It remains to check whether $\delta_1 > 0$ to guarantee exponential stability.

Proposition 4.3.1 *Defining u according to the control law presented in [55] using the values of $k_{\rm es}$ and $k_{\rm di}$ which stabilize the conservative model ($k_{\rm es} > 0$ and $k_{\rm di} > 0$), there exist positive values of β_1 and β_2 that make the closed-loop system (4.62) unstable.*

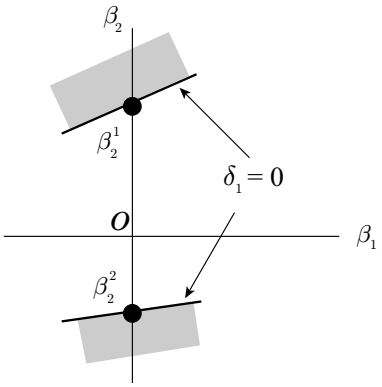

Figure 4.4: A schematic of the stability boundaries for the ball on the beam system.

Proof: It is clear from Eq. 4.71 that δ_1 is quadratic in β_2. Thus for a given β_1 and the pair $(k_{\rm es},\ k_{\rm di})$, there are two or no real roots to the equation $\delta_1(\beta_2) = 0$. When $\beta_1 = 0$, the equation $\delta_1 = 0$ can be solved to give the two roots,

$$\begin{aligned} \beta_2^1 &= \frac{\sqrt{2}k_{\rm di}(2-k_{\rm es}) + \sqrt{(\sqrt{2}k_{\rm di}(2-k_{\rm es}))^2 + 8k_{\rm es}k_{\rm di}^2}}{2k_{\rm es}} \\ \beta_2^2 &= \frac{\sqrt{2}k_{\rm di}(2-k_{\rm es}) - \sqrt{(\sqrt{2}k_{\rm di}(2-k_{\rm es}))^2 + 8k_{\rm es}k_{\rm di}^2}}{2k_{\rm es}}. \end{aligned} \tag{4.72}$$

It is clear that $\beta_2^1 > 0$ and $\beta_2^2 < 0$ for $k_{\rm es},\ k_{\rm di} > 0$. Since δ_1 is quadratic in β_2 and because of continuity of δ_1 in β_1, the curves $\delta_1 = 0$ will intersect the $\beta_1 = 0$ axis transversely at the points $(0, \beta_2^1)$ and $(0, \beta_2^2)$. This is schematically shown in Fig. 4.4. Note that the curves $\delta_1 = 0$ determine stability boundaries in the $(\beta_1,\ \beta_2)$ parameter space. Also, when $\beta_1 = \beta_2 = 0$,

$$\delta_1(0,0) = k_{\rm di}^2 > 0.$$

Thus the origin in the $(\beta_1,\ \beta_2)$ parameter space lies in the region of stabilizing damping values for $k_{\rm di} \neq 0$. Shaded regions in Fig. 4.4 represent destabilizing values of β_1 and β_2. Since $\beta_2^1 > 0$ and the curve $\delta_1 = 0$ intersects the $\beta_1 = 0$ axis transversely, there always exist values of β_1 and β_2 that make the closed-loop system (4.62) *unstable*. ■

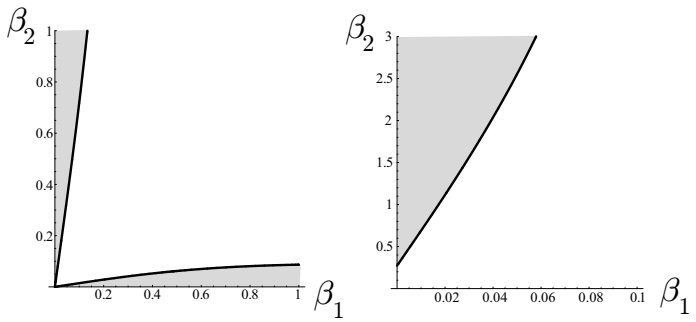

Figure 4.5: Stable and unstable values of damping coefficients for $M = 1$. (a) $k_{\text{es}} = 1$ and $k_{\text{di}} = 0$. (b) $k_{\text{es}} = 0.1$ and $k_{\text{di}} = 0.01$. Shaded regions represent destabilizing values of damping coefficients.

Figure 4.5 shows regions of unstable damping values for different gain values. Without damping injection (Case (a)), physically reasonable values of the damping constant β_1 destabilize the closed-loop system. For this example, one may tune the feedback gains so that physical damping in the unactuated direction does not destabilize the system. However, the example illustrates that asymptotic stability is not "automatic". *Simply ensuring that the desired equilibrium is a minimum of the control-modified energy does not ensure stability when there is physical damping.*

We conclude this chapter by summarizing the general matching and stabilization procedure.

4.4 A Quick Summary of the Matching Conditions

The open-loop Euler-Lagrange equations are written as

$$\boldsymbol{M}(\boldsymbol{q})\ddot{\boldsymbol{q}} + \boldsymbol{C}(\boldsymbol{q}, \dot{\boldsymbol{q}})\dot{\boldsymbol{q}} + \frac{\partial V}{\partial \boldsymbol{q}} = \boldsymbol{G}\boldsymbol{u}. \tag{4.73}$$

The method of controlled Lagrangians provides a control law for which the closed-loop equations become

$$\boldsymbol{M}_c(\boldsymbol{q})\ddot{\boldsymbol{q}} + \boldsymbol{C}_c(\boldsymbol{q}, \dot{\boldsymbol{q}})\dot{\boldsymbol{q}} + \frac{\partial V_c}{\partial \boldsymbol{q}} = \boldsymbol{\mathcal{S}}_c(\boldsymbol{q}, \dot{\boldsymbol{q}})\dot{\boldsymbol{q}}. \tag{4.74}$$

Comparing the open-loop and closed-loop equations above gives

$$\boldsymbol{\mathcal{S}}_c\dot{\boldsymbol{q}} = \boldsymbol{M}_c\boldsymbol{M}^{-1}\left(\boldsymbol{G}\boldsymbol{u} - \boldsymbol{C}\dot{\boldsymbol{q}} - \frac{\partial V}{\partial \boldsymbol{q}}\right) + \boldsymbol{C}_c\dot{\boldsymbol{q}} + \frac{\partial V_c}{\partial \boldsymbol{q}}. \tag{4.75}$$

Partition the control $\boldsymbol{u}$ as

$$\boldsymbol{u}(\boldsymbol{q},\dot{\boldsymbol{q}}) = \boldsymbol{u}^{\mathrm{k/g}}(\boldsymbol{q},\dot{\boldsymbol{q}}) + \boldsymbol{u}^{\mathrm{p}}(\boldsymbol{q}),$$

where $\boldsymbol{u}^{\mathrm{k/g}}$ is the kinetic shaping component and $\boldsymbol{u}^{\mathrm{p}}$ is the potential shaping component. Collecting the velocity dependent terms in (4.75) gives the kinetic matching condition

$$\boldsymbol{\mathcal{S}}_c\dot{\boldsymbol{q}} = \boldsymbol{M}_c\boldsymbol{M}^{-1}(\boldsymbol{G}\boldsymbol{u}^{\mathrm{k/g}} - \boldsymbol{C}\dot{\boldsymbol{q}}) + \boldsymbol{C}_c\dot{\boldsymbol{q}}. \tag{4.76}$$

Assuming $\boldsymbol{u}^{\mathrm{k/g}}$ to be quadratic in velocity, we may write

$$\boldsymbol{G}\boldsymbol{u}^{\mathrm{k/g}} = \boldsymbol{U}(\boldsymbol{q},\dot{\boldsymbol{q}})\dot{\boldsymbol{q}},$$

where the non-zero components of the matrix $\boldsymbol{U}$ are linear in velocity. Equation (4.76) becomes

$$\boldsymbol{\mathcal{S}}_c\dot{\boldsymbol{q}} = (\boldsymbol{M}_c\boldsymbol{M}^{-1}(\boldsymbol{U} - \boldsymbol{C}) + \boldsymbol{C}_c)\dot{\boldsymbol{q}}.$$

Skew-symmetry of $\boldsymbol{\mathcal{S}}_c$ implies

$$\dot{\boldsymbol{q}}^T(\boldsymbol{M}_c\boldsymbol{M}^{-1}(\boldsymbol{U} - \boldsymbol{C}) + \boldsymbol{C}_c)\dot{\boldsymbol{q}} = 0. \tag{4.77}$$

The scalar equation (4.77) represents the kinetic matching condition. It is cubic in velocity. Because the closed-loop dynamics are unconstrained, we may collect coefficients of velocity terms and set each to zero. Eliminating the control components from these equations gives the matching conditions. The matching conditions are solved to give $\boldsymbol{M}_c$. Then, one may solve for the control component $\boldsymbol{u}^{\mathrm{k/g}}$. The elements of $\boldsymbol{\mathcal{S}}_c$ are found by using (4.76).

Having solved the kinetic matching condition, one collects the velocity independent terms in (4.75) to give the potential matching condition as

$$\boldsymbol{M}_c\boldsymbol{M}^{-1}\left(\boldsymbol{G}\boldsymbol{u}^{\mathrm{p}} - \frac{\partial V}{\partial \boldsymbol{q}}\right) + \frac{\partial V_c}{\partial \boldsymbol{q}} = 0. \tag{4.78}$$

Equation (4.78) is solved for the unknowns V_c and $\boldsymbol{u}^{\mathrm{p}}$. Any freedom in $\boldsymbol{M}_c$ and $\boldsymbol{\mathcal{S}}_c$ may be used to solve the potential matching condition.

Alternatively, comparing the open-loop and closed-loop equations, we may write

$$\boldsymbol{G}\boldsymbol{u} = \boldsymbol{M}\boldsymbol{M}_c^{-1}\left(\boldsymbol{\mathcal{S}}_c\dot{\boldsymbol{q}} - \boldsymbol{C}_c\dot{\boldsymbol{q}} - \frac{\partial V_c}{\partial \boldsymbol{q}}\right) + \boldsymbol{C}\dot{\boldsymbol{q}} + \frac{\partial V}{\partial \boldsymbol{q}}. \tag{4.79}$$

If $\boldsymbol{G}^{\perp}$ denotes the left annihilator of $\boldsymbol{G}$, then $\boldsymbol{G}^{\perp}\boldsymbol{G} = 0$. Left multiplying (4.79) by $\boldsymbol{G}^{\perp}$ gives

$$\boldsymbol{G}^{\perp}\left[\boldsymbol{M}\boldsymbol{M}_c^{-1}\left(\boldsymbol{\mathcal{S}}_c\dot{\boldsymbol{q}} - \boldsymbol{C}_c\dot{\boldsymbol{q}} - \frac{\partial V_c}{\partial \boldsymbol{q}}\right) + \boldsymbol{C}\dot{\boldsymbol{q}} + \frac{\partial V}{\partial \boldsymbol{q}}\right] = 0. \tag{4.80}$$

Collecting the velocity dependent terms in (4.80) gives the kinetic matching condition

$$\boldsymbol{G}^{\perp}\left[\boldsymbol{M}\boldsymbol{M}_c^{-1}\left(\boldsymbol{\mathcal{S}}_c\dot{\boldsymbol{q}} - \boldsymbol{C}_c\dot{\boldsymbol{q}}\right) + \boldsymbol{C}\dot{\boldsymbol{q}}\right] = 0. \tag{4.81}$$

Equation (4.81) is a set of $n = \dim \boldsymbol{q}_{\mathrm{u}}$ equations quadratic in velocity. Setting the coefficients of the velocity terms to zero gives the matching conditions. Having solved the matching conditions for $\boldsymbol{M}_c$ and $\boldsymbol{\mathcal{S}}_c$, one collects the velocity independent terms in (4.80) to give the potential matching condition,

$$\boldsymbol{G}^{\perp}\left[\boldsymbol{M}\boldsymbol{M}_c^{-1}\left(-\frac{\partial V_c}{\partial \boldsymbol{q}}\right) + \frac{\partial V}{\partial \boldsymbol{q}}\right] = 0. \tag{4.82}$$

The potential matching conditions are a set of $n = \dim \boldsymbol{q}_{\mathrm{u}}$ partial differential equations in V_c. Having solved the potential matching condition for V_c, we obtain the control law as

$$\boldsymbol{u} = (\boldsymbol{G}^T\,\boldsymbol{G})^{-1}\boldsymbol{G}^T\left[\boldsymbol{M}\boldsymbol{M}_c^{-1}(\boldsymbol{\mathcal{S}}_c\dot{\boldsymbol{q}} - \boldsymbol{C}_c\dot{\boldsymbol{q}} - \frac{\partial V_c}{\partial \boldsymbol{q}}) + \boldsymbol{C}\dot{\boldsymbol{q}} + \frac{\partial V}{\partial \boldsymbol{q}}\right], \tag{4.83}$$

where $\boldsymbol{G}^T$ is the transpose of $\boldsymbol{G}$.

Following matching, one may study closed-loop stability of equilibria by treating the control-modified total energy

$$E_c(\boldsymbol{q}, \dot{\boldsymbol{q}}) = \frac{1}{2}\dot{\boldsymbol{q}}^T\boldsymbol{M}_c(\boldsymbol{q})\dot{\boldsymbol{q}} + V_c(\boldsymbol{q})$$

as a control Lyapunov function. Having found control parameters such that a given equilibrium is a minimum (or a maximum) of E_c, one may apply feedback dissipation to make $\dot{E}_c \leq 0$ (or $\dot{E}_c \geq 0$). One may then assess asymptotic stability using LaSalle's principle.

Chapter 5

Example: Inverted Pendulum on a Cart

The ubiquitous pendulum on a cart ..

To illustrate the results of § 4.2.3 and § 4.2.5, and to maintain continuity with previous work, we consider the problem of stabilizing an inverted pendulum on a cart. In [17], the "simplified matching conditions" led to a choice of feedback which recovered a closed-loop Lagrangian system with no gyroscopic forces. Conservation of the modified total energy and the modified translational momentum allowed the construction of a control Lyapunov function for the desired equilibrium. There, the desired equilibrium was the pendulum in the upright position with the cart moving at a prescribed constant velocity. Conservation of the translational momentum was used to reduce the order of the dynamics, and the desired equilibrium was shown to be a maximum of the closed-loop potential energy and of the horizontal component of the closed-loop kinetic energy.

In [10], the approach was made more powerful by introducing an additional control term to modify the closed-loop potential energy. The modified potential energy broke the symmetry, and the translational momentum was no longer conserved. In this case, the desired equilibrium, corresponding to

the pendulum in the upright position and the cart at rest at the origin, was made into a maximum of the closed-loop energy.

Here, we go a step further by allowing gyroscopic forces in the closed-loop system. The desired equilibrium, corresponding to the pendulum in the upright position and the cart at rest at the origin, becomes a minimum of the control-modified total energy. The basin of stability is the set of states for which the pendulum is elevated above the horizontal line through its pivot.

This same example has been considered in numerous other papers on energy shaping, including [3], [6], and [30]. Two features of our control design and analysis distinguish our treatment from others. First, the closed-loop Lagrangian system includes artificial gyroscopic forces, illustrating that such energy-conserving forces can play a useful role in the matching process. Second, we consider the issue of physical damping and its effect on the closed-loop dynamics. As the example illustrates, such analysis is crucial if one wishes to implement a feedback control law which modifies a system's kinetic energy.

The organization of the chapter is as follows. In § 5.1, we apply the method of controlled Lagrangians to the conservative cart-pendulum model. In § 5.2, the effect of physical dissipation on closed-loop stability is considered. Experimental results are reported in § 5.3.

5.1 Conservative Model

The "inverted pendulum on a cart" was introduced in § 3.2.1 to illustrate some concepts from geometric mechanics. In this section, we revisit the cart-pendulum system and apply the control technique outlined in Chapter 4. The inverted pendulum on a cart is depicted in Figure 5.1. The configuration space is $Q = S^1 \times \mathbb{R}$. The coordinates of any point $q \in Q$ are $(\phi, s) \in S^1 \times \mathbb{R}$, where ϕ is the pendulum angle and s is the cart location. A control force u is applied along the group direction, that is, along the cart direction. As seen in § 3.2.1, the uncontrolled dynamics are invariant under the action of $G = \mathbb{R}$ on Q.

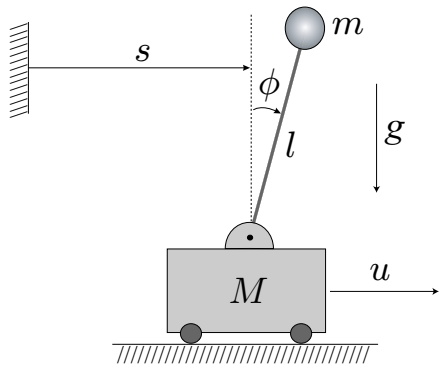

Figure 5.1: The inverted pendulum on a cart system.

The uncontrolled Lagrangian L for the cart-pendulum system is

$$L(\phi, s, \dot{\phi}, \dot{s}) == \frac{1}{2} \begin{pmatrix} \dot{\phi} \\ \dot{s} \end{pmatrix}^T \begin{pmatrix} ml^2 & ml\cos\phi \\ ml\cos\phi & M+m \end{pmatrix} \begin{pmatrix} \dot{\phi} \\ \dot{s} \end{pmatrix} - mgl\cos\phi, \tag{5.1}$$

where l is the pendulum length, m is the pendulum mass and M is the cart mass. We introduce the following nondimensional variables,

$$\bar{L} = \frac{L}{mgl}, \qquad \bar{s} = \frac{s}{l}, \qquad \gamma = \frac{M+m}{m}, \qquad \text{and} \qquad T = \omega t \qquad \text{where} \qquad \omega = \sqrt{\frac{g}{l}}. \tag{5.2}$$

We denote differentiation with respect to nondimensional time T with an overdot. Using the notation of [17], and dropping the overbar, the nondimensional Lagrangian is

$$L = \frac{1}{2} \begin{pmatrix} \dot{\phi} \\ \dot{s} \end{pmatrix}^T \begin{pmatrix} 1 & \cos\phi \\ \cos\phi & \gamma \end{pmatrix} \begin{pmatrix} \dot{\phi} \\ \dot{s} \end{pmatrix} - \cos\phi.$$

In the conservative setting, the open-loop equations of motion for this system are

$$\begin{pmatrix} \mathcal{E}_\phi(L) \\ \mathcal{E}_s(L) \end{pmatrix} = \begin{pmatrix} 0 \\ u \end{pmatrix}.$$

For the cart-pendulum system, following the notation in Chapter 4, we have

$$[g_{ab}] = \gamma \quad \text{and} \quad [g_{\alpha b}] = \cos\phi.$$

The connection coefficient is thus a scalar,

$$[\mathcal{A}^a_\alpha] = [g^{ab}][g_{\alpha b}] = \frac{1}{\gamma}\cos\phi,$$

and the vertical and horizontal vectors are respectively

$$\text{Ver } \boldsymbol{v}_q = (0,\ \dot{s} + \frac{1}{\gamma}\cos\phi\ \dot{\phi}) \ \text{ and } \ \text{Hor } \boldsymbol{v}_\text{q} = (\dot{\phi},\ -\frac{1}{\gamma}\cos\phi\ \dot{\phi}).$$

Because this is a two-degree-of-freedom problem, we may define the scalar parameters

$$\tau = [\tau^a_\alpha]\,, \qquad \sigma = [\sigma_{ab}]\,, \qquad \text{and} \qquad \rho = [\rho_{ab}]$$

without ambiguity. From (4.28), the modified kinetic energy metric is

$$\boldsymbol{M}_{\tau,\sigma,\rho} = \begin{pmatrix} \left(1 - \frac{1}{\gamma}\cos^2\phi\right) + \sigma\tau^2 + \rho\left(\tau + \frac{1}{\gamma}\cos\phi\right)^2 & \rho\left(\tau + \frac{1}{\gamma}\cos\phi\right) \\ \rho\left(\tau + \frac{1}{\gamma}\cos\phi\right) & \rho \end{pmatrix}. \tag{5.3}$$

As described at the end of Section 4.2.3, we first compute the terms U_{ab} and $U_{a\beta}$ from (4.46) and (4.47). We then consider the two PDEs obtained from (4.44). To preserve symmetry in the modified kinetic energy, τ, σ, and ρ are independent of the cart position s. The two PDEs reduce to a single ODE in the three unknown functions τ, σ, and ρ. As a two degree of freedom, single-input system, the cart-pendulum problem is obviously quite special. In general, solving the $\frac{1}{2}r(r+1)(r+n)$ PDEs for matching may be challenging.

Aided by Mathematica, one finds that the following choices satisfy the equation:

$$\begin{aligned} \tau &= \frac{2}{\cos\phi}, \\ \sigma &= \frac{4 - \left(2 + \cos^3\phi\right)\left(1 - \frac{1}{\gamma}\cos^2\phi\right)}{4\cos\phi}, \ \text{ and} \\ \rho &= \frac{2}{\cos\phi\left(1 - \frac{1}{\gamma}\cos^2\phi\right)}. \end{aligned}$$

For this matching solution, no parametric freedom remains in the control-modified kinetic energy. Remarkably, the closed-loop kinetic energy metric is positive definite and the parametric freedom obtained through potential shaping is sufficient to allow stabilization.

The velocity-dependent component of the energy shaping control law is

$$u^{\mathrm{k/g}} = \frac{1}{2\left(\gamma + \cos^2\phi\right)^2}\Big(\left(\gamma^2\left(5\gamma - 4\cos^2\phi\right)\sec\phi\tan\phi - 3\left(5\gamma + 2\cos^2\phi\right)\sin\phi\cos^2\phi\right)\dot{\phi}^2 + \left(\gamma^2\left(\gamma - 2\cos^2\phi\right)\tan\phi - 3\gamma\sin\phi\cos^3\phi\right)\dot{\phi}\dot{s}\Big). \tag{5.4}$$

Next, solving the potential shaping PDE (4.53) and substituting the solution into (4.52), we find that we may choose

$$u^{\mathrm{p}} = \frac{1}{2\left(\gamma + \cos^2\phi\right)}\left(4\gamma^2\tan\phi + \cos\phi\left(\gamma - \cos^2\phi\right)^2\frac{dv(\varphi(\phi,s))}{d\varphi}\right), \tag{5.5}$$

where $v(\cdot)$ is an arbitrary C^1 function and where

$$\varphi(\phi,s) = s + 6\,\mathrm{arctanh}\left(\tan\left(\frac{\phi}{2}\right)\right).$$

Note that φ is well-defined for all s and for all $\phi \in (-\frac{\pi}{2},\frac{\pi}{2})$. The input u^{p} effectively alters the system's potential energy; the modified potential function is

$$V'(\phi,s) = \left(\left(\frac{1}{\cos^2\phi} - 1\right) + v(\varphi(\phi,s))\right).$$

Figure (5.2) shows level sets of the modified potential energy with $v(\varphi) = \frac{1}{2}\kappa\varphi^2$ and with $\kappa = 0.5$.

Letting

$$u = u^{\mathrm{k/g}} + u^{\mathrm{p}}, \tag{5.6}$$

the closed-loop equations of motion are

$$\begin{pmatrix}\mathcal{E}_\phi(L_{\tau,\sigma,\rho})\\ \mathcal{E}_s(L_{\tau,\sigma,\rho})\end{pmatrix} = \begin{pmatrix}0 & \varsigma\\ -\varsigma & 0\end{pmatrix}\begin{pmatrix}\dot{\phi}\\ \dot{s}\end{pmatrix},$$

where the control-modified Lagrangian is

$$L_{\tau,\sigma,\rho} = \frac{1}{2}\begin{pmatrix}\dot{\phi}\\ \dot{s}\end{pmatrix}^T \boldsymbol{M}_{\tau,\sigma,\rho}\begin{pmatrix}\dot{\phi}\\ \dot{s}\end{pmatrix} - V'(\phi,s),$$

and where

$$\varsigma = -\frac{\gamma}{(\gamma - \cos^2\phi)^2}\left(\left(\gamma - 3\cos^2\phi\right)\sec^2\phi\tan\phi(3\dot{\phi} + \dot{s}\cos\phi)\right). \tag{5.7}$$

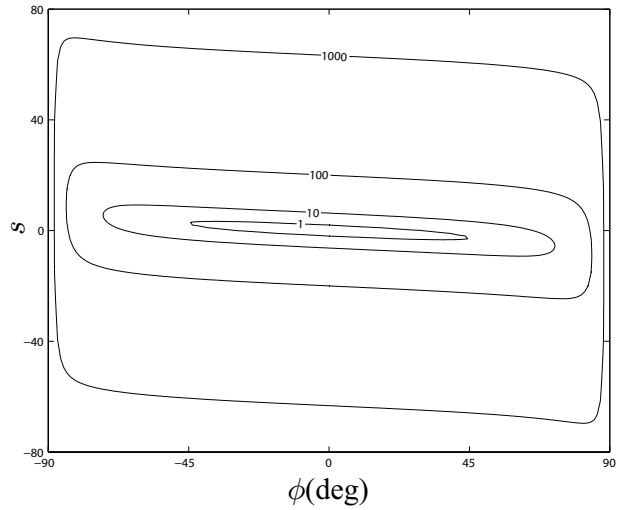

Figure 5.2: Level sets of $V'(\phi, s)$.

Proposition 5.1.1 *The control law (5.6), with $u^{\mathrm{k/g}}$ given by (5.4) and u^{p} given by (5.5), and with*

$$v(\varphi) = \frac{1}{2}\kappa\,\varphi^2, \tag{5.8}$$

stabilizes the equilibrium at the origin provided $\kappa > 0$. Moreover, for all initial states in the set

$$W = \{(\phi, s, \dot{\phi}, \dot{s}) \in S^1 \times \mathbb{R}^3 \mid |\phi| < \frac{\pi}{2}\}, \tag{5.9}$$

trajectories exist for all time and are confined to compact, invariant, level sets of the modified total energy

$$E_{\tau,\sigma,\rho} = \frac{1}{2}\begin{pmatrix}\dot{\phi}\\ \dot{s}\end{pmatrix}^T \boldsymbol{M}_{\tau,\sigma,\rho}\begin{pmatrix}\dot{\phi}\\ \dot{s}\end{pmatrix} + \left(\left(\frac{1}{\cos^2\phi} - 1\right) + v(\varphi(\phi, s))\right). \tag{5.10}$$

Proof : The desired equilibrium is a strict minimum of the control-modified energy, which is conserved under the closed-loop dynamics. Thus $E_{\tau,\sigma,\rho}$ is a Lyapunov function and stability of the origin follows by Lyapunov's second method. Level sets of $E_{\tau,\sigma,\rho}$ which are contained in W are invariant because $E_{\tau,\sigma,\rho}$ is conserved. To check that these level sets are compact, apply the change

of coordinates

$$(\phi, s, \dot{\phi}, \dot{s}) \mapsto (\chi, s, \dot{\chi}, \dot{s}),$$

where $\chi = \tan\phi$. This change of variables defines a diffeomorphism from W to $\mathbb{R}^4$. In the transformed coordinates, the control-modified energy $E_{\tau,\sigma,\rho}$ is radially unbounded. It follows that the level sets of $E_{\tau,\sigma,\rho}$ contained in W are compact; see [40]. ■

5.1.1 Conservative Model with Feedback Dissipation

Next, we apply dissipative feedback, as described in Remark 4.2.2. The complete feedback control law is

$$u = u^{\mathrm{k/g}} + u^{\mathrm{p}} + u^{\mathrm{diss}}. \tag{5.11}$$

Setting

$$u^{\mathrm{diss}} = k_{\mathrm{diss}} \left(-\frac{2\sec^2\phi(\gamma + \cos^2\phi)(3\dot{\phi} + \dot{s}\cos\phi)}{(\gamma - \cos^2\phi)^2} \right), \tag{5.12}$$

where k_{diss} is a dimensionless dissipative control gain, gives

$$\dot{E}_{\tau,\sigma,\rho} = k_{\mathrm{diss}} \left(\frac{2\sec^2\phi(\gamma + \cos^2\phi)(3\dot{\phi} + \dot{s}\cos\phi)}{(\gamma - \cos^2\phi)^2} \right)^2. \tag{5.13}$$

Choosing $k_{\mathrm{diss}} < 0$ makes $\dot{E}_{\tau,\sigma,\rho}$ negative semidefinite.

Proposition 5.1.2 *The control law (5.11), with $u^{\mathrm{k/g}}$ and u^{p} given as in Proposition 5.1.1 and with u^{diss} given by (5.12), asymptotically stabilizes the origin provided $k_{\mathrm{diss}} < 0$. The region of attraction is the set W (5.9) of states for which the pendulum is elevated above the horizontal plane.*

Proof : The proof is given in Appendix C. ■

5.2 Dissipative Model

We have shown that one may choose κ to make the equilibrium a strict minimum of the control-modified energy $E_{\tau,\sigma,\rho}$. We have also shown that one may choose k_{diss} to drive $E_{\tau,\sigma,\rho}$ to that

minimum value, in the absence of other dissipative forces. Interestingly, when $k_{\text{diss}} = 0$ and physical damping is present, the control law does not provide asymptotic stability. Suppose a damping force opposes the cart's motion in proportion to the cart's velocity. Suppose also that a damping moment opposes the pendulum's motion in proportion to the pendulum angular rate. This simple linear damping destabilizes the inverted equilibrium unless it is properly countered through feedback. This phenomenon is consistent with previous control designs based on the method of controlled Lagrangians, as discussed in [82].

Assume that the closed-loop system described in Section 5.1 is subject to (nondimensional) dissipative external forces of the form

$$[F_\alpha] = -d_\phi \dot{\phi} \qquad \text{and} \qquad [F_a] = -d_s \dot{s}, \tag{5.14}$$

where d_ϕ and d_s are dimensionless damping constants. We assume that $d_\phi > 0$. The value of d_s, on the other hand, can be modified directly through feedback. Indeed, one may impose arbitrary dissipative forces in the controlled directions and may thus modify the components in the bottom row of the matrix $\boldsymbol{R}$ through feedback. Regardless, it can be shown that there is *no* choice of linear feedback dissipation which makes inequality (4.59) hold for this example. We prove the following result.

Lemma 5.2.1 *Given real, symmetric matrices*

$$\boldsymbol{M} = \begin{pmatrix} a & b \\ b & c \end{pmatrix} > 0 \quad \text{and} \quad \boldsymbol{M}_c = \begin{pmatrix} \alpha & \beta \\ \beta & \chi \end{pmatrix} > 0$$

and

$$\boldsymbol{R} = \begin{pmatrix} r_1 & 0 \\ 0 & r_2 \end{pmatrix},$$

where $r_1 > 0$, there exists a range of values of r_2 such that

$$\Big(\big(\boldsymbol{M}_c \boldsymbol{M}^{-1} \boldsymbol{R} \big) + \big(\boldsymbol{M}_c \boldsymbol{M}^{-1} \boldsymbol{R} \big)^T \Big) > 0 \tag{5.15}$$

if and only if

$$a\chi - b\beta > 0, \quad c\alpha - b\beta > 0, \quad \text{and}$$
$$b\beta(c\alpha + a\chi) + ac(\beta^2 - 2\alpha\chi) + b^2(2\beta^2 - \alpha\chi) < 0.$$

Proof: Let $\boldsymbol{Q} = \frac{1}{2}\left(\left(\boldsymbol{M}_c\boldsymbol{M}^{-1}\boldsymbol{R}\right) + \left(\boldsymbol{M}_c\boldsymbol{M}^{-1}\boldsymbol{R}\right)^T\right)$. If $\boldsymbol{K}$ is any nonsingular matrix of compatible dimensions, then $\boldsymbol{Q} > 0 \Leftrightarrow \boldsymbol{K}^T\boldsymbol{Q}\boldsymbol{K} > 0$. Note that $\boldsymbol{M},\ \boldsymbol{M}_c$ are both nonsingular. Let

$$\boldsymbol{Q}^1 = \boldsymbol{K}^T\boldsymbol{Q}\boldsymbol{K},$$

where $\boldsymbol{K} = \boldsymbol{M}_c^{-1}\boldsymbol{M}$. Note that $\boldsymbol{Q} > 0 \Leftrightarrow \bar{\boldsymbol{Q}} > 0$. Calculating the elements of $\boldsymbol{Q}$, we get

$$\begin{aligned} Q_{11} &= \frac{r_1(c\alpha - b\beta)}{ac - b^2}, \\ Q_{22} &= \frac{r_2(a\chi - b\beta)}{ac - b^2}, \\ \mathrm{Det}(\boldsymbol{Q}) &= -\frac{1}{4(ac - b^2)^2}(Ar_2^2 + Br_2 + C), \end{aligned} \tag{5.16}$$

where

$$\begin{aligned} A &= (b\alpha - a\beta)^2, \\ B &= 2r_1(b\beta(c\alpha + a\chi) + ac(\beta^2 - 2\alpha\chi) + b^2(a\chi - 2\beta^2)), \\ C &= r_1^2(c\beta - b\chi)^2. \end{aligned}$$

For $\boldsymbol{Q} > 0$, we need $Q_{11} > 0, Q_{22} > 0$ and $\mathrm{Det}(\boldsymbol{Q}) > 0$. From the first equation in (5.16), we need $c\alpha - b\beta > 0$ for $Q_{11} > 0$, since $r_1 > 0$ and $ac - b^2 > 0$. Calculating the elements of $\bar{\boldsymbol{Q}}$, we get

$$\begin{aligned} \bar{Q}_{11} &= \frac{r_1(a\chi - b\beta)}{\alpha\chi - \beta^2}, \\ \bar{Q}_{22} &= \frac{r_2(c\alpha - b\beta)}{\alpha\chi - \beta^2}, \quad \text{and} \\ \mathrm{Det}(\bar{\boldsymbol{Q}}) &= -\frac{1}{4(\alpha\chi - \beta^2)^2}(Ar_2^2 + Br_2 + C). \end{aligned} \tag{5.17}$$

From the first equation in (5.17), we need $a\chi - b\beta > 0$ for $\bar{Q}_{11} > 0$, since $r_1 > 0$ and $\alpha\chi - \beta^2 > 0$. We need

$$\bar{Q}_{22} = \frac{r_2(c\alpha - b\beta)}{\alpha\chi - \beta^2} > 0.$$

Since from (5.16), we have $c\alpha - b\beta > 0$, we need $r_2 > 0$. Finally, we see that for $\mathrm{Det}(\boldsymbol{Q}) > 0$, we need $\psi(r_2) := Ar_2^2 + Br_2 + C < 0$. $\psi(r_2)$ is a quadratic equation in r_2 with $A > 0$ and $C > 0$. Thus, $\psi(r_2)$ is upward quadratic. Also, $B^2 - 4AC > 0$. This means that the equation $\psi(r_2) = 0$ has two real roots so that $\psi(r_2) < 0$ for some range of values of r_2. The sign of B determines the nature of the roots. If $B > 0$, we have two negative roots. But from (5.17), we need $r_2 > 0$. If $B < 0$, then we have two positive roots and $\psi(r_2) < 0$ for values of r_2 between the two positive roots. Thus we need $B < 0$ for $\mathrm{Det}(\boldsymbol{Q}) > 0$. Thus, if

$$\begin{aligned} &a\chi - b\beta > 0, \quad c\alpha - b\beta > 0, \quad \text{and} \\ &b\beta(c\alpha + a\chi) + ac(\beta^2 - 2\alpha\chi) + b^2(2\beta^2 - \alpha\chi) < 0, \end{aligned}$$

then there exits a range of positive values of r_2 such that

$$\frac{1}{2}\left(\left(\boldsymbol{M}_c\boldsymbol{M}^{-1}\boldsymbol{R}\right) + \left(\boldsymbol{M}_c\boldsymbol{M}-1\boldsymbol{R}\right)^T\right) > 0.$$

■

In the proof, we have taken $\boldsymbol{R}$ to be diagonal. The element $\boldsymbol{R}_{21}$ can be changed through feedback. However, even when $\boldsymbol{R}_{21} \neq 0$, we find that the condition $a\chi - b\beta > 0$ still holds.

For the inverted pendulum example, $a\chi - b\beta < 0$. Therefore, there is *no* choice of d_s for which (5.15) is satisfied. Because $\dot{E}_{\tau,\sigma,\rho}$ cannot be made negative semidefinite when $d_\phi > 0$, $E_{\tau,\sigma,\rho}$ is no longer a Lyapunov function in this case.

Rather than search for a new Lyapunov function, we analyze nonlinear stability locally using Lyapunov's first method. That is, we examine the spectrum associated with the linearized dynamics. The local analysis provides a valuable assessment of the nonlinear controller's performance. In

practice, one would not likely implement a nonlinear control law whose local performance compares poorly with available linear control laws.

As will be shown, the given controller, with an appropriate choice of linear feedback dissipation, is still quite effective at stabilizing the desired equilibrium. Moreover, even though we lose the Lyapunov function, and thus the proof of a large region of attraction, simulations suggest that the region of attraction remains quite large.

Encouraged by converse theorems for Lyapunov stability, one might search for a new Lyapunov function for the given controller. One approach might involve complementing $\dot{E}_{\tau,\sigma,\rho}$ with another function, and an appropriately defined switching sequence, such that the pair of functions proves asymptotic stability; see [20], for example. A more challenging approach, perhaps, would be to seek a new modified energy for the given control law, for which the equilibrium is a minimum (or a maximum) and for which a dissipation inequality such as (4.59) can be made to hold with suitably defined feedback dissipation. (In the case of nonlinear damping, the inequality (4.59) would have to be modified. Nonlinear damping often arises in real systems, including the system considered here; see [60]). Additional freedom can be obtained in the matching process by relaxing the symmetry requirements and allowing a more general Ehresmann connection [9]; see § 7.2.

Linearizing the closed-loop equations about the desired equilibrium gives

$$\dot{\boldsymbol{x}} = \boldsymbol{A}\boldsymbol{x} + \text{h.o.t.}, \tag{5.18}$$

where $\boldsymbol{x} = [\phi,\ s,\ \dot{\phi},\ \dot{s}]^T$ is the state vector and the state matrix

$$\boldsymbol{A} = \begin{pmatrix} 0 & 0 & 1 & 0 \\ 0 & 0 & 0 & 1 \\ -a - 3b\kappa & -b\kappa & -\frac{d_\phi \gamma}{\gamma - 1} + 3\, c\, k_{\text{diss}} & \frac{d_s}{\gamma - 1} + c\, k_{\text{diss}} \\ 2a + 3b\kappa + \frac{1}{\gamma + 1} & b\kappa & -\frac{d_\phi}{\gamma - 1} - 3\, c\, k_{\text{diss}} & -\frac{d_s}{\gamma - 1} - c\, k_{\text{diss}} \end{pmatrix} \tag{5.19}$$

with

$$a = \frac{\gamma}{\gamma + 1}, \qquad b = \frac{\gamma - 1}{2(\gamma + 1)}, \qquad \text{and} \qquad c = \frac{2(\gamma + 1)}{(\gamma - 1)^3}.$$

We point out that κ and k_{diss} are control parameters and γ and d_ϕ are system parameters. Because the dissipative force corresponding to the parameter d_s enters in the controlled direction, this parameter can be modified through feedback; still, we treat d_s as a system parameter. Because $\gamma > 1$, the constants $a,\ b$, and c are all positive. We examine stability in the $(\kappa,\ k_{\text{diss}})$ parameter space for different system parameter values. Specifically, using Routh's criterion, we find values of κ and k_{diss} such that every eigenvalue of $\boldsymbol{A}$ has a negative real part for given system parameter values. We use Routh's criterion to find conditions on κ and k_{diss} such that exponential stability is guaranteed.

The eigenvalues λ of $\boldsymbol{A}$ satisfy the fourth-order polynomial

$$\lambda^4 + p_3\lambda^3 + p_2\lambda^2 + p_1\lambda + p_0 = 0 \tag{5.20}$$

where the coefficients are

$$\begin{aligned} p_0 &= b\kappa & p_2 &= a + \frac{d_\phi d_s}{\gamma - 1} + 2b\kappa + c\, d_\phi\, k_{\text{diss}} \\ p_1 &= \frac{-d_s}{\gamma - 1} - b\, d_\phi\, \kappa - c\, k_{\text{diss}} & p_3 &= \frac{\gamma d_\phi + d_s}{\gamma - 1} - 2c\, k_{\text{diss}} \end{aligned} \tag{5.21}$$

Necessary and sufficient conditions for every eigenvalue to have negative real part are that

$$p_0 > 0, \quad p_1 > 0, \quad p_2 > 0, \quad \text{and} \quad p_3 > 0, \tag{5.22}$$

and that

$$\begin{aligned} \delta &= p_2 p_3 - p_1 \quad > 0 \\ \delta_1 &= \delta\, p_1 - p_3^2\, p_0 > 0. \end{aligned} \tag{5.23}$$

First, consider the simpler case where there is no physical dissipation, i.e., $d_\phi = d_s = 0$. Figure 5.3 shows the curves

$$p_0 = 0, \quad p_1 = 0, \quad p_2 = 0, \quad p_3 = 0, \quad \delta = 0, \quad \delta_1 = 0$$

in the $(\kappa,\ k_{\text{diss}})$ plane. The hashed areas are control parameter values for which the conditions for asymptotic stability are violated. The region of stabilizing control parameter values is seen to be the entire fourth quadrant, which is consistent with Remark 4.2.2.

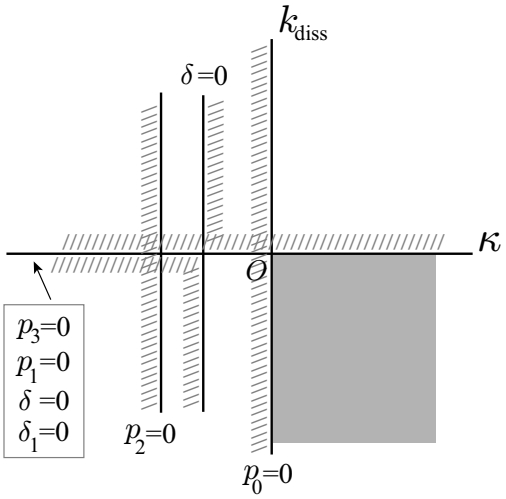

Figure 5.3: Stabilizing values of control parameters for $d_\phi = d_s = 0$ shown in gray.

If d_s and d_ϕ are nonzero, the region of stabilizing control parameter values shown in Figure 5.3 changes slightly.

Proposition 5.2.2 *If $\sqrt{2} > d_\phi \geq 0$ and $d_s > -\gamma d_\phi$, then there exist control parameter values κ and k_{diss} which exponentially stabilize the origin of the linearized dynamics (5.18)-(5.19).*

Proof : We note that the coefficients p_0 through p_3 given in (5.21) are linear in k_{diss} and κ. For convenience, we let

$$\begin{aligned} p_0 &= -b_0\kappa & p_2 &= a_2 - b_2\kappa + c_2 k_{\text{diss}} \\ p_1 &= a_1 - b_1\kappa + c_1 k_{\text{diss}} & p_3 &= a_3 + c_3 k_{\text{diss}} \end{aligned} \tag{5.24}$$

where the coefficients a_i, b_i and c_i are defined by comparing with (5.21). Referring to (5.22), we have

$$\begin{aligned} p_0 > 0 &\Leftrightarrow -b_0\kappa > 0 & p_2 > 0 &\Leftrightarrow k_{\text{diss}} > \frac{b_2}{c_2}\kappa - \frac{a_2}{c_2} \\ p_1 > 0 &\Leftrightarrow k_{\text{diss}} < \frac{b_1}{c_1}\kappa - \frac{a_1}{c_1} & p_3 > 0 &\Leftrightarrow k_{\text{diss}} < -\frac{a_3}{c_3} \end{aligned} \tag{5.25}$$

The condition on p_0 implies that $\kappa > 0$, since $b_0 = -b < 0$. The lines (in the $(\kappa,\ k_{\text{diss}})$ plane)

$$k_{\text{diss}} = -\frac{a_3}{c_3}, \quad k_{\text{diss}} = \frac{b_2}{c_2}\kappa - \frac{a_2}{c_2}, \quad k_{\text{diss}} = \frac{b_1}{c_1}\kappa - \frac{a_1}{c_1} \ \text{ and } \ \kappa = 0$$

are boundaries of stability. It can be checked that $-\frac{a_2}{c_2} < -\frac{a_1}{c_1} < 0$ and $\frac{b_2}{c_2} < \frac{b_1}{c_1} < 0$ for $0 < d_\phi < \sqrt{2}$. The two lines $p_1 = 0$ and $p_2 = 0$ have negative slopes and negative k_{diss}-axis intercepts. Moreover, the line $p_2 = 0$ is steeper than $p_1 = 0$ when $d_\phi < \sqrt{2}$ and the k_{diss}-axis intercept of $p_2 = 0$ is greater in magnitude than that of $p_1 = 0$. Assume that $d_s > -\gamma d_\phi$, so that the line $p_3 = 0$ is above the κ axis. See Figure 5.4.

Next, we need $\delta > 0$ where

$$\delta = p_2 p_3 - p_1. \tag{5.26}$$

We make the following observations:

- By the definition (5.26) of δ, we see that

  $$p_2 = p_1 = 0 \Rightarrow \delta = 0 \ \text{ and } \ p_3 = p_1 = 0 \Rightarrow \delta = 0.$$

  Thus the curve $\delta = 0$ passes through the intersection of $p_1 = 0$ with $p_2 = 0$ and also through the intersection of $p_1 = 0$ with $p_3 = 0$.

- Using (5.24) and (5.26), we have

  $$\begin{aligned} \delta = 0 &\Rightarrow (a_3 + c_3 k_{\text{diss}})(a_2 - b_2\kappa + c_2 k_{\text{diss}}) - (a_1 - b_1\kappa + c_1 k_{\text{diss}}) = 0 \\ &\Rightarrow \kappa = \frac{(a_3 + c_3 k_{\text{diss}})(a_2 + c_2 k_{\text{diss}}) - (a_1 + c_1 k_{\text{diss}})}{b_2(a_3 + c_3 k_{\text{diss}}) - b_1}. \end{aligned} \tag{5.27}$$

  It can be seen that

  $$\kappa \to \pm\infty \ \text{ as } \ k_{\text{diss}} \to -\frac{a_3}{c_3} + \frac{b_1}{b_2 c_3} \tag{5.28}$$

  Thus the line $k_{\text{diss}} = -\frac{a_3}{c_3} + \frac{b_1}{b_2 c_3}$ is an asymptote for $\delta = 0$. Also $\frac{b_1}{b_2 c_3} = \frac{d_\phi}{4c} > 0$. This implies that the asymptote lies above the line $p_3 = 0$. From (5.27), we see that

  $$\kappa \to \frac{c_2 k_{\text{diss}}}{b_2} + \frac{a_2}{b_2} + \frac{a_3 c_2 - c_1}{c_3 b_2} \ \text{ as } \ k_{\text{diss}} \to \pm\infty. \tag{5.29}$$

Now, $p_2 = 0$ has the form

$$k = \frac{c_2 k_{\text{diss}}}{b_2} + \frac{a_2}{b_2}$$

This means that the asymptote given by (5.29) is parallel to $p_2 = 0$ and to the right since

$$\frac{a_3 c_2 - c_1}{c_3 b_2} = \frac{(\gamma d_\phi + d_s) d_\phi}{4b(\gamma - 1)} + \frac{1}{4b} > 0$$

since $d_s > -\gamma d_\phi$.

The observations made so far are illustrated in Figure 5.4. The asymptotes given in (5.28) and (5.29) are shown by dashed lines. There are two possible cases. In the first case, shown in Figure 5.4(a), the point of intersection of the lines $p_1 = 0$ and $p_2 = 0$ lies below the point of intersection of $p_1 = 0$ and $p_3 = 0$. In the second case, shown in Figure 5.4(b), the point of intersection lies above that of $p_1 = 0$ and $p_3 = 0$. Since $\delta = 0$ is quadratic in k_{diss} and linear in κ, it cannot intersect $p_1 = 0$ or $p_2 = 0$ at points other than those shown by the filled circles. Thus, the possible branches of $\delta = 0$ must be as shown in Figure 5.4, for the cases considered above. The above observations help us to determine the possible regions of stabilizing control parameter values. At the origin,

$$\delta = p_3 p_2 - p_1 = a_3 a_2 - a_1 > 0 \quad \text{since} \quad a_3, a_2 > 0 > a_1$$

Thus, by continuity of δ in κ and k_{diss}, the possible region of stabilizing control parameter values ($\delta > 0$) lies between the curves for $\delta = 0$ in one case (Figure 5.4(a)) and does not lie between the curves in the other case (Figure 5.4(b)).

Next, we need

$$\delta_1 = \delta p_1 - p_3^2 p_0 > 0.$$

Thus $\delta_1 = 0$ forms another boundary on the range of stabilizing parameter values.

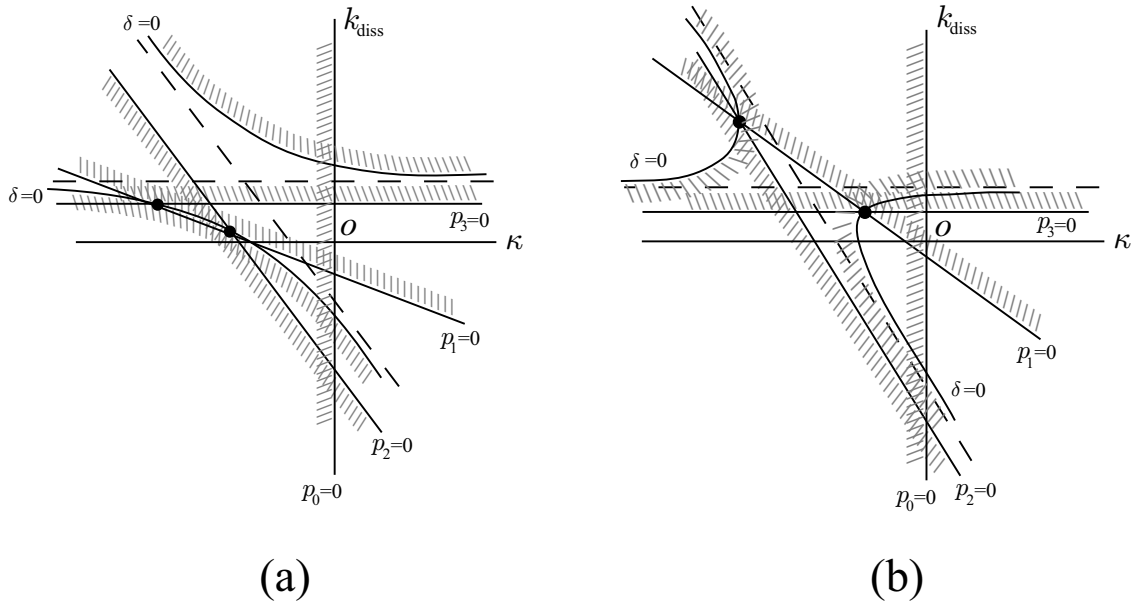

Figure 5.4: Preliminary boundaries for stabilizing control parameter values. Hashes denote regions where the conditions for exponential stability are violated.

- Note that

$$\begin{aligned} \delta_1 = 0 \qquad & \text{when} \qquad \delta = 0 \ \text{ and } \ p_3 = 0, \\ & \text{and when} \quad \delta = 0 \ \text{ and } \ p_0 = 0, \\ & \text{and when} \quad p_1 = 0 \ \text{ and } \ p_3 = 0, \\ & \text{and when} \quad p_1 = 0 \ \text{ and } \ p_0 = 0. \end{aligned}$$

  Thus the curve $\delta_1 = 0$ passes through the intersections of $\delta = 0$ with $p_0 = 0$ and $p_3 = 0$ and also through the intersections of $p_1 = 0$ with $p_0 = 0$ and $p_3 = 0$.

- One can check that

$$\begin{aligned} 0 = \delta_1 = &((a_3 + c_3 k_{\text{diss}})(a_2 - b_2\kappa + c_2 k_{\text{diss}}) - (a_1 - b_1\kappa + c_1 k_{\text{diss}}))(a_1 - b_1\kappa + c_1 k_{\text{diss}}) \\ &+ (a_3 + c_3 k_{\text{diss}})^2 b_0 \kappa \\ \Rightarrow 0 &= (a_3 + c_3 k_{\text{diss}}) b_2 - b_1 \quad \text{for large} \quad \kappa \\ \Rightarrow k_{\text{diss}} &= -\frac{a_3}{c_3} + \frac{b_1}{b_2 c_3} \quad \text{for large} \quad \kappa. \end{aligned}$$

  Thus $k_{\text{diss}} = -\frac{a_3}{c_3} + \frac{b_1}{b_2 c_3}$ is an asymptote for $\delta_1 = 0$.

- We note that $\delta_1 = 0$ is quadratic in κ and cubic in k_{diss}. This means that for a given k_{diss}, there can be two roots for κ (including repeated roots) or none. Likewise, for a given κ, there can be three roots for k_{diss} (including repeated roots) or one.

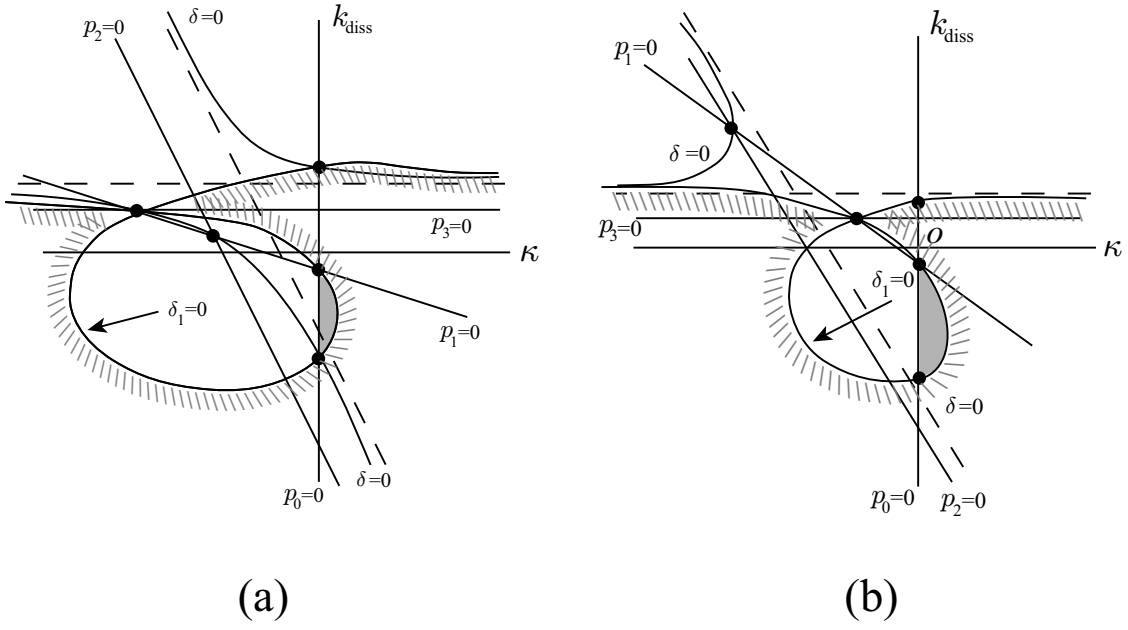

Figure 5.5: Sketch showing the region of stabilizing control parameter values (in gray).

The above observations, along with an examination of Figure 5.4, give a clear idea about the nature of $\delta_1 = 0$. This is schematically shown in Figure 5.5 where $\delta_1 = 0$ is sketched along with the

other curves. Figure 5.5(a) corresponds to the case discussed in Figure 5.4(a) and Figure 5.5(b) corresponds to the case discussed in Figure 5.4(b).

The crucial observation is that there is some part of $\delta_1 = 0$ that lies in the fourth quadrant. At the origin ($\kappa = k_{\text{diss}} = 0$),

$$\delta_1 = (a_3 a_2 - a_1)a_1 < 0,$$

since $a_3,\ a_2 > 0 > a_1$. Thus, by the continuity of δ_1 in κ and k_{diss}, $\delta_1 > 0$ inside the $\delta_1 = 0$ loop as shown in Figure 5.5. The region of stabilizing control parameter values is shown in gray in Figure 5.5. ■

The proof of the above result also shows that if $k_{\text{diss}} = 0$, one can *not* find a stabilizing value of κ when $d_s > 0$ and $d_\phi > 0$. That is, the control law developed for the conservative system model will fail to stabilize a system with generic, linear damping. One must introduce feedback dissipation to stabilize the system.

As an alternative to the feedback dissipation term (5.12), one may instead apply feedback which makes d_s negative. (Although we have treated d_s as a system parameter, the damping force associated with this parameter occurs in the controlled direction, so one may effectively change d_s through feedback.) If d_s satisfies $-\gamma d_\phi < d_s < 0$, one may obtain closed-loop stability even with $k_{\text{diss}} = 0$; see the sketch on the right-hand side of Figure 5.6. Applying feedback to make d_s negative corresponds to reversing the natural damping force acting on the cart.

Proposition 5.2.2 asserts that, under quite reasonable conditions on the physical parameter values, there exist control parameter values which exponentially stabilize the linearized dynamics. For these parameter values, it follows from Lyapunov's first method that the nonlinear system is locally exponentially stable. In fact, simulations suggest that the region of attraction is once again the set W of states for which the pendulum is elevated above the horizontal plane. We point out that exponential stability of the linearized dynamics also implies that the control law is, at least locally, robust to small uncertainties in the model parameters.

Numerical results. Figure 5.6 shows the region of stabilizing control parameter values for par-

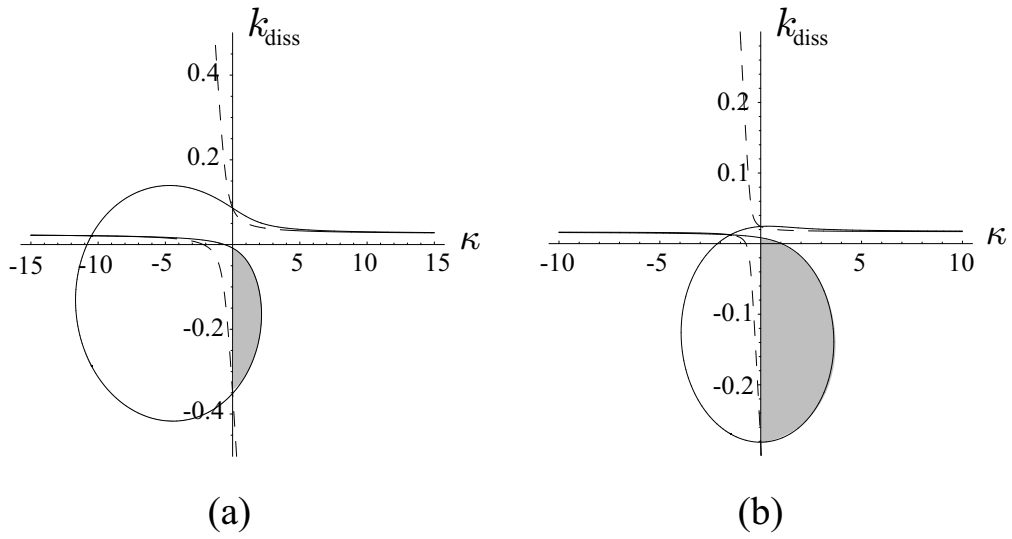

Figure 5.6: Stabilizing control parameter values (in gray) for $\gamma = 2$ and $d_\phi = 0.1$ with (a) $d_s = 0.05$ and (b) $d_s = -0.05$. The solid line is $\delta_1 = 0$; the dashed line is $\delta = 0$.

ticular values of the system parameters. We fix $\gamma = 2$ and $d_\phi = 0.1$ and consider the two cases $d_s = 0.05$ and $d_s = -0.05$. Figure 5.6(a) shows that, when $d_s = 0.05$, the κ-axis lies outside the region of stabilizing control parameter values. Thus, in absence of feedback dissipation (i.e., with $k_{\text{diss}} = 0$), no value of the control parameter κ can stabilize the system when $d_s > 0$. When $d_s < 0$, however, a portion of the κ-axis lies within the region of stabilizing control parameter values. This observation is illustrated in Figure 5.6(b) for the case $d_s = -0.05$.

From Figure 5.6(b), we see that the values $\kappa = 0.5$ and $k_{\text{diss}} = -0.25$ lie in the region of stabilizing parameter values. Figure 5.7 shows closed-loop system trajectories with these parameter choices in response to the (nondimensional) initial conditions

$$\phi(0) = \left(\frac{89}{90}\right)\frac{\pi}{2} \qquad s(0) = 0 \qquad \dot{\phi}(0) = \pi \qquad \dot{s}(0) = 0.$$

Note that this initial state is far outside the region where the linearized equations provide a reasonable model for the nonlinear dynamics. It corresponds to an almost horizontal pendulum which is rotating downward. We assume a perfect actuator; the magnitude of the control force is unlimited

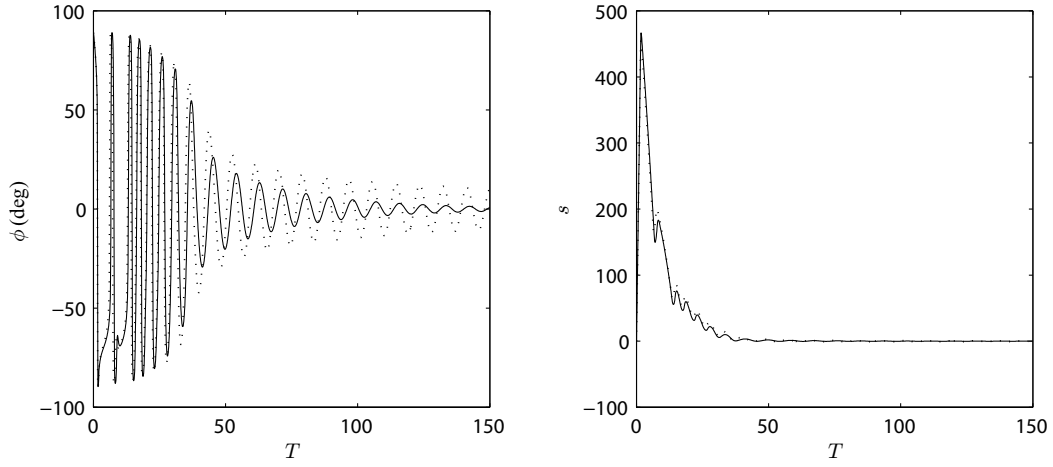

Figure 5.7: Pendulum angle and cart location versus time with $d_\phi = 0$ (solid) and $d_\phi = 0.1$ (dashed).

and the actuator responds instantaneously to reference commands.

Figure 5.7 shows two cases. In the first case, denoted by solid lines, only feedback dissipation is applied ($d_\phi = d_s = 0$). In the second case, denoted by dashed lines, there is also physical damping in the unactuated direction ($d_\phi = 0.1$) and "reversed damping" in the actuated direction ($d_s = -0.05$). In both cases, the system converges to the desired equilibrium, although more slowly in the latter case.

Figure 5.8 shows the control-modified energy for the two cases described above. In both cases, the energy decays to its minimum value. In the presence of physical damping, however, the function does not decay monotonically. The control-modified total energy is *not* a Lyapunov function when physical damping is present.

5.3 Experimental Results

The experimental setup, shown in Figure 5.9, is available as a commercial teaching aid [35]. The motor-driven cart moves along the track through a rack and pinion arrangement. One optical

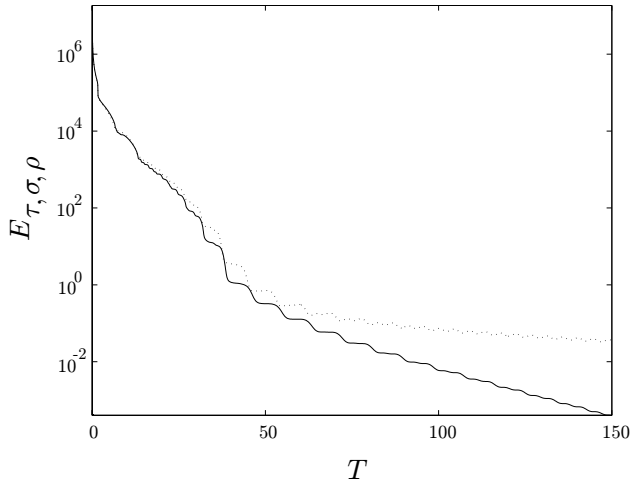

Figure 5.8: Control-modified energy $E_{\tau,\sigma,\rho}$ versus time with $d_\phi = 0$ (solid) and $d_\phi = 0.1$ (dashed). Note the non-monotonic convergence in the case where physical damping is present.

encoder measures the pendulum angle and another measures the cart position. The maximum cart travel is 0.814 m.

The inverted pendulum in the experiment is best modelled by a uniform rod of mass M and length $2l$. If we redefine the nondimensional mass and time parameters as

$$\gamma = \frac{4}{3}\frac{M+m}{m} \quad \text{and} \quad \omega = \sqrt{\frac{3g}{4l}},$$

then we retain the non-dimensional equations of § 5.1 and we can use the results therein. It was noted in Section 5.2 that one may choose stabilizing control parameter values, even when the mechanism is subject to linear damping. In reality, damping of the cart's motion is better modelled by nonlinear (static and Coulomb) friction. For control gains which are predicted to stabilize the system, this nonlinear friction degrades the system's performance, introducing an asymptotically stable limit cycle in experiments. This is a well-known phenomenon; see [32] and references therein. In many cases, it may be impossible to eliminate such oscillations without modifying the system itself. On the other hand, in terms of system performance, it may be acceptable to simply minimize the amplitude of the limit cycle oscillations.

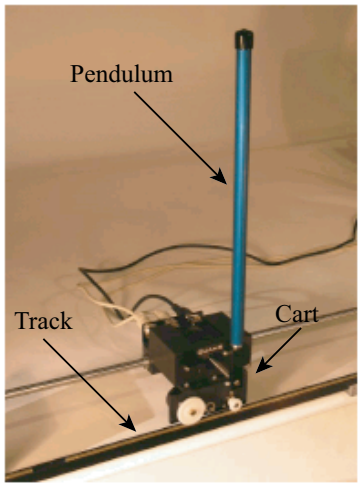

Figure 5.9: Experimental apparatus. (Photo courtesy Quanser Consulting, Inc.)

To verify that the limit cycle oscillations are induced by friction, we have simulated the closed loop dynamics with a model for static and coulomb friction. The system parameters are

$$M = 0.7031 \text{ kg}, \qquad m = 0.127 \text{ kg}, \qquad l = 0.1778 \text{ m}.$$

The control gains are

$$\kappa = -0.5 \qquad \text{and} \qquad k_{\text{diss}} = -30.$$

Experimental parameter identification gave the following values for static and dynamic friction coefficients for the cart's motion:

$$\mu_s \approx 0.14 \qquad \text{and} \qquad \mu_d \approx 0.10.$$

Figure 5.10(a) shows the limit cycle oscillations for the experiment. Figure 5.10(b) shows the simulated limit cycle using the estimated values of the friction coefficients. Though the simulated limit cycle amplitude is smaller than that observed in the experiment, the simulations qualitatively match the experimental behavior. Assuming errors in the friction estimation, we vary the friction coefficients to match the experimental data. Figure 5.10(c) shows simulations using

$$\mu_s \approx 0.15 \qquad \text{and} \qquad \mu_d \approx 0.14.$$

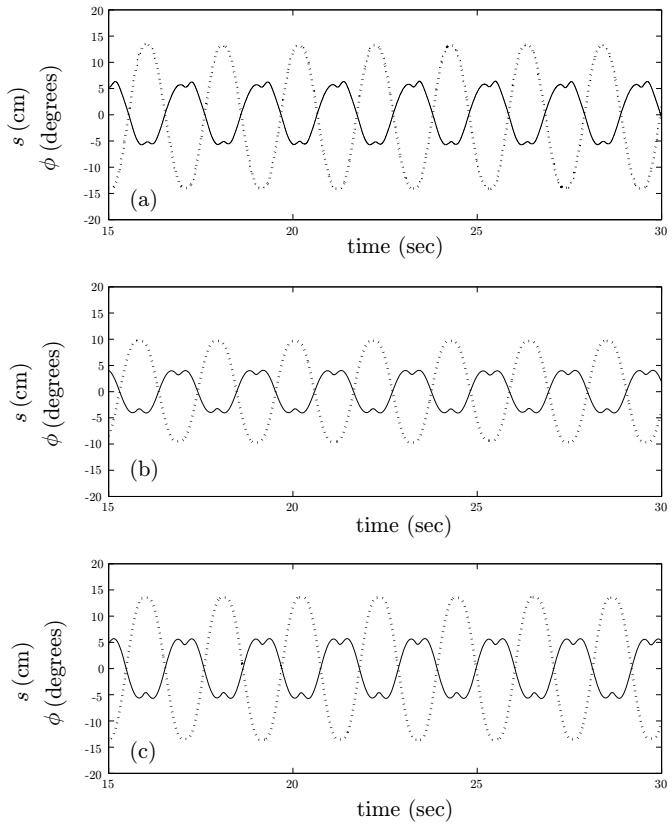

Figure 5.10: Friction-induced limit cycle oscillations. Pendulum angle shown solid. Cart position shown dashed. (a) Experimental results (b) Simulation with experimentally determined friction coefficients (c) Simulation with adjusted friction coefficients.

There is excellent agreement with experimental data; these friction parameters are certainly within the experimental error of the measured values. These results strongly suggest that the experimentally observed limit cycles are induced by static and coulomb friction. To minimize the effect of static and dynamic friction in later experiments, a compensatory force was applied to the cart.

While the control law derived using the method of controlled Lagrangians provides good regional performance, the local performance is less satisfactory. The nonlinear control law provides only two parameters with which to tune performance while linear state feedback provides four. These observations suggest a switching control strategy to obtain good closed-loop performance both

regionally and locally. We employ a Lyapunov-based switching rule to switch from the nonlinear controller, for states far from the equilibrium, to a linear controller for states nearer the equilibrium. The Lyapunov-based switching rule ensures that, in the absence of disturbances, at most one switch occurs. The strategy therefore satisfies a "dwell time" condition which is sufficient for stability of the switched system [44].

5.3.1 Lyapunov Based Switching

Suppose that the open-loop dynamics for the cart-pendulum system are written in the state space form as

$$\dot{\boldsymbol{x}} = \boldsymbol{f}(\boldsymbol{x}, u), \tag{5.30}$$

where $\boldsymbol{x} = [\phi,\ s,\ \dot{\phi},\ \dot{s}]^T \in \mathbb{R}^4$ and u is some control law. Let

$$\boldsymbol{f}(\boldsymbol{x}, 0) = \boldsymbol{A}\boldsymbol{x} + \boldsymbol{g}(\boldsymbol{x}), \tag{5.31}$$

where $\boldsymbol{A}\boldsymbol{x}$ represents the linearization of $\boldsymbol{f}(\boldsymbol{x}, 0)$ about the equilibrium $\boldsymbol{x}^* = \boldsymbol{0}$ and

$$\lim_{||\boldsymbol{x}|| \to \boldsymbol{0}} \frac{||\boldsymbol{g}(\boldsymbol{x})||}{||\boldsymbol{x}||} = \boldsymbol{0}.$$

Suppose we have designed a linear state feedback control law $u = -\boldsymbol{K}\boldsymbol{x}$. We have

$$\dot{\boldsymbol{x}} = \boldsymbol{A}\boldsymbol{x} + \boldsymbol{g}(\boldsymbol{x}) + \boldsymbol{B}\boldsymbol{u} = \boldsymbol{A}\boldsymbol{x} - \boldsymbol{B}\boldsymbol{K}\boldsymbol{x} + \boldsymbol{g}(\boldsymbol{x}) = \bar{\boldsymbol{A}}\boldsymbol{x} + \boldsymbol{g}(\boldsymbol{x}), \tag{5.32}$$

where $\bar{\boldsymbol{A}} = \boldsymbol{A} - \boldsymbol{B}\boldsymbol{K}$ is *Hurwitz*. If $\bar{\boldsymbol{A}}$ is Hurwitz, then given any symmetric, positive definite matrix $\boldsymbol{Q}$, there exists a symmetric, positive definite matrix $\boldsymbol{P}$ that satisfies the Lyapunov equation [40]

$$\boldsymbol{P}\bar{\boldsymbol{A}} + \bar{\boldsymbol{A}}^T\boldsymbol{P} = -\boldsymbol{Q}. \tag{5.33}$$

A good choice for a Lyapunov function is the positive definite quadratic function,

$$V(\boldsymbol{x}) = \boldsymbol{x}^T\boldsymbol{P}\boldsymbol{x}. \tag{5.34}$$

For the nonlinear system dynamics (5.30) with linear state feedback law, one can estimate an open ball around the equilibrium, $\mathcal{B} = \{\boldsymbol{x} \in \mathbb{R}^4 \mid ||\boldsymbol{x}|| < r\}$, such that

$$V(\boldsymbol{x}) > 0 \;\text{ and }\; \dot{V}(\boldsymbol{x}) < 0 \;\;\forall\;\; \boldsymbol{x} \in \mathcal{B}.$$

The reader is referred to [40] for details about estimating the basin of attraction. For states outside of $\mathcal{B}$, we use the energy shaping control law u given by (5.11). We track the value of V as the system evolves. When the value of V reaches a critical value, so that the state $\boldsymbol{x}$ lies within the ball $\mathcal{B}$, we switch to the linear controller. A quadratic positive definite function $V(\boldsymbol{x}) = \boldsymbol{x}^T\boldsymbol{P}\boldsymbol{x}$ satisfies [40]

$$\lambda_{\min}(\boldsymbol{P})||\boldsymbol{x}||^2 \leq \boldsymbol{x}^T\boldsymbol{P}\boldsymbol{x} \leq \lambda_{\max}(\boldsymbol{P})||\boldsymbol{x}||^2,$$

where $\lambda_{\min}(\boldsymbol{P})$ and $\lambda_{\max}(\boldsymbol{P})$ are minimum and maximum eigenvalues of $\boldsymbol{P}$ respectively. The critical switching value is given by $\bar{V} = \lambda_{\min}(\boldsymbol{P})r^2$. ■.

Figure 5.11 compares the performance of the controlled Lagrangian controller and the switching controller. The system parameters are

$$M = 1.07031 \text{ kg}, \qquad m = 0.127 \text{ kg}, \qquad l = 0.1778 \text{ m}.$$

The nonlinear controller gains are

$$\kappa = 0.5 \qquad \text{and} \qquad k_{\text{diss}} = -50.$$

For the linear controller, the gains were chosen according to an Linear Quadratic Regulator (LQR) design provided with the apparatus [35].

Figure 5.11(a) illustrates the poor local performance of the nonlinear controller; the system appears to converge to a large-amplitude limit cycle. Figure 5.11(c) shows the significantly improved performance of the switching controller. The switching signal is chosen based on the value of a quadratic Lyapunov function V chosen for the linearized, LQR-controlled dynamics. For the experiment shown, the switching value was chosen to be $V = \bar{V} = 0.08$. Figures 5.11 (b) and (d) show the value of this function for the two simulations. Note that V is *not* a Lyapunov function for the

controlled Lagrangian system; thus, one can not expect monotonic convergence in Figure 5.11 (b). The non-monotonic nature of V in Figure 5.11 (d) is attributed to stick-slip. Note that, for the switched system, the cart position converges to a small offset, probably due to static friction; this offset can be removed by adding integral feedback.

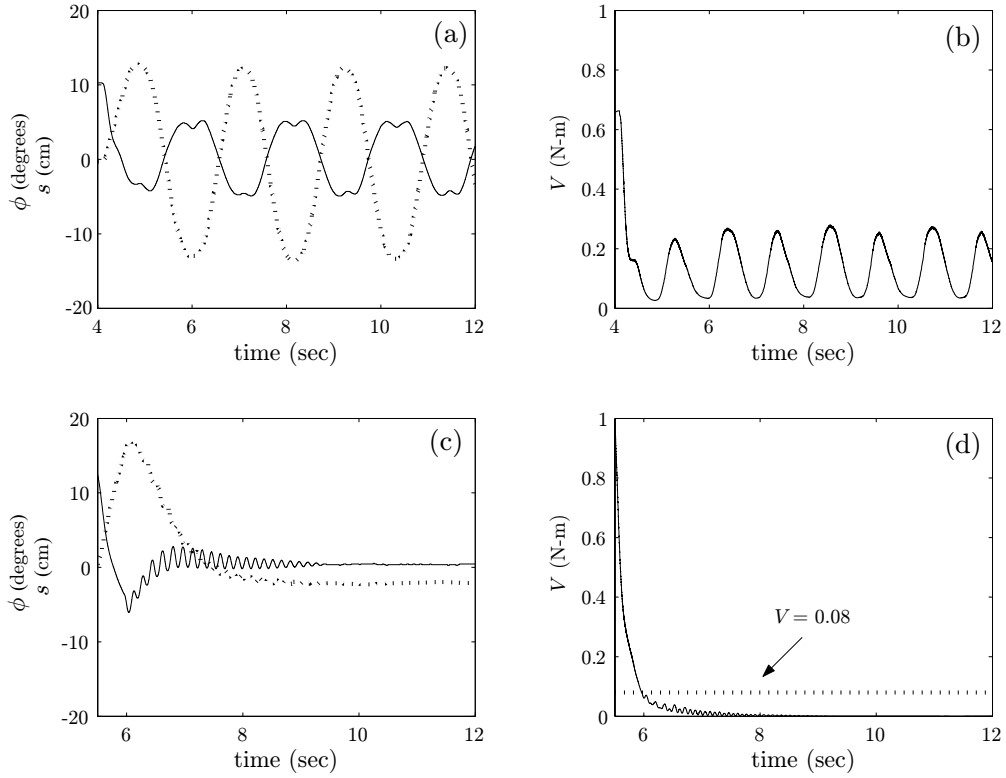

Figure 5.11: Closed-loop performance of (a-b) Nonlinear controller and (c-d) Switched Controller. Pendulum angle shown solid. Cart position shown dashed.

Chapter 6

Energy Shaping for Vehicles with Point Mass Actuators

The principal objective of this chapter is to illustrate the applicability of controlled Lagrangians to simple models for vehicles with moving mass actuators (MMAs). We anticipate that this approach may be ultimately used to develop nonlinear controllers for complex vehicle control problems such as underwater gliders.

In § 6.1, we derive the reduced Euler-Lagrange equations for a system consisting of a rigid body with n internal moving masses immersed in an ideal fluid. We show that the Lagrangian is G-invariant and this leads to reduced dynamics. In § 6.2, we consider two special cases of the general system, examples of which are considered in § 6.4 and § 6.5. In § 6.3, we derive a set of sufficient algebraic matching conditions. We show that there is always at least one solution to the matching conditions and present an algorithm for matching and stabilization. Section 6.4 describes a simple example of a spinning disk with a single MMA. In § 6.5, we consider a slightly more complicated example, a streamlined underwater vehicle in planar motion.

6.1 Rigid Body with n Internal Moving Masses: Dynamic Equations

Figure 6.1 depicts a rigid body, immersed in an ideal fluid, and n internal point masses. For now, we assume that the point masses are free to move in three dimensions. In general, the body may apply control forces to these point masses, thus coupling the elements of the system. In the examples considered in this chapter, we will consider the case of a single MMA that is confined to a linear track. Let m_{rb} be the mass of the rigid body and let m_i be the mass of the i^{th} point mass. We assume that the system is neutrally buoyant; that is, we assume that

$$m = m_{\text{rb}} + \sum_{i=1}^{n} m_i$$

is equal to the mass of fluid displaced by the rigid body. Let $\boldsymbol{u}_i$ denote a control force applied to the i^{th} point mass by the body. The examples given in § 6.4 and § 6.5 involve planar systems for which the effect of gravity vanishes. Although it is straightforward to include forces and moments due to gravity in the dynamic model (see [80], for example), our model ignores gravity in the interest of brevity.

6.1.1 Geometry of the System

Introduce the reference frame $\Sigma_{\text{inertial}} = (O_{\text{inertial}}, \{\boldsymbol{i}_i, \boldsymbol{i}_2, \boldsymbol{i}_3\})$ fixed in space and the reference frame $\Sigma_{\text{body}} = (O_{\text{body}}, \{\boldsymbol{b}_i, \boldsymbol{b}_2, \boldsymbol{b}_3\})$ fixed in the body. Let the vector $\boldsymbol{p} \in \mathbb{R}^3$ connect the origin O_{inertial} of the frame Σ_{inertial} to the origin O_{body} of the frame Σ_{body}. Let $\boldsymbol{a}_s$ be any vector expressed in the inertial reference frame and let $\boldsymbol{a}_b$ be the same vector expressed in the body reference frame. The vectors $\boldsymbol{a}_s$ and $\boldsymbol{a}_b$ are related through the affine transformation

$$\boldsymbol{a}_s = \boldsymbol{\mathcal{R}}\boldsymbol{a}_b + \boldsymbol{p},$$

where $\boldsymbol{\mathcal{R}} \in SO(3)$ is the proper rotation matrix. Thus, the pair $(\boldsymbol{p}, \boldsymbol{\mathcal{R}}) \in SE(3)$ maps the coordinates of any point relative to Σ_{body} to its coordinates relative to Σ_{inertial}. For any point on the

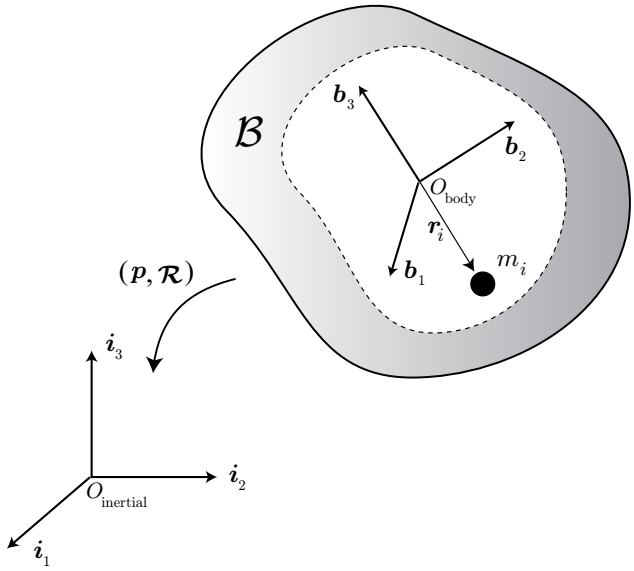

Figure 6.1: A rigid body in an ideal fluid with n internal point masses.

rigid body we have

$$\boldsymbol{x}_s = \boldsymbol{\mathcal{R}}\boldsymbol{x}_b + \boldsymbol{p}.$$

Let $\boldsymbol{r}_i$ denote the position of the i^{th} mass relative to the frame Σ_{body}. Suppose that the body frame rotates with angular velocity $\boldsymbol{\omega}$ and translates with velocity $\boldsymbol{v}$ with respect to the inertial frame, where both vectors are expressed in the body frame. For i^{th} point mass we have the relation

$$\boldsymbol{\rho}_i = \boldsymbol{\mathcal{R}}\boldsymbol{r}_i + \boldsymbol{p},$$

where $\boldsymbol{\rho}_i \in \mathbb{R}^3$ are the inertial coordinates of the i^{th} point mass. The configuration space for the above system is

$$Q = G \times M = SE(3) \times \underbrace{\mathbb{R}^3 \times \cdots \times \mathbb{R}^3}_{n \text{ times}}.$$

6.1.2 Invariance of the Lagrangian

The Lagrangian $L : TQ \to \mathbb{R}$ is the total kinetic energy of the system. The kinetic energy of the rigid body is given by

$$\begin{aligned} KE_{\text{rb}} &= \frac{1}{2}\int_{\mathcal{B}} ||\dot{\boldsymbol{x}}_s||^2 \, dm \\ &= \frac{1}{2}\int_{\mathcal{B}} ||\dot{\boldsymbol{\mathcal{R}}}\boldsymbol{x}_b + \dot{\boldsymbol{p}}||^2 dm \\ &= \frac{1}{2}\int_{\mathcal{B}} ||\boldsymbol{\mathcal{R}}(\hat{\boldsymbol{\omega}}\boldsymbol{x}_b + \boldsymbol{v})||^2 dm, \end{aligned} \tag{6.1}$$

since $\dot{\boldsymbol{\mathcal{R}}} = \boldsymbol{\mathcal{R}}\hat{\boldsymbol{\omega}}$ and $\dot{\boldsymbol{p}} = \boldsymbol{\mathcal{R}}\boldsymbol{v}$. The kinetic energy of the i^{th} point mass is

$$\begin{aligned} KE_i &= \frac{1}{2} m_i ||\dot{\boldsymbol{\rho}}_i||^2 \\ &= \frac{1}{2} m_i ||\dot{\boldsymbol{p}} + \dot{\boldsymbol{\mathcal{R}}}\boldsymbol{r}_i + \boldsymbol{\mathcal{R}}\dot{\boldsymbol{r}}_i||^2 \\ &= \frac{1}{2} m_i ||\boldsymbol{\mathcal{R}}(\boldsymbol{v} + \hat{\boldsymbol{\omega}}\boldsymbol{r}_i + \dot{\boldsymbol{r}}_i)||^2. \end{aligned} \tag{6.2}$$

The Lagrangian is

$$\begin{aligned} L &= KE_{\text{rb}} + \sum_{i=1}^{n} KE_i \\ &= \frac{1}{2}\left(\int_{\mathcal{B}} ||\boldsymbol{\mathcal{R}}(\hat{\boldsymbol{\omega}}\boldsymbol{x}_b + \boldsymbol{v})||^2 dm + \sum_{i=1}^{n} m_i ||\boldsymbol{\mathcal{R}}(\boldsymbol{v} + \hat{\boldsymbol{\omega}}\boldsymbol{r}_i + \dot{\boldsymbol{r}}_i)||^2 \right). \end{aligned} \tag{6.3}$$

We claim that L is G-invariant. Let $q = (h, x) \in Q$ where

$$h = (\boldsymbol{p}, \boldsymbol{\mathcal{R}}) \in SE(3) \;\text{ and }\; x = (\boldsymbol{r}_1,\ \boldsymbol{r}_2, \ldots,\ \boldsymbol{r}_n) \in \mathbb{R}^3 \times \cdots \times \mathbb{R}^3.$$

The left action of an element $g = (\bar{\boldsymbol{p}}, \bar{\boldsymbol{\mathcal{R}}}) \in SE(3)$ on Q is

$$\Phi_g(h, x) = (gh, x) = (\bar{\boldsymbol{\mathcal{R}}}\boldsymbol{p} + \bar{\boldsymbol{p}}, \bar{\boldsymbol{\mathcal{R}}}\boldsymbol{\mathcal{R}}, \boldsymbol{r}_1,\ \boldsymbol{r}_2, \ldots,\ \boldsymbol{r}_n).$$

Also,

$$T_q\Phi_g(\dot{q}) = (\bar{\boldsymbol{\mathcal{R}}}\boldsymbol{\mathcal{R}}\boldsymbol{v}, \bar{\boldsymbol{\mathcal{R}}}\boldsymbol{\mathcal{R}}\hat{\boldsymbol{\omega}}, \dot{\boldsymbol{r}}_1,\ \dot{\boldsymbol{r}}_2, \ldots,\ \dot{\boldsymbol{r}}_n).$$

The Lagrangian is G-invariant if $L(\Phi_g(q), T_q\Phi_g(\dot{q})) = L(q, \dot{q})$. We have,

$$\begin{aligned} L(\Phi_g(q), T_q\Phi_g(\dot{q})) &= \frac{1}{2}\left(\int_{\mathcal{B}} ||\bar{\boldsymbol{\mathcal{R}}}\boldsymbol{\mathcal{R}}(\hat{\boldsymbol{\omega}}\boldsymbol{x}_b + \boldsymbol{v})||^2 dm + \sum_{i=1}^{n} m_i ||\bar{\boldsymbol{\mathcal{R}}}\boldsymbol{\mathcal{R}}(\boldsymbol{v} + \hat{\boldsymbol{\omega}}\boldsymbol{r}_i + \dot{\boldsymbol{r}}_i)||^2\right) \\ &= L(q, \dot{q}) \end{aligned}$$

since $\bar{\boldsymbol{\mathcal{R}}}^T = \bar{\boldsymbol{\mathcal{R}}}^{-1}$. ■

6.1.3 Reduced Euler-Lagrange Equations

The G-invariance of L induces a reduced Lagrangian $l : \mathfrak{se}(3) \times T\mathbb{R} \times \cdots \times T\mathbb{R} \to \mathbb{R}$. The Euler-Lagrange equations for L are equivalent to the reduced Euler-Lagrange equations for l given by (3.19),

$$\begin{aligned} \frac{d}{dt}\frac{\partial l}{\partial \xi} &= \mathrm{ad}^*_\xi \frac{\partial l}{\partial \xi}, \\ \frac{d}{dt}\frac{\partial l}{\partial \dot{\boldsymbol{r}}} - \frac{\partial l}{\partial \boldsymbol{r}} &= \boldsymbol{u}, \end{aligned} \tag{6.4}$$

where $\xi = (\boldsymbol{\omega},\ \boldsymbol{v}) \in \mathfrak{se}(3)$, $\frac{\partial l}{\partial \xi} = \left(\frac{\partial l}{\partial \boldsymbol{\omega}}\ ,\ \frac{\partial l}{\partial \boldsymbol{v}}\right) \in \mathfrak{se}(3)^*$,

$$\boldsymbol{r} = \begin{pmatrix} \boldsymbol{r}_1 \\ \vdots \\ \boldsymbol{r}_n \end{pmatrix} \quad \text{and} \quad \boldsymbol{u} = \begin{pmatrix} \boldsymbol{u}_1 \\ \vdots \\ \boldsymbol{u}_n \end{pmatrix}.$$

The coadjoint action of $\mathfrak{se}(3)$ on its dual $\mathfrak{se}(3)^*$ is computed to be [46]

$$\mathrm{ad}^*_\xi \frac{\partial l}{\partial \xi} = \left(\frac{\hat{\partial} l}{\partial \boldsymbol{\omega}}\boldsymbol{\omega} + \frac{\hat{\partial} l}{\partial \boldsymbol{v}}\boldsymbol{v},\ \frac{\hat{\partial} l}{\partial \boldsymbol{v}}\boldsymbol{\omega}\right), \tag{6.5}$$

where both $\mathfrak{se}(3)$ and $\mathfrak{se}(3)^*$ are identified with $\mathbb{R}^6$. Using (6.5) in (6.4), the dynamic equations for a rigid body with n internal point masses are

$$\begin{aligned} \frac{d}{dt}\frac{\partial l}{\partial \boldsymbol{\omega}} &= \frac{\hat{\partial} l}{\partial \boldsymbol{\omega}}\boldsymbol{\omega} + \frac{\hat{\partial} l}{\partial \boldsymbol{v}}\boldsymbol{v}, \\ \frac{d}{dt}\frac{\partial l}{\partial \boldsymbol{v}} &= \frac{\hat{\partial} l}{\partial \boldsymbol{v}}\boldsymbol{\omega}, \\ \frac{d}{dt}\frac{\partial l}{\partial \dot{\boldsymbol{r}}} - \frac{\partial l}{\partial \boldsymbol{r}} &= \boldsymbol{u}. \end{aligned} \tag{6.6}$$

6.1.4 Structure of Reduced Lagrangian

We use Eq. (6.3) to determine the structure of the reduced Lagrangian. Since $\boldsymbol{\mathcal{R}}\boldsymbol{\mathcal{R}}^T = \mathbb{I}$, we have

$$\begin{aligned} l &= \frac{1}{2}\left[\int_{\mathcal{B}} (\hat{\boldsymbol{\omega}}\boldsymbol{x}_b + \boldsymbol{v})^T(\hat{\boldsymbol{\omega}}\boldsymbol{x}_b + \boldsymbol{v})dm + \sum_{i=1}^{n} m_i(\boldsymbol{v} + \hat{\boldsymbol{\omega}}\boldsymbol{r}_i + \dot{\boldsymbol{r}}_i)^T(\boldsymbol{v} + \hat{\boldsymbol{\omega}}\boldsymbol{r}_i + \dot{\boldsymbol{r}}_i)\right] \\ &= \frac{1}{2}\left[\int_{\mathcal{B}} (-\hat{\boldsymbol{x}}_b\boldsymbol{\omega} + \boldsymbol{v})^T(-\hat{\boldsymbol{x}}_b\boldsymbol{\omega} + \boldsymbol{v})dm + \sum_{i=1}^{n} m_i(\boldsymbol{v} - \hat{\boldsymbol{r}}_i\boldsymbol{\omega} + \dot{\boldsymbol{r}}_i)^T(\boldsymbol{v} - \hat{\boldsymbol{r}}_i\boldsymbol{\omega} + \dot{\boldsymbol{r}}_i)\right] \\ &= \frac{1}{2}\boldsymbol{\omega}^T\boldsymbol{I}_{\mathrm{b}}\,\boldsymbol{\omega} + \frac{1}{2}\boldsymbol{v}^T\boldsymbol{M}_{\mathrm{b}}\,\boldsymbol{v} + \frac{1}{2}\sum_{i=1}^{n} m_i(\boldsymbol{v} - \hat{\boldsymbol{r}}_i\boldsymbol{\omega} + \dot{\boldsymbol{r}}_i)^T(\boldsymbol{v} - \hat{\boldsymbol{r}}_i\boldsymbol{\omega} + \dot{\boldsymbol{r}}_i), \end{aligned} \tag{6.7}$$

where $\boldsymbol{I}_{\mathrm{b}} = \int_{\mathcal{B}}(-\hat{\boldsymbol{x}}_b\hat{\boldsymbol{x}}_b)dm$ and $\boldsymbol{M}_{\mathrm{b}} = m_{\mathrm{rb}}\mathbb{I}$ are the rigid body inertia and mass matrices respectively. Because the system is immersed in an ideal fluid, the body's motion induces motion in the surrounding fluid (and vice versa). The effect is captured by *added inertia* and *added mass*, which account for the additional energy that is necessary to accelerate the fluid around the body as it moves. If the rigid body has uniformly distributed mass and three planes of symmetry, and if the body frame is chosen appropriately, then the combined body/fluid inertia and mass matrices $\boldsymbol{I}_{\mathrm{b/f}}$ and $\boldsymbol{M}_{\mathrm{b/f}}$ are diagonal.

As shown in [80], Eq. (6.7) can be expressed in matrix form as

$$l(\boldsymbol{\omega}, \boldsymbol{v}, \boldsymbol{r}, \dot{\boldsymbol{r}}) = \frac{1}{2}\boldsymbol{\psi}^T\boldsymbol{M}(\boldsymbol{r})\boldsymbol{\psi}, \tag{6.8}$$

where

$$\boldsymbol{\psi} = \begin{pmatrix} \boldsymbol{\omega} \\ \boldsymbol{v} \\ \dot{\boldsymbol{r}} \end{pmatrix} \quad \text{and} \quad \boldsymbol{M} = \begin{pmatrix} \boldsymbol{M}_1 & \boldsymbol{M}_4 & \boldsymbol{M}_5 \\ \boldsymbol{M}_4^T & \boldsymbol{M}_2 & \boldsymbol{M}_6 \\ \boldsymbol{M}_5^T & \boldsymbol{M}_6^T & \boldsymbol{M}_3 \end{pmatrix}$$

is the kinetic energy metric with components

$$\begin{aligned}
\boldsymbol{M}_1 &= \boldsymbol{I}_{\mathrm{b/f}} - \sum_{i=1}^{n} m_i \hat{\boldsymbol{r}}_i \hat{\boldsymbol{r}}_i, \\
\boldsymbol{M}_2 &= \boldsymbol{M}_{\mathrm{b/f}} + \left(\sum_{i=1}^{n} m_i \right) \mathbb{I}, \\
\boldsymbol{M}_3 &= \mathrm{diag}(m_1 \mathbb{I},\ m_2 \mathbb{I}, \ldots,\ m_n \mathbb{I}), \\
\boldsymbol{M}_4 &= \sum_{i=1}^{n} m_i \hat{\boldsymbol{r}}_i, \\
\boldsymbol{M}_5 &= [m_1 \hat{\boldsymbol{r}}_1 \ \ m_2 \hat{\boldsymbol{r}}_2 \ \ \ldots \ \ m_n \hat{\boldsymbol{r}}_n], \\
\boldsymbol{M}_6 &= [m_1 \mathbb{I} \ \ m_2 \mathbb{I} \ \ \ldots \ \ m_n \mathbb{I}].
\end{aligned}$$

In the above expressions, $\mathbb{I}$ represents the 3×3 identity matrix. For both of the two examples considered in this chapter, there is only one moving point mass which is constrained to move along a linear track. It is a simple matter to adapt the above equations to this case. For example, suppose that the linear track is parallel to the body $\boldsymbol{b}_1$-axis. Then one simply requires that $\dot{\boldsymbol{r}}_1 \cdot \boldsymbol{e}_2 = 0$ and $\dot{\boldsymbol{r}}_1 \cdot \boldsymbol{e}_3 = 0$, where $\boldsymbol{e}_i$ is the i^{th} basis vector for $\mathbb{R}^3$.

The reduced Euler-Lagrange equations (6.4) can be cast in a form that is amenable for the controlled Lagrangian formulation as

$$\boldsymbol{M}\dot{\boldsymbol{\psi}} + \boldsymbol{C}\boldsymbol{\psi} = \boldsymbol{\mathcal{S}}\boldsymbol{\psi} + \boldsymbol{G}\boldsymbol{u}, \tag{6.9}$$

where

$$\boldsymbol{\mathcal{S}} = -\boldsymbol{\mathcal{S}}^T = \begin{pmatrix} \frac{\hat{\partial} l}{\partial \boldsymbol{\omega}} & \frac{\hat{\partial} l}{\partial \boldsymbol{v}} & \boldsymbol{0} \\ \frac{\hat{\partial} l}{\partial \boldsymbol{v}} & \boldsymbol{0} & \boldsymbol{0} \\ \boldsymbol{0} & \boldsymbol{0} & \boldsymbol{0} \end{pmatrix} \quad \text{and} \quad \boldsymbol{G} = \begin{pmatrix} \boldsymbol{0} \\ \boldsymbol{0} \\ \mathbb{I} \end{pmatrix}.$$

Recall that the matrix $\boldsymbol{C}$ is the "Coriolis and centripetal" matrix corresponding to $\boldsymbol{M}$. The matrix $\mathbb{I}$ is the identity matrix of appropriate dimensions.

6.2 Special Cases

6.2.1 $Q = SO(2) \times \mathbb{R}$

In this case, the reduced Euler-Lagrange equations are given by

$$\begin{aligned} \frac{d}{dt}\frac{\partial l}{\partial \xi} &= \mathrm{ad}^*_\xi \frac{\partial l}{\partial \xi}, \\ \frac{d}{dt}\frac{\partial l}{\partial \dot{y}} - \frac{\partial l}{\partial y} &= u, \end{aligned} \tag{6.10}$$

$\xi \in \mathfrak{so}(2),\ y \in \mathbb{R}$ and $l(\xi, y, \dot{y}) : \mathfrak{so}(2) \times T\mathbb{R} \to \mathbb{R}$ is the reduced Lagrangian. The coadjoint action of $\mathfrak{g}$ on its dual $\mathfrak{g}^*$ is the map $\mathrm{ad}^*_\xi : \mathfrak{g}^* \to \mathfrak{g}^*$ defined as

$$\left\langle \mathrm{ad}^*_\xi(\alpha), \eta \right\rangle := \left\langle \alpha, [\xi, \eta] \right\rangle,$$

where $\alpha \in \mathfrak{g}^*,\ \xi, \eta \in \mathfrak{g}$ and $[\xi, \eta]$ denotes the Lie bracket on $\mathfrak{g}$. Recall that any element in $\mathfrak{so}(2)$ can be identified with a 2×2 skew symmetric matrix of the form

$$\hat{\xi} = \begin{pmatrix} 0 & -\omega \\ \omega & 0 \end{pmatrix}.$$

The Lie bracket is defined as $[\xi, \eta] = \hat{\xi}\hat{\eta} - \hat{\eta}\hat{\xi}$ which gives

$$[\xi, \eta] = 0 \Rightarrow \mathrm{ad}^*_\xi(\alpha) = 0.$$

Thus, the reduced Euler-Lagrange equations (6.10) become

$$\begin{aligned} \frac{d}{dt}\frac{\partial l}{\partial \omega} &= 0, \\ \frac{d}{dt}\frac{\partial l}{\partial \dot{y}} - \frac{\partial l}{\partial y} &= u, \end{aligned} \tag{6.11}$$

where $\mathfrak{so}(2)$ is identified with $\mathbb{R}$.

6.2.2 $Q = SE(2) \times \mathbb{R}$

In this case, the reduced Lagrangian l is a function

$$l(\xi, y, \dot{y}) : \mathfrak{se}(2) \times T\mathbb{R} \to \mathbb{R},$$

where $\xi = (\omega, \boldsymbol{v}) \in \mathfrak{se}(2)$ and $(y, \dot{y}) \in T\mathbb{R}$. The reduced equations are given by (6.10) where $\mathrm{ad}^*_\xi \frac{\partial l}{\partial \xi}$ is the coadjoint action of $\mathfrak{se}(2)$ on its dual $\mathfrak{se}(2)^*$. The coadjoint action is given by (see [46])

$$\mathrm{ad}^*_{(x,\boldsymbol{y})}(\mu, \boldsymbol{\alpha}) = (-\boldsymbol{y}^T \mathbb{J}\boldsymbol{\alpha}, x\mathbb{J}\boldsymbol{\alpha}), \tag{6.12}$$

where $(x, \boldsymbol{y}) \in \mathfrak{se}(2)$, $(\mu, \boldsymbol{\alpha}) \in \mathfrak{se}(2)^*$ and

$$\mathbb{J} = \begin{pmatrix} 0 & 1 \\ -1 & 0 \end{pmatrix}.$$

Using $\xi = (\omega, \boldsymbol{v})$ and $\frac{\partial l}{\partial \xi} = (\frac{\partial l}{\partial \omega}, \frac{\partial l}{\partial \boldsymbol{v}})$ in (6.12), we have

$$\mathrm{ad}^*_\xi \frac{\partial l}{\partial \xi} = \begin{pmatrix} 0 & v_2 & -v_1 \\ 0 & 0 & \omega \\ 0 & -\omega & 0 \end{pmatrix} \begin{pmatrix} \frac{\partial l}{\partial \omega} \\ \frac{\partial l}{\partial v_1} \\ \frac{\partial l}{\partial v_2} \end{pmatrix}, \tag{6.13}$$

where $\boldsymbol{v} = [v_1,\ v_2]^T$. Using (6.13) in (6.10), the reduced Euler-Lagrange equations are

$$\begin{pmatrix} \frac{d}{dt}\frac{\partial l}{\partial \omega} \\ \frac{d}{dt}\frac{\partial l}{\partial v_1} \\ \frac{d}{dt}\frac{\partial l}{\partial v_2} \\ \frac{d}{dt}\frac{\partial l}{\partial \dot{y}} - \frac{\partial l}{\partial y} \end{pmatrix} = \begin{pmatrix} 0 & -\frac{\partial l}{\partial v_2} & \frac{\partial l}{\partial v_1} & 0 \\ \frac{\partial l}{\partial v_2} & 0 & 0 & 0 \\ -\frac{\partial l}{\partial v_1} & 0 & 0 & 0 \\ 0 & 0 & 0 & 0 \end{pmatrix} \begin{pmatrix} \omega \\ v_1 \\ v_2 \\ \dot{y} \end{pmatrix} + \begin{pmatrix} 0 \\ 0 \\ 0 \\ u \end{pmatrix}. \tag{6.14}$$

6.3 Simplified Matching Conditions

Let us write the open-loop reduced Lagrangian in the block matrix form as

$$l = \frac{1}{2} \begin{pmatrix} \boldsymbol{\eta} \\ \dot{\boldsymbol{r}} \end{pmatrix}^T \begin{pmatrix} \boldsymbol{M}_1 & \boldsymbol{M}_2 \\ \boldsymbol{M}_2^T & \boldsymbol{M}_3 \end{pmatrix} \begin{pmatrix} \boldsymbol{\eta} \\ \dot{\boldsymbol{r}} \end{pmatrix},$$

where $\boldsymbol{\eta}^T = [\boldsymbol{\omega}^T, \boldsymbol{v}^T]$. We seek a control law $\boldsymbol{u}$ such that the closed-loop equations are derived from a control-modified Lagrangian

$$\begin{aligned} l_c &= \frac{1}{2}\boldsymbol{\psi}^T \boldsymbol{M}_c(\boldsymbol{r})\boldsymbol{\psi} - V_c(\boldsymbol{r}) \\ &= \frac{1}{2} \begin{pmatrix} \boldsymbol{\eta} \\ \dot{\boldsymbol{r}} \end{pmatrix}^T \begin{pmatrix} \boldsymbol{M}_{c1} & \boldsymbol{M}_{c2} \\ \boldsymbol{M}_{c2}^T & \boldsymbol{M}_{c3} \end{pmatrix} \begin{pmatrix} \boldsymbol{\eta} \\ \dot{\boldsymbol{r}} \end{pmatrix} - V_c(\boldsymbol{r}), \end{aligned} \tag{6.15}$$

where $\boldsymbol{M}_c$ is the control-modified kinetic energy metric and V_c is some artificial potential energy introduced in the closed-loop. Let the closed-loop equations be of the form,

$$\boldsymbol{M}_c\dot{\boldsymbol{\psi}} + \boldsymbol{C}_c\boldsymbol{\psi} + \begin{pmatrix} \mathbf{0} \\ \frac{\partial V_c}{\partial \boldsymbol{r}} \end{pmatrix} = \boldsymbol{\mathcal{S}}_c\boldsymbol{\psi}. \tag{6.16}$$

Equation (4.79) gives the general matching conditions,

$$\boldsymbol{G}^{\perp}\left[\boldsymbol{M}\boldsymbol{M}_c^{-1}\left(\boldsymbol{\mathcal{S}}_c\boldsymbol{\psi} - \boldsymbol{C}_c\boldsymbol{\psi} - \begin{pmatrix} \mathbf{0} \\ \frac{\partial V_c}{\partial \boldsymbol{r}} \end{pmatrix}\right) + \boldsymbol{C}\boldsymbol{\psi} - \boldsymbol{\mathcal{S}}\boldsymbol{\psi}\right] = \mathbf{0}, \tag{6.17}$$

where

$$\boldsymbol{G}^{\perp} = [\mathbb{I} \;\; \mathbf{0}], \;\; \boldsymbol{\mathcal{S}} = \begin{pmatrix} \boldsymbol{\Lambda} & \mathbf{0} \\ \mathbf{0} & \mathbf{0} \end{pmatrix}, \;\; \boldsymbol{\Lambda}^T = -\boldsymbol{\Lambda}.$$

The matching conditions in (6.17) are a set of coupled nonlinear ordinary differential equations in the elements of $\boldsymbol{M}_c$ and generally difficult to solve. We derive sufficient matching conditions that are algebraic in nature. This considerably reduces the complexity of solving the matching conditions.

Let $\boldsymbol{\lambda} = \boldsymbol{M}\boldsymbol{M}_c^{-1}$ as in [5]. Since $\boldsymbol{M}_c = \boldsymbol{M}_c^T$, we have

$$\boldsymbol{\lambda}\boldsymbol{M} = \boldsymbol{M}\boldsymbol{\lambda}^T. \tag{6.18}$$

Let us partition $\boldsymbol{\lambda}$ as

$$\boldsymbol{\lambda} = \begin{pmatrix} \boldsymbol{\lambda}_1 & \boldsymbol{\lambda}_2 \\ \boldsymbol{\lambda}_3 & \boldsymbol{\lambda}_4 \end{pmatrix}.$$

Rearranging Eq. (6.17), we get

$$\begin{aligned} \mathbf{0} &= \boldsymbol{G}^{\perp}\left[\boldsymbol{\lambda}\left(\boldsymbol{\mathcal{S}}_c\boldsymbol{\psi} - \boldsymbol{C}_c\boldsymbol{\psi} - \begin{pmatrix} \mathbf{0} \\ \frac{\partial V_c}{\partial \boldsymbol{r}} \end{pmatrix}\right) + \boldsymbol{C}\boldsymbol{\psi} - \boldsymbol{\mathcal{S}}\boldsymbol{\psi}\right] \\ &= \boldsymbol{G}^{\perp}\left[\boldsymbol{\lambda}\left(\boldsymbol{\mathcal{S}}_c\boldsymbol{\psi} - \boldsymbol{C}_c\boldsymbol{\psi}\right) + \boldsymbol{C}\boldsymbol{\psi} - \boldsymbol{\mathcal{S}}\boldsymbol{\psi}\right] - \boldsymbol{G}^{\perp}\boldsymbol{\lambda}\begin{pmatrix} \mathbf{0} \\ \frac{\partial V_c}{\partial \boldsymbol{r}} \end{pmatrix}. \end{aligned}$$

The kinetic matching condition is

$$\boldsymbol{G}^{\perp}\left[\boldsymbol{\lambda}\left(\boldsymbol{\mathcal{S}}_c\boldsymbol{\psi}-\boldsymbol{C}_c\boldsymbol{\psi}\right)+\boldsymbol{C}\boldsymbol{\psi}-\boldsymbol{\mathcal{S}}\boldsymbol{\psi}\right]=\mathbf{0}, \tag{6.19}$$

and the potential matching condition is

$$\boldsymbol{G}^{\perp}\boldsymbol{\lambda}\begin{pmatrix}\mathbf{0}\\ \frac{\partial V_c}{\partial \boldsymbol{r}}\end{pmatrix}=\mathbf{0}. \tag{6.20}$$

We claim that $\boldsymbol{\lambda}$ of the form

$$\boldsymbol{\lambda}=\begin{pmatrix}\boldsymbol{\lambda}_1 & \mathbf{0}\\ \boldsymbol{\lambda}_3 & \boldsymbol{\lambda}_4\end{pmatrix} \tag{6.21}$$

satisfies the potential matching condition (6.20). To see this, note that

$$\boldsymbol{G}^{\perp}\boldsymbol{\lambda}\begin{pmatrix}\mathbf{0}\\ \frac{\partial V_c}{\partial \boldsymbol{r}}\end{pmatrix}=[\mathbb{I}\ \ \mathbf{0}]\begin{pmatrix}\boldsymbol{\lambda}_1 & \mathbf{0}\\ \boldsymbol{\lambda}_3 & \boldsymbol{\lambda}_4\end{pmatrix}\begin{pmatrix}\mathbf{0}\\ \frac{\partial V_c}{\partial \boldsymbol{r}}\end{pmatrix}=\mathbf{0}.$$

To solve the kinetic matching condition, partition $\boldsymbol{\mathcal{S}}_c$ as

$$\begin{aligned}\boldsymbol{\mathcal{S}}_c &= \boldsymbol{\mathcal{S}}_{c1}+\boldsymbol{\mathcal{S}}_{c2}\\ &= \begin{pmatrix}\boldsymbol{\Lambda}_c & \mathbf{0}\\ \mathbf{0} & \mathbf{0}\end{pmatrix}+\begin{pmatrix}\mathbf{0} & \boldsymbol{\mathcal{D}}\\ -\boldsymbol{\mathcal{D}}^T & \mathbf{0}\end{pmatrix},\end{aligned}$$

where $\boldsymbol{\Lambda}_c^T=-\boldsymbol{\Lambda}_c^T$. Rewrite the kinetic matching condition (6.19) as

$$\boldsymbol{G}^{\perp}\left[\boldsymbol{\lambda}\boldsymbol{\mathcal{S}}_{c1}\boldsymbol{\psi}-\boldsymbol{\mathcal{S}}\boldsymbol{\psi}\right]+\boldsymbol{G}^{\perp}\left[\boldsymbol{\lambda}\boldsymbol{\mathcal{S}}_{c2}\boldsymbol{\psi}-\left(\boldsymbol{G}^{\perp}\boldsymbol{\lambda}\boldsymbol{C}_c\boldsymbol{\psi}-\boldsymbol{C}\boldsymbol{\psi}\right)\right]=\mathbf{0}.$$

Sufficient conditions for kinetic matching are

$$\boldsymbol{G}^{\perp}\left[\boldsymbol{\lambda}\boldsymbol{\mathcal{S}}_{c1}\boldsymbol{\psi}-\boldsymbol{\mathcal{S}}\boldsymbol{\psi}\right]=\mathbf{0}, \tag{6.22}$$

and

$$\boldsymbol{G}^{\perp}\boldsymbol{\lambda}\boldsymbol{\mathcal{S}}_{c2}\boldsymbol{\psi}=\boldsymbol{G}^{\perp}\left[\boldsymbol{\lambda}\boldsymbol{C}_c\boldsymbol{\psi}-\boldsymbol{C}\boldsymbol{\psi}\right]. \tag{6.23}$$

Using the form of $\boldsymbol{\lambda}$ that solves the potential matching condition, Eq. (6.22) reduces to

$$\boldsymbol{\lambda}_1\boldsymbol{\Lambda}_c\boldsymbol{\eta}=\boldsymbol{\Lambda}\boldsymbol{\eta}. \tag{6.24}$$

Skew symmetry of $\boldsymbol{\Lambda}_c$ gives

$$\boldsymbol{\eta}^T \boldsymbol{\lambda}_1^{-1} \boldsymbol{\Lambda} \boldsymbol{\eta} = 0 \tag{6.25}$$

Equation (6.25) is a scalar equation that is cubic in the velocities.

We claim that it is enough to solve condition (6.22) to solve the kinetic matching condition (6.19). Suppose we solve (6.18) and (6.25) for $\boldsymbol{\lambda}$ and therefore $\boldsymbol{M}_c$. Note that we can write $\boldsymbol{C}$ and $\boldsymbol{C}_c$ as

$$\boldsymbol{C} = \begin{pmatrix} \mathbf{0} & \boldsymbol{\mathcal{P}} \\ \boldsymbol{\mathcal{Q}} & \boldsymbol{\mathcal{R}} \end{pmatrix} \text{ and } \boldsymbol{C}_c = \begin{pmatrix} \mathbf{0} & \boldsymbol{\mathcal{P}}_c \\ \boldsymbol{\mathcal{Q}}_c & \boldsymbol{\mathcal{R}}_c \end{pmatrix},$$

where the entries in $\boldsymbol{C}$ and $\boldsymbol{C}_c$ are affine in the velocities. This is possible because the entries in $\boldsymbol{M}$ and $\boldsymbol{M}_c$ only depend on $\boldsymbol{r}$. Condition (6.23) reduces to

$$\boldsymbol{\lambda}_1 \boldsymbol{\mathcal{D}} \dot{\boldsymbol{r}} = \left(\boldsymbol{\lambda}_1 \boldsymbol{\mathcal{P}}_c - \boldsymbol{\mathcal{P}} \right) \dot{\boldsymbol{r}},$$

which gives

$$\boldsymbol{\mathcal{D}} = \boldsymbol{\mathcal{P}}_c - \boldsymbol{\lambda}_1^{-1} \boldsymbol{\mathcal{P}}. \tag{6.26}$$

Thus, condition (6.23) can always be satisfied once $\boldsymbol{\lambda}$ is known. The following proposition summarizes the above discussion.

Proposition 6.3.1 *Choosing $\boldsymbol{\lambda}$ of the form as given in (6.21), equations (6.18) and (6.24) provide sufficient matching conditions such that (6.17) holds.*

Corollary 6.3.2 *There always exists at least one matching solution to (6.17).*

Proof : Choosing $\boldsymbol{\Lambda}_c = \boldsymbol{\Lambda}$, Eq. (6.24) gives $\boldsymbol{\lambda}_1 = \mathbb{I}$. From Eq. (6.26), it follows that $\boldsymbol{\mathcal{D}} = \mathbf{0}$ and therefore $\boldsymbol{\mathcal{S}}_c = \boldsymbol{\mathcal{S}}$. Finally, using $\boldsymbol{\lambda} \boldsymbol{M}_c = \boldsymbol{M}$ gives

$$\boldsymbol{M}_{c1} = \boldsymbol{M}_c \text{ and } \boldsymbol{M}_{c2} = \boldsymbol{M}_2 \Rightarrow \boldsymbol{M}_c = \begin{pmatrix} \boldsymbol{M}_1 & \boldsymbol{M}_2 \\ \boldsymbol{M}_2^T & \boldsymbol{\rho} \end{pmatrix}, \tag{6.27}$$

where $\boldsymbol{\rho}$ is free to choose. The entries of $\boldsymbol{\rho}$ act as control parameters. We refer to this matching law as the *trivial* matching solution. ■

The following proposition shows the connection to the kinetic energy shaping technique outlined in Chapter 4. We follow the notation in Chapter 4.

Proposition 6.3.3 *The trivial matching law (6.27) corresponds to the following choice of* τ_α^a, σ_{ab} *and* ρ_{ab} *:*

$$\tau_\alpha^a = -\sigma^{ac} g_{c\alpha} \quad \text{and} \quad \sigma^{ab} + \rho^{ab} = g^{ab}. \tag{6.28}$$

Proof : Let $\boldsymbol{\tau}, \boldsymbol{\sigma}$ and $\boldsymbol{\rho}$ be the matrix representations for $\tau_\alpha^a, \sigma_{ab}$ and ρ_{ab}. In matrix form, the conditions given in (6.28) are

$$\boldsymbol{\sigma}^{-1} + \boldsymbol{\rho}^{-1} = \boldsymbol{M}_3^{-1}; \quad \boldsymbol{\tau} = -\boldsymbol{M}_2 \boldsymbol{\sigma}^{-\mathbf{1}}.$$

Also, the matrix form for the mechanical connection is given by (see Eq. (4.20))

$$\mathcal{A} = \boldsymbol{M}_2 \boldsymbol{M}_3^{-1}.$$

Equations (4.26), (4.27) and (4.28) give the elements of $\boldsymbol{M}_c$. In matrix notation, they are

$$\begin{aligned}
\boldsymbol{M}_{c3} &= \boldsymbol{\rho}, \\
\boldsymbol{M}_{c2} &= (\mathcal{A} + \boldsymbol{\tau})\boldsymbol{\rho} \\
&= \boldsymbol{M}_2(\boldsymbol{M}_3^{-1} - \boldsymbol{\sigma}^{-1})\boldsymbol{\rho} \\
&= \boldsymbol{M}_2 \boldsymbol{\rho}^{-1} \boldsymbol{\rho} \\
&= \boldsymbol{M}_2, \\
\boldsymbol{M}_{c1} &= \boldsymbol{M}_1 - \boldsymbol{M}_2 \boldsymbol{M}_3^{-1} \boldsymbol{M}_2^T + \boldsymbol{\tau}\boldsymbol{\sigma}\boldsymbol{\tau}^T + (\mathcal{A} + \boldsymbol{\tau})\boldsymbol{\rho}(\mathcal{A} + \boldsymbol{\tau})^T \\
&= \boldsymbol{M}_1 - \boldsymbol{M}_2(-\boldsymbol{M}_3^{-1} + \boldsymbol{\sigma}^{-1} + \boldsymbol{\rho}^{-1})\boldsymbol{M}_2^T \\
&= \boldsymbol{M}_1.
\end{aligned}$$

Thus,

$$\boldsymbol{M}_c = \begin{pmatrix} \boldsymbol{M}_1 & \boldsymbol{M}_2 \\ \boldsymbol{M}_2^T & \boldsymbol{\rho} \end{pmatrix}$$

which is the trivial matching law.

6.3.1 An Algorithm for Matching and Stabilization

The matching conditions given by (6.18), (6.24) and (6.26) lead to an algorithmic approach to the matching and stabilization process. We outline the algorithm below.

1. With $\boldsymbol{\lambda}$ assumed to be of the form (6.21), choose a form for $\boldsymbol{\Lambda}_c$ so that (6.18) and (6.25) are satisfied. This gives us $\boldsymbol{\lambda}$ and thus $\boldsymbol{M}_c$.
2. Compute $\boldsymbol{\mathcal{D}}$ from (6.26). $\boldsymbol{\Lambda}_c$ and $\boldsymbol{\mathcal{D}}$ give $\boldsymbol{\mathcal{S}}_c$.
3. The closed-loop energy $E_c = \frac{1}{2}\boldsymbol{\psi}^T \boldsymbol{M}_c \boldsymbol{\psi} + V_c$ is conserved. The matching process in steps (1) and (2) typically leaves free parameters that can be used for stabilization.
4. Identify other conserved quantities in the system. Usually, the total angular or total linear momenta are conserved. Suppose C is a conserved quantity.
5. Construct the candidate Lyapunov function $E_\phi = E_c + \phi(C)$ where $\phi(.)$ is as-yet-undetermined smooth function. E_ϕ is conserved by construction.
6. Asses nonlinear stability using Lyapunov's direct method.

Steps (4) to (6) constitute the Energy-Casimir method [46]. The *trivial* matching solution (6.27) should be tried first. If the trivial matching solution does not lead to a proof of nonlinear stability, other matching solutions should be found. If the trivial matching solution is the only solution, spectral stability can be assessed in lieu of a proof of nonlinear stability.

6.4 Example: A Planar Spinning Disk

In this section, we illustrate the controlled Lagrangian technique by considering the simple example of a spinning disk with a single mass moving along a slot. Consider a planar disk spinning about its center O shown in Figure 6.2. A point mass m moves, under the influence of a control force,

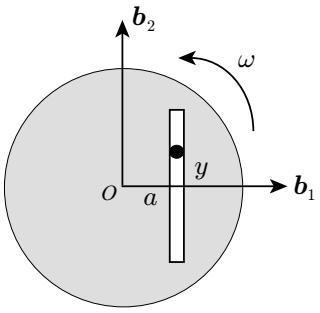

Figure 6.2: A spinning disk with a point mass moving along a slot

along a slot in the disk which is displaced some distance a from the center (where $a \neq 0$). Let I be the moment of inertia of the disk about the its spin axis. The configuration space of the spinning disk is $Q = SO(2) \times \mathbb{R}$. As seen in § 6.1.2, the Lagrangian $L : TQ \to \mathbb{R}$ is invariant under the action of $G = SO(2)$. This allows us to write the reduced Euler-Lagrange equations for the above system. The reduced Lagrangian l is the kinetic energy of the system given by

$$l(\omega, y, \dot{y}) = \frac{1}{2} \begin{pmatrix} \omega \\ \dot{y} \end{pmatrix}^T \begin{pmatrix} I + m(a^2 + y^2) & ma \\ ma & m \end{pmatrix} \begin{pmatrix} \omega \\ \dot{y} \end{pmatrix}. \tag{6.29}$$

Define the non-dimensional quantities:

$$\bar{y} = \frac{y}{a}; \quad \bar{\omega} = \frac{\omega}{\omega_0}; \quad \bar{t} = \omega_0 t, \ \alpha = \frac{I}{ma^2} + 1, \quad \text{and} \quad \bar{l} = \frac{l}{ma^2\omega_0^2},$$

where $\omega_0 \neq 0$ is some equilibrium angular rate. Dropping the bar for convenience, the non-dimensional reduced Lagrangian is

$$l = \frac{1}{2} \begin{pmatrix} \omega \\ \dot{y} \end{pmatrix}^T \begin{pmatrix} \alpha + y^2 & 1 \\ 1 & 1 \end{pmatrix} \begin{pmatrix} \omega \\ \dot{y} \end{pmatrix}. \tag{6.30}$$

In the absence of physical dissipation, the controlled dynamics are given by (6.11) as

$$\begin{aligned} \frac{d}{dt}\left(\frac{\partial l}{\partial \omega}\right) &= 0, \\ \frac{d}{dt}\left(\frac{\partial l}{\partial \dot{y}}\right) - \frac{\partial l}{\partial y} &= u, \end{aligned} \tag{6.31}$$

where u is the control applied to the point mass. Clearly, the total angular momentum

$$\pi_s = \frac{\partial l}{\partial \omega} = (\alpha + y^2)\omega + \dot{y} \tag{6.32}$$

is conserved at all times. Thus, the dynamics evolves on a constant angular momentum surface, that is, on the surface

$$(\alpha + y^2)\omega + \dot{y} = \text{constant}.$$

6.4.1 Stability of the Uncontrolled Dynamics

The relative equilibrium of interest is $(\omega, y, \dot{y}) = (1, 0, 0)$. This corresponds to the disk spinning at a constant angular rate ω_0 and the mass being stationary at the center of the slot. The eigenvalues corresponding to the equilibrium e are

$$\lambda_1 = 0 \quad \text{and} \quad \lambda_{2,3} = \pm\sqrt{\frac{\alpha}{(\alpha - 1)}}\ .$$

Since $\alpha > 1$, the equilibrium is a saddle point. The zero eigenvalue corresponds to conservation of π_s. We denote the value of a quantity δ at the equilibrium by $\delta|_e$. At equilibrium,

$$\pi_s|_e = \pi_0 = \alpha.$$

The control objective is to stabilize the equilibrium with respect to perturbations that preserve the angular momentum, that is, perturbations that lie on the surface

$$(\alpha + y^2)\omega + \dot{y} = \alpha.$$

6.4.2 A Matching Solution

The open-loop equations (6.31) can be written as

$$\boldsymbol{M}\dot{\boldsymbol{\psi}} + \boldsymbol{C}\boldsymbol{\psi} = \boldsymbol{G}u, \tag{6.33}$$

where

$$\boldsymbol{\psi} = \begin{pmatrix} \omega \\ \dot{y} \end{pmatrix}, \quad \boldsymbol{M} = \begin{pmatrix} \alpha + y^2 & 1 \\ 1 & 1 \end{pmatrix}, \quad \boldsymbol{C} = \begin{pmatrix} y\dot{y} & y\omega \\ -y\omega & 0 \end{pmatrix} \quad \text{and} \quad \boldsymbol{G} = \begin{pmatrix} 0 \\ 1 \end{pmatrix}.$$

We seek an energy shaping control law u_{es} such that the closed-loop equations are

$$\boldsymbol{M}_c\dot{\boldsymbol{\psi}} + \boldsymbol{C}_c\boldsymbol{\psi} = \boldsymbol{\mathcal{S}}_c\boldsymbol{\psi}, \tag{6.34}$$

where $\boldsymbol{\mathcal{S}}_c^T = -\boldsymbol{\mathcal{S}}_c$. A matching solution is given by Eq. (6.27) as

$$\boldsymbol{M}_c = \begin{pmatrix} \alpha + y^2 & 1 \\ 1 & \beta(y) \end{pmatrix} \quad \text{and} \quad \boldsymbol{\mathcal{S}}_c = \boldsymbol{0}, \tag{6.35}$$

where $\beta(y)$ is as-yet-undetermined function of y. We need

$$\text{Det}(\boldsymbol{M}_c) \;\neq\; 0 \quad \Rightarrow \quad (\alpha + y^2)\beta(y) \;\neq\; 1.$$

Setting

$$\beta(y) \;=\; \frac{\tilde{\beta}}{\alpha + y^2} \;\Rightarrow\; \tilde{\beta} \;\neq\; 1,$$

where $\tilde{\beta}$ acts as a control parameter.

Note: The above matching solution belongs to a set of more general solutions given by the matching conditions derived in Appendix D. The above matching solution can be obtained by setting $a_c = a$, $b_c = b$ and $s_1 = s_2 = 0$, where $a,\ a_c,\ b,\ b_c,\ s_1$ and s_2 are defined in Appendix D.

The energy shaping control is given by (4.83),

$$\begin{aligned} u_{\text{es}} &= (\boldsymbol{G}^T\ \boldsymbol{G})^{-1}\boldsymbol{G}^T\left[\boldsymbol{M}\boldsymbol{M}_c^{-1}(\boldsymbol{\mathcal{S}}_c\boldsymbol{\psi} - \boldsymbol{C}_c\boldsymbol{\psi}) + \boldsymbol{C}\boldsymbol{\psi}\right] \\ &= \frac{y\left((\alpha+y^2)^2(\alpha+y^2-\tilde{\beta})\omega^2 + 2(\alpha+y^2)(\alpha+y^2-\tilde{\beta})\omega\dot{y} + \tilde{\beta}(\alpha+y^2-1)\dot{y}^2\right)}{(\tilde{\beta}-1)(\alpha+y^2)} \end{aligned} \tag{6.36}$$

6.4.3 Nonlinear Stability

We prove nonlinear stability of the equilibrium using the Energy-Casimir Method [46]. For the spinning disk, the control-modified energy

$$E_c = l_c = \frac{1}{2} \begin{pmatrix} \omega \\ \dot{y} \end{pmatrix}^T \begin{pmatrix} \alpha + y^2 & 1 \\ 1 & \frac{\tilde{\beta}}{\alpha + y^2} \end{pmatrix} \begin{pmatrix} \omega \\ \dot{y} \end{pmatrix} \tag{6.37}$$

is a conserved quantity.

Proposition 6.4.1 *The energy shaping control* u_{es} *stabilizes the relative equilibrium* $(\omega, y, \dot{y}) = (1, 0, 0)$ *with* $\tilde{\beta} < 1$.

Proof: Let

$$E_\phi = E_c + \phi(\pi_s) \tag{6.38}$$

be a candidate Lyapunov function where $\phi(.)$ is an as-yet-undetermined smooth function of π_s. The function E_ϕ is conserved by construction. Thus, nonlinear stability of the equilibrium will follow from Lyapunov's direct method if

$$\nabla E_\phi\big|_e = 0 \;\text{ and }\; \nabla^2 E_\phi\big|_e > 0 \text{ (or } < 0),$$

where ∇E_ϕ and $\nabla^2 E_\phi$ denote the gradient and Hessian of E_ϕ respectively. Upon calculation,

$$\nabla E_\phi\big|_e = \begin{pmatrix} \alpha \left(\frac{\partial \phi}{\partial \pi_s}\Big|_e + 1 \right) \\ 0 \\ \frac{\partial \phi}{\partial \pi_s}\Big|_e + 1 \end{pmatrix} \tag{6.39}$$

and

$$\nabla^2 E_\phi\big|_e = \begin{pmatrix} \alpha \left(1 + \alpha \;\frac{\partial^2 \phi}{\partial \pi_s^2}\Big|_e \right) & 0 & 1 + \alpha \;\frac{\partial^2 \phi}{\partial \pi_s^2}\Big|_e \\ 0 & 1 + 2\;\frac{\partial \phi}{\partial \pi_s}\Big|_e & 0 \\ 1 + \alpha \;\frac{\partial^2 \phi}{\partial \pi_s^2}\Big|_e & 0 & \frac{\partial^2 \phi}{\partial \pi_s^2}\Big|_e + \frac{\tilde{\beta}}{\alpha} \end{pmatrix}. \tag{6.40}$$

Note that

$$\text{Det } \left(\nabla^2 E_\phi\big|_e\right) = \left(1 + 2\ \frac{\partial \phi}{\partial \pi_s}\bigg|_e\right)\left(1 + \alpha\ \frac{\partial^2 \phi}{\partial \pi_s^2}\bigg|_e\right)\left(\tilde{\beta} - 1\right). \tag{6.41}$$

The equilibrium can be made a maximum of E_ϕ by choosing

$$\frac{\partial \phi}{\partial \pi_s}\bigg|_e = -1;\ \ \frac{\partial^2 \phi}{\partial \pi_s^2}\bigg|_e < -\frac{1}{\alpha}\ \text{ and }\ \tilde{\beta} < 1.$$

A choice for ϕ is

$$\phi(\pi_s) = \frac{\delta}{2}\pi_s^2 - (1 + \delta\alpha)\pi_s,$$

where $\delta < -\frac{1}{\alpha}$. ■

6.4.4 Feedback Dissipation and Asymptotic Stability

Let us augment the energy shaping control with feedback dissipation, that is,

$$u = u_{\text{es}} + u_{\text{diss}}.$$

In this case, the closed-loop equations become

$$\boldsymbol{M}_c\dot{\boldsymbol{\psi}} + \boldsymbol{C}_c\boldsymbol{\psi} = \boldsymbol{\mathcal{S}}_c\boldsymbol{\psi} + \boldsymbol{M}_c\boldsymbol{M}^{-1}\ \boldsymbol{G}u_{\text{diss}}. \tag{6.42}$$

The control-modified energy is no longer conserved and its rate is given by

$$\dot{E}_c = \boldsymbol{\psi}^T\boldsymbol{M}_c\boldsymbol{M}^{-1}\ \boldsymbol{G}u_{\text{diss}}. \tag{6.43}$$

Choosing

$$\boldsymbol{G}u_{\text{diss}} = \boldsymbol{M}\boldsymbol{M}_c^{-1}\boldsymbol{R}\boldsymbol{\psi}$$

gives

$$\dot{E}_c = \boldsymbol{\psi}^T\boldsymbol{R}\boldsymbol{\psi}, \tag{6.44}$$

where $\boldsymbol{R}$ is the dissipation matrix. Let

$$\boldsymbol{R} = \begin{pmatrix} 0 & 0 \\ 0 & k_{\text{diss}} \end{pmatrix},$$

where k_{diss} is the dissipation parameter. The feedback dissipation u_{diss} is

$$\begin{aligned} u_{\text{diss}} &= (\boldsymbol{G}^T\boldsymbol{G})^{-1}\boldsymbol{G}^T\boldsymbol{M}\boldsymbol{M}_c^{-1}\boldsymbol{R}\boldsymbol{\psi} \\ &= \frac{k_{\text{diss}}\ \dot{y}\ (\alpha + y^2 - 1)}{\tilde{\beta} - 1} \end{aligned} \tag{6.45}$$

We use LaSalle's invariance principle (2.4.4) to prove asymptotic stability when $u = u_{\text{es}} + u_{\text{diss}}$, where u_{es} is given by (6.36) and u_{diss} is given by (6.45).

Proposition 6.4.2 *The relative equilibrium $(\omega, y, \dot{y}) = (1, 0, 0)$ is leaf-wise asymptotically stable (that is, asymptotically stable with respect to perturbations constrained to the surface $\pi_s = \alpha$) for $k_{\text{diss}} > 0$.*

Proof : Let

$$W = \{(\omega, y, \dot{y}) \mid (\alpha + y^2)\omega + \dot{y} = \alpha\}.$$

Consider any compact, positively invariant set $\Omega \subset W$ containing the equilibrium. Let E be the set of all points in Ω at which $\dot{E}_\phi = 0$. Since π_s is conserved at all times,

$$\dot{E}_\phi = \dot{E}_c = \boldsymbol{\psi}^T\boldsymbol{R}\boldsymbol{\psi} = k_{\text{diss}}\dot{y}^2 \geq 0 \ \text{ since } \ k_{\text{diss}} > 0. \tag{6.46}$$

Thus,

$$E = \{(\omega, y, \dot{y}) \in \Omega \mid \dot{y} = 0\}. \tag{6.47}$$

LaSalle's invariance principle asserts that every trajectory starting in Ω approaches the largest invariant set $\mathcal{M}$ contained in E as $t \to \infty$. If the set $\mathcal{M}$ contains only the equilibrium, it follows that the equilibrium is asymptotically stable. From (6.47), for any set $\mathcal{M} \subset E$ to be invariant, we need

$$\dot{y}(t) \equiv 0 \text{ (zero for all times)} \ \Rightarrow \ddot{y}(t) = 0.$$

Writing $\ddot{y}$ explicitly, we get

$$\ddot{y} = \frac{1}{\tilde{\beta} - 1}\left[2y\dot{y}\omega + (\alpha + y^2)(k_{\text{diss}}\dot{y} + y\omega^2) + \frac{\tilde{\beta}\dot{y}}{\alpha + y^2}\right]. \tag{6.48}$$

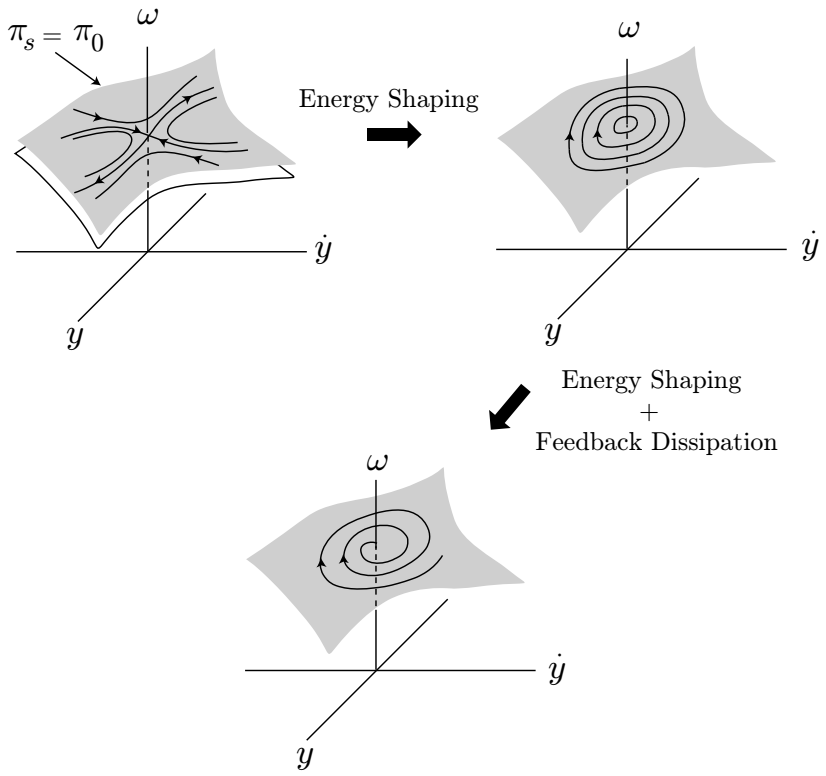

Figure 6.3: Stabilization for the spinning disk using energy shaping and feedback dissipation.

Setting $\dot{y} = 0$ in (6.48) gives

$$\ddot{y} = \frac{1}{\tilde{\beta} - 1}(\alpha + y^2)y\omega^2 \Rightarrow \ddot{y} = 0 \text{ iff } y = 0$$

since $\omega \neq 0$. Conservation of π_s gives

$$\mathcal{M} = (1, 0, 0).$$

Asymptotic stability of the equilibrium follows from LaSalle's invariance principle. ■

The stabilization process is illustrated in Fig. 6.3. Figure 6.4 shows simulations for the spinning disk with feedback dissipation.

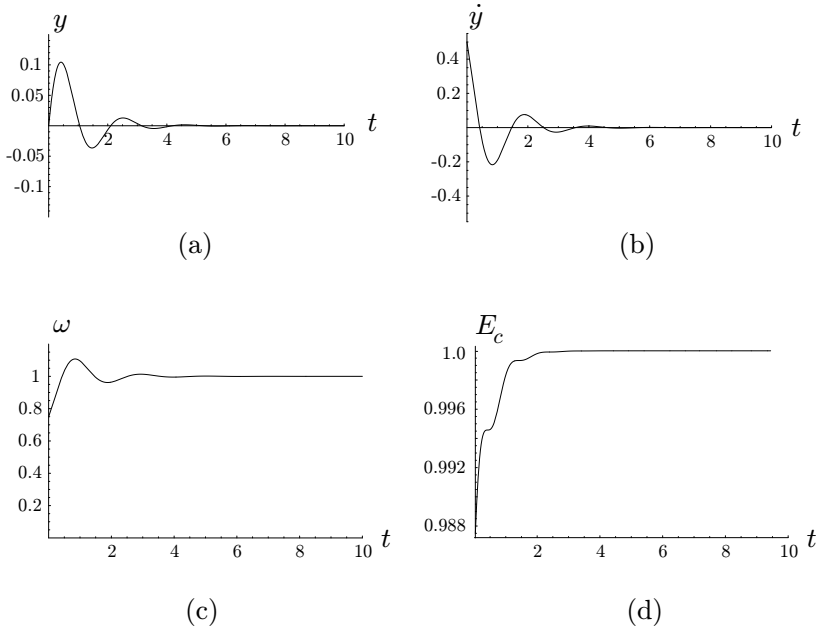

Figure 6.4: Time histories for (a) y, (b) $\dot{y}$, (c) ω and (d) E_c. The simulation parameters are $\alpha = 2,\ \tilde{\beta} = 0.8,\ k_{\text{diss}} = 0.2$. The initial conditions are $(\omega,\ y,\ \dot{y})(0) = (0.75,\ 0,\ 0.5)$.

6.5 Example: A Streamlined Planar Underwater Vehicle

In this section, we consider the problem of stabilizing steady, long-axis translation of a streamlined underwater vehicle using a single moving mass actuator (MMA) mounted orthogonally to this axis. We restrict our attention to the planar case. While the problem may seem academic, it is quite relevant to the problem of directional stabilization for rudderless underwater gliders. These vehicles use moving mass actuators for attitude control because external actuators, such as control planes and thrusters, foul or corrode overtime

Figure 6.5 depicts an elliptical planar underwater vehicle with a single MMA. Let the translational velocity of the vehicle expressed in the body frame $(\boldsymbol{b}_1, \boldsymbol{b}_2)$ be $\boldsymbol{v} = [v_1,\ v_2]^T$. Let ω denote the angular velocity of the vehicle. The actuated mass m_1 moves along a track which is parallel to the body $\boldsymbol{b}_2$-axis and offset some distance a forward of the geometric center. (In this analysis, it makes

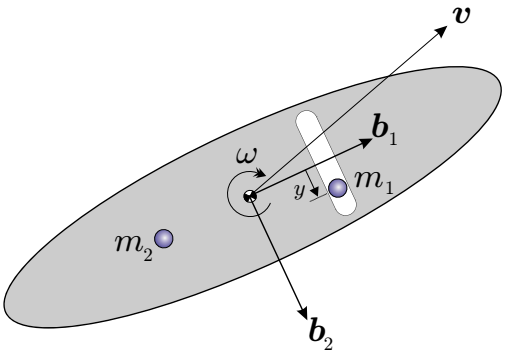

Figure 6.5: A planar underwater vehicle with two point masses. One mass is fixed and the other moves along a track under the influence of a control force u.

no difference whether the mass is forward or aft of the geometric center.) Thus, the position of the actuated mass relative to the body reference frame is $\boldsymbol{r}_1 = (a, y(t))$. To simplify analysis, another point mass $m_2 = m_1 = m$ is fixed at the location $\boldsymbol{r}_2 = (-a, 0)$.

The configuration space of the system is $Q = SE(2) \times \mathbb{R}$, where an element in $SE(2)$ represents the position and orientation of the vehicle and $y(t) \in \mathbb{R}$. The invariance of the Lagrangian $L : TSE(2) \times T\mathbb{R} \to \mathbb{R}$ under the action of $SE(2)$ induces a reduced Lagrangian $l : \mathfrak{se}(2) \times T\mathbb{R} \to \mathbb{R}$. The reduced Lagrangian is the kinetic energy of the system given by (6.8),

$$\begin{aligned} l &= \frac{1}{2}\boldsymbol{\psi}^T \boldsymbol{M}(y)\boldsymbol{\psi} \\ &= \frac{1}{2}\begin{pmatrix} \omega \\ v_1 \\ v_2 \\ \dot{y} \end{pmatrix}^T \begin{pmatrix} I + 2ma^2 + my^2 & -my & 0 & ma \\ -my & M_1 + 2m & 0 & 0 \\ 0 & 0 & M_2 + 2m & m \\ ma & 0 & m & m \end{pmatrix} \begin{pmatrix} \omega \\ v_1 \\ v_2 \\ \dot{y} \end{pmatrix}, \end{aligned} \tag{6.49}$$

where

$$\boldsymbol{I}_{\mathrm{b/f}} = I \quad \text{and} \quad \boldsymbol{M}_{\mathrm{b/f}} = \begin{pmatrix} M_1 & 0 \\ 0 & M_2 \end{pmatrix}$$

represent the body/fluid inertia and mass matrix respectively. Let l_i represent the length of the vehicle along the $\boldsymbol{b}_i$ axis. Assuming $l_1 > l_2$, it follows that $M_2 > M_1$. Define the following

non-dimensional quantities:

$$\bar{y} = \frac{y}{a},\ \bar{v}_i = \frac{v_i}{v_0},\ \bar{\omega} = \frac{\omega a}{v_0},\ \bar{t} = \frac{v_0}{a}t,\ \bar{I} = \frac{I}{ma^2} + 2,\ \bar{M}_i = \frac{M_i}{m} + 2,\ \bar{l} = \frac{l}{mv_0^2},$$

where v_o is some desired steady translation speed along $\boldsymbol{b}_1$. Dropping the bar for convenience, the non-dimensional reduced Lagrangian is

$$l = \frac{1}{2}\begin{pmatrix} \omega \\ v_1 \\ v_2 \\ \dot{y} \end{pmatrix}^T \begin{pmatrix} I + y^2 & -y & 0 & 1 \\ -y & M_1 & 0 & 0 \\ 0 & 0 & M_2 & 1 \\ 1 & 0 & 1 & 1 \end{pmatrix} \begin{pmatrix} \omega \\ v_1 \\ v_2 \\ \dot{y} \end{pmatrix}, \tag{6.50}$$

where $I > 2$ and $M_2 > M_1 > 2$.

Equation (6.14) gives the controlled dynamics as

$$\frac{d}{dt}\left(\frac{\partial l}{\partial \omega}\right) = -\frac{\partial l}{\partial v_2}v_1 + \frac{\partial l}{\partial v_1}v_2, \tag{6.51}$$

$$\frac{d}{dt}\left(\frac{\partial l}{\partial v_1}\right) = \frac{\partial l}{\partial v_2}\omega, \tag{6.52}$$

$$\frac{d}{dt}\left(\frac{\partial l}{\partial v_2}\right) = -\frac{\partial l}{\partial v_1}\omega, \tag{6.53}$$

$$\frac{d}{dt}\left(\frac{\partial l}{\partial \dot{y}}\right) - \frac{\partial l}{\partial y} = u, \tag{6.54}$$

where u is the control applied to the moving mass. Equations (6.51)-(6.54) can be expressed as

$$\boldsymbol{M}\dot{\boldsymbol{\psi}} + \boldsymbol{C}\boldsymbol{\psi} = \boldsymbol{\mathcal{S}}\boldsymbol{\psi} + \boldsymbol{G}\boldsymbol{u},$$

where

$$\boldsymbol{\mathcal{S}} = \begin{pmatrix} 0 & -\frac{\partial l}{\partial v_2} & \frac{\partial l}{\partial v_1} & 0 \\ \frac{\partial l}{\partial v_2} & 0 & 0 & 0 \\ -\frac{\partial l}{\partial v_1} & 0 & 0 & 0 \\ 0 & 0 & 0 & 0 \end{pmatrix} \quad \text{and} \quad \boldsymbol{G} = \begin{pmatrix} 0 \\ 0 \\ 0 \\ 1 \end{pmatrix}.$$

The total linear momentum of the system is

$$P_s = \left(\frac{\partial l}{\partial v_1}\right)^2 + \left(\frac{\partial l}{\partial v_2}\right)^2. \tag{6.55}$$

From (6.52) and (6.53), we get $\dot{P}_s = 0$. Thus, the total linear momentum is conserved at all times and the dynamics evolve on a surface of constant P_s.

6.5.1 Stability of the Uncontrolled Dynamics

We are interested in stability of the equilibrium

$$(\omega,\ v_1,\ v_2,\ y,\ \dot{y})^T = (0, 1, 0, 0, 0)^T. \tag{6.56}$$

This corresponds to steady, long axis translation of the vehicle with a desired velocity v_0 and the moving mass being stationary at $(a, 0)$. Because the system is Hamiltonian (see [80]), the eigenvalues of the linearized dynamics are distributed symmetrically about the real and imaginary axis. The total linear momentum of the system is conserved, so one of the eigenvalues is zero. The remaining four eigenvalues either appear in pure real conjugate pairs, pure imaginary conjugate pairs, or as a complex conjugate quartet. Spectral stability requires that all eigenvalues be located on the imaginary axis. For the uncontrolled system (i.e., with $u = 0$), the eigenvalues corresponding to the equilibrium are

$$\lambda_{1,2,3} = 0 \text{ and } \lambda_{4,5} = \pm\sqrt{\frac{(M_2 - M_1)(M_1 - 1)}{I(M_2 - 1) - M_2}}.$$

We have

$$I(M_2 - 1) - M_2 = IM_2\left[1 - \left(\frac{1}{I} + \frac{1}{M_2}\right)\right].$$

Since $I, M_2 > 2$, it follows that

$$\frac{1}{I} + \frac{1}{M_2} < 1 \Rightarrow I(M_2 - 1) - M_2 > 0.$$

Since $M_2 > M_1$, $\lambda_{4,5}$ constitutes a real conjugate pair and the equilibrium is a saddle. The two additional zero eigenvalues reflect the degenerate nature of the equilibrium, which is not isolated. Indeed, any state of the form $(\omega,\ v_1,\ v_2,\ y,\ \dot{y})^T = (0, 1, 0, \tilde{y}, 0)^T$ is an equilibrium.

6.5.2 Stabilization of Streamlined Translation

The trivial matching law (6.27) is given by

$$\boldsymbol{M}_c = \begin{pmatrix} I+y^2 & -y & 0 & 1 \\ -y & M_1 & 0 & 0 \\ 0 & 0 & M_2 & 1 \\ 1 & 0 & 1 & \rho \end{pmatrix} \quad \text{and} \quad \boldsymbol{\mathcal{S}}_c = \boldsymbol{\mathcal{S}}. \tag{6.57}$$

In order to make the equilibrium an isolated equilibrium, we introduce a potential energy term by setting $V_c = \frac{1}{2}ky^2$ (i.e., a fictitious spring). The control parameters are ρ and k. Following the procedure described in § 6.3.1, we write the Lyapunov function as

$$E_\phi = E_c + \phi(P_s) = \frac{1}{2}\boldsymbol{\psi}^T \boldsymbol{M}_c \boldsymbol{\psi} + V_c + \phi(P_s),$$

where the total linear momentum P_s is conserved. However, we observed that the above matching solution (6.57) does not lead to a proof of nonlinear stability. Moreover, the trivial matching solution seems to be the only solution. In absence of a proof for nonlinear stability, we assess the stability of the equilibrium via a spectral analysis. First, we study controllability for the linearized dynamics.

Linear Controllability

The linearized open-loop dynamics are given by

$$\dot{\boldsymbol{x}} = \boldsymbol{A}\boldsymbol{x} + \boldsymbol{B}u$$

where $\boldsymbol{x} = [\omega,\ v_1,\ v_2,\ y,\ \dot{y}]^T$ is the state vector and the state matrices are

$$\boldsymbol{A} = \frac{1}{\Delta}\begin{pmatrix} M_2-M_1 & 0 & -(M_2-1)(M_2-M_1) & 0 & 0 \\ 0 & 0 & 0 & 0 & 0 \\ I+M_1-IM_1 & 0 & -(M_2-M_1) & 0 & 0 \\ 0 & 0 & 0 & 0 & 1 \\ -I(M_2-M_1) & 0 & (M_2-M_1)M_2 & 0 & 0 \end{pmatrix} \quad \text{and} \quad \boldsymbol{B} = \frac{1}{\Delta}\begin{pmatrix} -M_2 \\ 0 \\ -I \\ 0 \\ IM_2 \end{pmatrix},$$

where $\Delta = IM_2 - I - M_2 > 0$. The rank of the controllability matrix $\boldsymbol{C} = [\boldsymbol{B}\ \boldsymbol{AB}\ \boldsymbol{A}^2\boldsymbol{B}\ \boldsymbol{A}^3\boldsymbol{B}\ \boldsymbol{A}^4\boldsymbol{B}]$ is found to be 4. Since the total linear momentum P_s is conserved at all times, one of the eigenvalues is always zero. Hence the rank of $\boldsymbol{C}$ has to be at least 4 for the system to be linearly controllable. ■

Even though the system is linearly controllable and one can design a well-tuned linear controller, it might not have a large region of stability. On the other hand, the nonlinear controller might provide stability in a large basin. As a first step, we determine values of k and ρ for spectral stability. We have the following result.

Proposition 6.5.1 *There exist values of k and ρ for which* (6.56) *is spectrally stable.*

Proof: The eigenvalue λ for the closed-loop system satisfies

$$\lambda(\lambda^4 + \frac{\mu_1}{\mu_3}\lambda^2 + \frac{\mu_2}{\mu_3}) = 0 \tag{6.58}$$

where

$$\begin{aligned} \mu_1 &= -kIM_2 + (\rho M_1 - 1)(M_2 - M_1), \\ \mu_2 &= kM_1(M_2 - M_1), \\ \mu_3 &= I + (1 - \rho I)M_2. \end{aligned}$$

As noted earlier, the zero eigenvalue corresponds to conservation of total linear momentum. For spectral stability, the remaining eigenvalues must lie on the imaginary axis. This will occur only if

$$\frac{\mu_1}{\mu_3} > 0, \quad \frac{\mu_2}{\mu_3} > 0, \quad \text{and} \quad \mu_1^2 - 4\mu_2\mu_3 > 0. \tag{6.59}$$

Let us assume $I < \frac{M_1M_2}{M_2 - M_1}$. A similar proof follows when $I > \frac{M_1M_2}{M_2 - M_1}$. The curve $\phi(k, \rho) = \mu_1^2 - 4\mu_2\mu_3 = 0$ passes through the intersection of $\mu_1 = 0$ and $\mu_3 = 0$ and the intersection of $\mu_1 = 0$ and $\mu_2 = 0$. The lines $\mu_1 = 0$, $\mu_2 = 0$, and $\mu_3 = 0$ are shown schematically in Figure 6.6 (a), where

$$\rho_1 = \frac{1}{M_1} \quad \text{and} \quad \rho_2 = \frac{I + M_2}{IM_2} > \frac{1}{M_1}.$$

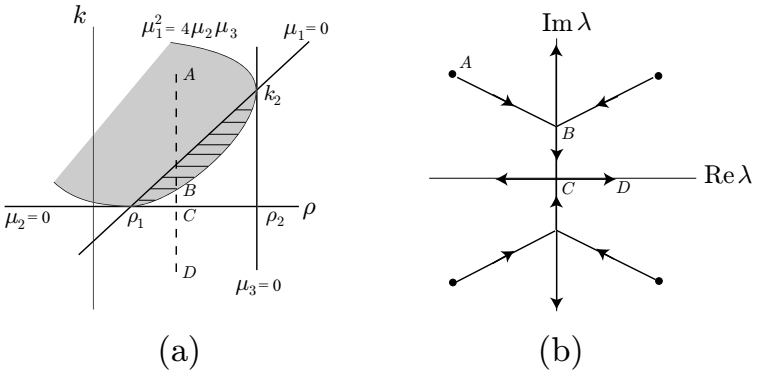

Figure 6.6: (a) Linear stability boundaries in the $(k,\ \rho)$ space. (b) Eigenvalue movement as k is decreased.

Note that the curve $\phi(k, \rho) = 0$ is quadratic in k and ρ. When $k = 0$,

$$\phi(0, \rho) = (M_2 - M_1)^2(1 - M_1\rho)^2.$$

Thus $\phi(0, \rho) = 0$ has a double root at $\rho = 1/M_1$. This implies that the ρ axis is tangent to the curve $\phi = 0$ at $\rho = 1/M_1$. Similarly, the line $\mu_3 = 0$ is tangent to the curve at (ρ_2, k_2). Since $\phi = 0$ is quadratic, the above observations suggest that the curve $\phi = 0$ has the form as shown schematically in Figure 6.6 (a). Also,

$$\phi(0, 0) = (M_2 - M_1)^2 > 0.$$

Thus, $\phi > 0$ outside the shaded region in 6.6 (a). The triangle formed by $\mu_1 = 0,\ \mu_2 = 0$ and $\mu_3 = 0$ represents the region where $\frac{\mu_1}{\mu_3} > 0$ and $\frac{\mu_2}{\mu_3} > 0$. Thus, the hashed region represents the parameter values of k and ρ for which the spectral stability conditions in (6.59) are satisfied. ■

The movement of the eigenvalues as k is varied is shown schematically in Figure 6.6 (b). At point A, as shown in 6.6 (a), there exists a symmetric quartet of eigenvalues. As k is decreased, the eigenvalues move towards the imaginary axis. At point B, $\phi = 0$ and the system undergoes a Hamiltonian Hopf bifurcation. From B to C, the eigenvalues move along the imaginary axis. One pair moves towards the origin and coalesces at C $(k = 0)$. As k is decreased further, this pair splits apart, moving in opposite directions along the real axis.

Corollary 6.5.2 *The equilibrium cannot be stabilized using potential shaping alone.*

Proof: Note that $\rho = 1$ corresponds to the case where there is no kinetic shaping. The proof follows from the observation that $1 > \rho_2 = \frac{1}{I} + \frac{1}{M_2}$ as $I > 2$ and $M_2 > 2$. Thus, the line $\rho = 1$ lies outside the stability region shown in Figure 6.6 (a). ■

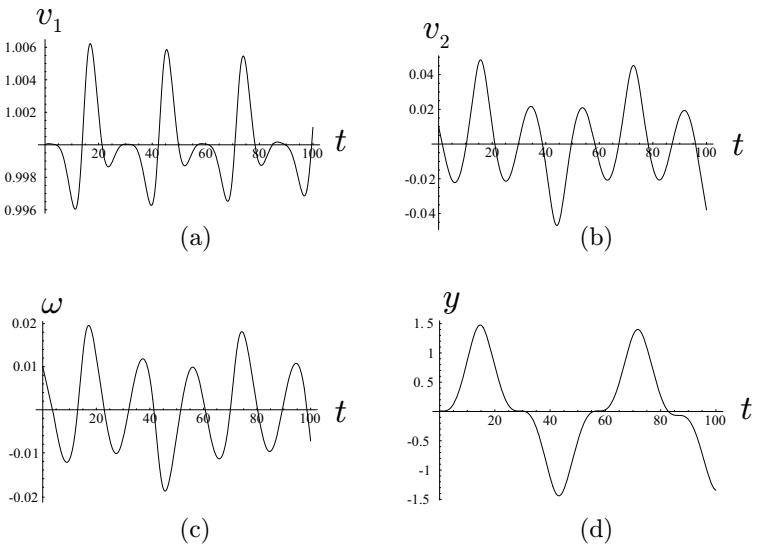

Figure 6.7: Time histories for (a) v_1, (b) v_2, (c) ω and (d) y. The simulation parameters are $M_1 = 4,\ M_2 = 5,\ I = 3,\ \rho = 1/3$ and $k = 0.001$. The initial conditions are $(\omega,\ v_1,\ v_2,\ y,\ \dot{y})(0) = (0.01,\ 1,\ 0.01,\ 0.01,\ 0)$.

Figure (6.7) shows simulations for values of k and ρ within the stability region. The simulation illustrates that the equilibrium is stable; a small perturbation leads to small oscillations about the equilibrium. The amplitude of moving mass motion is presumably influenced by the mass m_1 and the offset distance a. Note that, for the given parameter values, the movement of the mass is 50% greater than the offset distance a.

Chapter 7

Concluding Remarks

Here, we summarize the main findings of our research and discuss some future research work.

7.1 Summary

This dissertation has addressed two important problems related to the theory and application of the method of controlled Lagrangians. The first problem is to investigate the use of artificial gyroscopic forces in the closed-loop equations in order to allow more freedom in matching the open-loop and closed-loop equations and to enhance the closed-loop performance of the energy shaping nonlinear controller. The second problem is to apply the controlled Lagrangian formulation to develop nonlinear control strategies for vehicle systems that use internal moving mass actuators.

The method of controlled Lagrangians, as originally presented in [17] and [10], was modified to include artificial gyroscopic forces in the closed-loop system. While on one hand, these energy conserving forces retain the role of the control-modified energy as a control Lyapunov function, on the other hand, they provide additional freedom that can be used to expand the basin of stability and to tune the closed-loop system performance. We have described a general, algorithmic

procedure to match the closed-loop equations with the original dynamic equations when gyroscopic forces are introduced in the closed-loop system.

In energy shaping control techniques, physical damping effects that are neglected in the control design process may enter the closed-loop equations in a way that can affect stability. If the system is underactuated and kinetic energy is shaped using feedback, physical damping terms along the unactuated directions do not necessarily enter the system as dissipation with respect to the closed-loop energy. This is an important control design issue. Unless carefully accounted for, physical dissipation may destabilize the system. Loss of stability in presence of physical dissipation is not specific to the method of controlled Lagrangians but is inherent to any technique which uses feedback to shape the kinetic energy of the system. The detrimental effect of physical dissipation on closed-loop stability in the Hamiltonian setting (IDA-PBC technique) is illustrated through the "ball on a beam" example.

The controlled Lagrangian technique was applied to the classic inverted pendulum on a cart system. For the conservative model, a feedback control law is derived which makes the desired equilibrium a strict minimum of the control-modified energy. In the absence of physical damping, the control law provided stability in a basin that includes all states for which the pendulum is elevated above the horizontal plane. Addition of feedback dissipation asymptotically stabilized the equilibrium. The addition of feedback dissipation provided asymptotic stability within this same stability basin. This region of attraction is larger than any given earlier by the method of controlled Lagrangians. However, when physical dissipation was introduced, the control-modified energy rate became indefinite, thus invalidating the nonlinear stability argument. Rather than search for a new Lyapunov function, we investigated spectral stability for the closed-loop dynamics and showed that there exists a range of system and control parameter values which ensure that the desired equilibrium is locally exponentially stable. The simulations suggested that the region of attraction remained quite large.

The cart-pendulum example has been considered in numerous other papers on energy shaping, including [3], [6], and [30]. Two features of our control design and analysis distinguish our treatment

from others. First, the closed-loop Lagrangian system included artificial gyroscopic forces, illustrating that such energy-conserving forces can play a useful role in the matching process. Second, we have considered the issue of physical damping and its effect on the closed-loop dynamics in detail. As illustrated by the cart-pendulum example, such analysis is crucial if one wishes to implement a feedback control law which modifies a system's kinetic energy.

The nonlinear controller was tested experimentally. For the experimental apparatus, the damping of the pendulum motion is well-modelled as linear in angular rate. However, cart damping is accurately modelled by static and Coulomb friction. We showed through experiments and simulations that static and Coulomb friction degrades the energy-shaping controller's local performance by inducing limit cycle oscillations. However, we observed that a well-designed linear state feedback control law eliminates the limit cycle oscillations. The nonlinear controller has only two parameters for tuning the controller's regional performance. A well-tuned linear controller, on the other hand, provides four parameters to tune the local performance. We successfully implemented a Lyapunov based switching control law to recover the best features of both controllers; a large region of attraction with quick convergence towards the equilibrium along with desirable local performance. The experimental results further illustrate the importance of considering physical dissipation in systems whose kinetic energy has been modified through feedback.

We have applied the controlled Lagrangian technique to vehicle systems with internal moving mass actuators. Control design using moving mass actuators is challenging because the dynamic models are relatively high-dimensional and are often underactuated. We derived reduced Euler-Lagrange equations for a rigid body with n internal moving masses immersed in an ideal fluid. The equations of motion were cast in a form suitable for the application of the method of controlled Lagrangians. The use of gyroscopic forces in the matching process is illustrated and sufficient algebraic matching conditions were derived. We showed that there always exists a trivial matching solution and an algorithm for matching and stabilization was presented. We studied two examples to illustrate the application of the control design procedure. For the example of a spinning disk with a single moving mass actuator, a nonlinear controller was designed that asymptotically stabilizes

the equilibrium. For the second example of a streamlined planar underwater, the trivial matching control law did not yield a proof of nonlinear stability. With no other matching law available to us, we investigated spectral stability of the closed-loop system. We showed that there exist system and control parameter values that ensure local exponential stability.

7.2 Future Research

Based on the research findings, we have identified some control challenges that one faces when applying the method of controlled Lagrangians to practical engineering problems. We suggest ways to overcome these challenges and possible extensions of the present work.

Vertical/Horizontal Decomposition using the Ehresmann Connection

In Chapter 4, we observed that the nonlinear control law for the cart-pendulum system had only two control parameters for tuning the closed-loop performance. This resulted in poor local performance during the experiments. Next, we show that a more general way to shape the kinetic energy using the *Ehresmann* connection [9], as suggested by colleague J. E. Marsden, might provide extra freedom in the matching process and enhance closed-loop performance.

In § 3.4, a mechanical connection was used to decompose the tangent space at any point $q \in Q$ into vertical and horizontal subspaces. Here, we use the more general notion of a connection, namely the Ehresmann connection, to define V_qQ and H_qQ. We do not place any symmetry requirements on the system.

The following definition is taken from Bloch [9].

Definition 7.2.1 (Ehresmann Connection) *An Ehresmann connection $\mathcal{A}$ is a vector valued one-form on Q that satisfies,*

- *$\mathcal{A}$ is vertical valued: $\mathcal{A}_q : T_qQ \to V_qQ$ is a linear map for each $q \in Q$.*

- $\mathcal{A}$ *is a projection :* $\mathcal{A}(\boldsymbol{v}_q) = \boldsymbol{v}_q \ \forall \ \boldsymbol{v}_q \in V_qQ$.

Assume $Q = \mathbb{R}^2$ for purposes of illustrating the idea. Let $[x_1, x_2]^T \in Q$ and $\boldsymbol{v}_q = [\dot{x}_1, \dot{x}_2]^T \in T_qQ$. For $Q = \mathbb{R}^2$, we can represent $\mathcal{A}$ by a 2×2 matrix. Since $\mathcal{A}$ is a projection, we have

$$\mathcal{A}^2 = \mathcal{A}. \tag{7.1}$$

Let

$$\mathcal{A} = \begin{pmatrix} a & b \\ c & d \end{pmatrix}.$$

For (7.1) to hold, we need

$$a + d = 1 \Rightarrow a = 1 - d,$$
$$ad - bc = 0 \Rightarrow bc = d(1 - d).$$

Let $d \neq 0$. When $d = 1,\ a = 0$ and either $b = 0$ or $c = 0$. We have the following three cases.

Case 1: $d = 1$ and $b = 0$. In this case, we have

$$\mathcal{A} = \begin{pmatrix} 0 & 0 \\ c & 1 \end{pmatrix}.$$

The vertical and horizontal vectors are

$$\text{Ver } \boldsymbol{v}_q = \mathcal{A}(\boldsymbol{v}_q) = [0,\ c\dot{x}_1 + \dot{x}_2]^T \ \text{ and } \ \text{Hor } \boldsymbol{v}_q = \mathcal{A}(\boldsymbol{v}_q) - \text{Ver } \boldsymbol{v}_q = [\dot{x}_1,\ \ -c\dot{x}_1]^T.$$

This splitting of T_qQ is shown schematically in Fig. 7.1(a).

Case 2: $d = 1$ and $c = 0$. In this case,

$$\mathcal{A} = \begin{pmatrix} 0 & b \\ 0 & 1 \end{pmatrix} \Rightarrow \text{Ver } \boldsymbol{v}_q = [b\dot{x}_2,\ \dot{x}_2]^T \ \text{ and } \ \text{Hor } \boldsymbol{v}_q = [\dot{x}_1 - b\dot{x}_2,\ 0]^T.$$

This case is shown schematically in Fig. 7.1(b).

Case 3: $d \neq 0, 1$ and $b, c \neq 0$. This case gives

$$\mathcal{A} = \begin{pmatrix} 1-d & b \\ \frac{d(1-d)}{b} & d \end{pmatrix},$$

which leads to

$$\text{Ver } \boldsymbol{v}_q = [(1-d)\dot{x}_1 + b\dot{x}_2,\ \frac{d(1-d)}{b}\dot{x}_1 + d\dot{x}_2]^T \text{ and } \text{Hor } \boldsymbol{v}_q = [d\dot{x}_1 - b\dot{x}_2,\ -\frac{d(1-d)}{b}\dot{x}_1 + (1-d)\dot{x}_2]^T.$$

as seen schematically in Fig. 7.1(c).

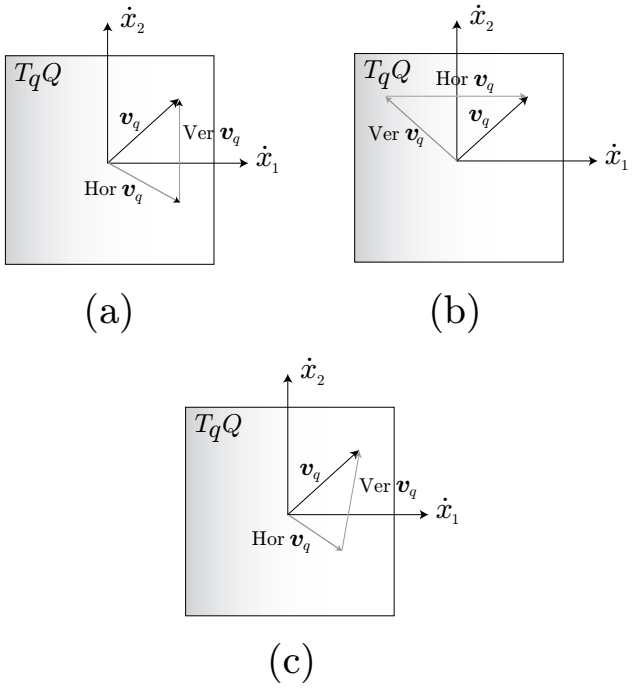

Figure 7.1: Three choices for decomposition of T_qQ

Let the kinetic energy metric be

$$g = \begin{pmatrix} g_{11} & g_{12} \\ g_{12} & g_{22} \end{pmatrix}.$$

Suppose that the horizontal and vertical spaces obtained using the Ehresmann connection are

metric orthogonal, that is,

$$g(\text{Ver } \boldsymbol{v}_q, \text{Hor } \boldsymbol{v}_q) = 0.$$

Metric orthogonality for the above three cases gives

Case 1: $c = \frac{g_{12}}{g_{22}}$.

Case 2: $b = \frac{-g_{12}}{g_{11}}$.

Case 3: $b^2 g_{11} + b(2d-1)g_{12} + d(d-1)g_{22} = 0$.

Cases 1 and 2 do not leave any free parameters. However, case 3 has one free parameter, either b or d. This simple example illustrates that a more general way of shaping the kinetic energy might provide extra freedom during matching and stabilization.

Effect of Unmodelled Dynamics on Closed-Loop Performance

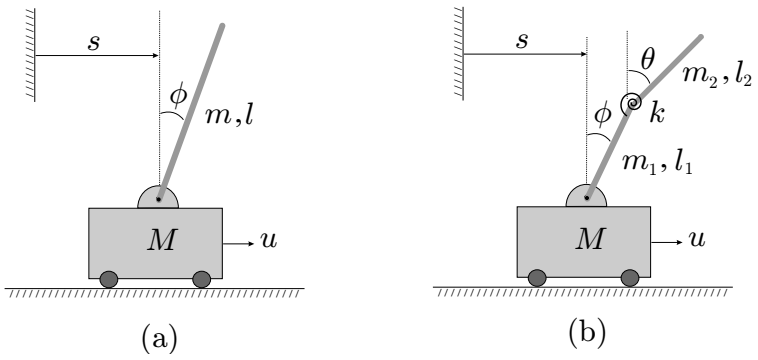

Figure 7.2: Effect of extra degrees of freedom on closed-loop stability.

Consider the system shown in Fig. 7.2. Figure 7.2(a) shows the inverted pendulum on a cart system. The pendulum is modelled as a rigid rod of uniform mass m and length l. Suppose we apply the method of controlled Lagrangians to the system in 7.2(a) and derive an asymptotically stabilizing control law u. What if the pendulum were not truly rigid? Figure 7.2(b) shows the pendulum modelled as a two degree of freedom system, θ representing the first flexible mode with stiffness k.

We pose the problem as : *Can u asymptotically stabilize the upright equilibrium for the system in 7.2(b)*?

A quick observation is that the configuration manifolds for the systems in 7.2(a) and 7.2(b) are different. When we add degrees of freedom we increase the dimension of the system and make the system more underactuated. Research in this direction will help answer as to how "underactuated" the system can be before it *cannot* be stabilized.

Nonlinear Stability for Vehicle Systems with MMAs

It was seen in § 6.5 that the trivial matching solution does not yield a proof of nonlinear stability. A similar problem was encountered while studying spin stabilization of a satellite about its intermediate axis using a single moving mass actuator. A schematic of this system is shown in Fig. 7.3. The moving mass actuator moves parallel to the intermediate $\boldsymbol{b}_3$ axis and the translational dynamics for the satellite are ignored.

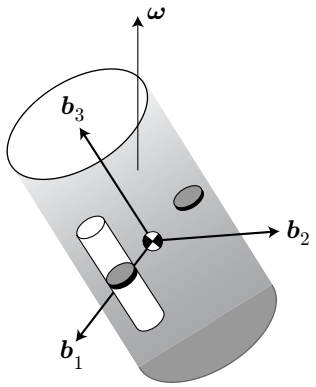

Figure 7.3: Spin stabilization of a satellite using a moving mass actuator.

One might be tempted to claim this is a generic problem. We do not know the answer. However, this warrants further research. We recommend the following as future research.

- Characterize the solution set for (6.18) and (6.24) given the most general form for $\boldsymbol{\Lambda}$ and $\boldsymbol{\Lambda}_c$.

- Determine conditions for nonlinear stability for the each of the solutions obtained.
- In absence of a proof of nonlinear stability, estimate the basin of attraction for the linearized closed-loop dynamics. Compare the region of attraction with that obtained using a well-tuned linear controller, if the system is linearly stabilizable.
- Investigate the effect of physical dissipation, gravity and buoyancy terms on the closed-loop performance.

Appendix A

General Tensors

This discussion is adapted from Frankel [28].

Covariant Tensors

Let T_pM be the tangent space at the point p of an n-dimensional manifold M and let T_p^*M be the dual space of T_pM. Let $\boldsymbol{e} = (\frac{\partial}{\partial x^1},\ \frac{\partial}{\partial x^2}, \ldots,\ \frac{\partial}{\partial x^n})$ be a basis for T_pM and $\sigma = (dx^1,\ dx^2, \ldots,\ dx^n)$ be the dual basis.

A *covariant tensor of rank r* is a multilinear real valued function

$$R : \underbrace{T_pM \times T_pM \times \cdots \times T_pM}_{r \text{ times}} \to \mathbb{R}$$

of r-tuples of vectors. $R(\boldsymbol{v}_1,\ \boldsymbol{v}_2, \ldots,\ \boldsymbol{v}_r)$ is multilinear if it is linear in each entry provided that the remaining entries are fixed. Note that the value of this function is independent of the basis used. As an example, a covector $\omega_p \in T_p^*M$ is a covariant tensor of rank 1. A familiar example of a covariant tensor of rank 2 is the metric tensor

$$g(\boldsymbol{v}, \boldsymbol{w}) = g_{ij} v^i w^j,$$

where g_{ij} are the components of g. Using $i_1,\ i_2,\ i_3, \ldots$ for the indices $i,\ j,\ k, \ldots$, we have by multilinearity,

$$R(\boldsymbol{v}_1,\ \boldsymbol{v}_2, \ldots,\ \boldsymbol{v}_r) = R_{i_1\ i_2 \ldots\ i_r} v_1^{i_1} \ldots v_r^{i_r},$$

where $R_{i_1\ i_2 \ldots\ i_r} := R(\frac{\partial}{\partial x^{i_1}},\ \frac{\partial}{\partial x^{i_2}}, \ldots,\ \frac{\partial}{\partial x^{i_r}})$ are the components of R. The set of all covariant tensors of rank r forms a vector space under the usual operations of addition and multiplication by real numbers. We denote the vector space of r^{th} rank covariant tensors by

$$T_p^*M \otimes T_p^*M \otimes \cdots \otimes T_p^*M = \otimes^r\ T_p^*M.$$

If $\alpha,\ \beta \in T_p^*M$, the *tensor product* of α and β, $\alpha \otimes \beta : T_pM \times T_pM \to \mathbb{R}$, defined as

$$\alpha \otimes \beta(\boldsymbol{v}, \boldsymbol{w}) := \alpha(\boldsymbol{v})\beta(\boldsymbol{w})$$

is a covariant tensor of rank 2. If $\alpha = \alpha_i dx^i$ and $\beta = \beta_j dx^j$, then

$$(\alpha \otimes \beta)_{ij} = \alpha \otimes \beta(\frac{\partial}{\partial x^i}, \frac{\partial}{\partial x^j}) = \alpha(\frac{\partial}{\partial x^i})\ \beta(\frac{\partial}{\partial x^j}) = \alpha_i \beta_j$$

are the components of $\alpha \otimes \beta$. Locally, $\alpha \otimes \beta$ is expressed as

$$\alpha \otimes \beta = \alpha_i \beta_j\ dx^i \otimes dx^j.$$

More generally, if $\alpha \in \otimes^p\ T_p^*M$ and $\beta \in \otimes^q\ T_p^*M$, then their tensor product is a covariant tensor of rank $(p+q)$ given by

$$\alpha \otimes \beta(\boldsymbol{v}_1,\ \boldsymbol{v}_2, \ldots,\ \boldsymbol{v}_{p+q}) := \alpha(\boldsymbol{v}_1,\ \boldsymbol{v}_2, \ldots,\ \boldsymbol{v}_p)\ \beta(\boldsymbol{v}_{p+1},\ \boldsymbol{v}_{p+2}, \ldots,\ \boldsymbol{v}_{p+q}).$$

Contravariant Tensors

A *contravariant vector* or simply a vector, that is, an element of T_pM, can be thought of as a linear functional on covectors by defining

$$\boldsymbol{v}(\alpha) := \alpha(\boldsymbol{v}).$$

This leads to the definition of a contravariant tensor of rank s. A *contravariant tensor* of rank s is a multilinear function of s-tuples of covectors

$$S : \underbrace{T_p^*M \times T_p^*M \times \cdots \times T_p^*M}_{s \text{ times}} \to \mathbb{R}.$$

We have,

$$S(\alpha_1,\ \alpha_2, \ldots,\ \alpha_s) = \alpha_{1\ i_1} ... \alpha_{s\ i_s} S^{i_1\ i_2\ \cdots\ i_s},$$

where $\alpha_1,\ \alpha_2, \ldots,\ \alpha_s$ are covectors and $S^{i_1\ i_2\ \cdots\ i_s} := S(dx^{i_1},\ dx^{i_2}, ...,\ dx^{i_s})$ are the components of S. The space of s rank contravariant tensors is the vector space

$$T_pM \otimes T_pM \otimes \cdots \otimes T_pM := \otimes^s\ T_pM.$$

Vectors are contravariant tensors of rank 1. An example of a contravariant tensor of rank 2 is the inverse of the metric tensor, g^{-1}, given by

$$g^{-1}(\alpha, \beta) = g^{ij}\alpha_i\beta_j,$$

where g^{ij} are the components of g^{-1}.

Given a pair of contravariant vectors, $\boldsymbol{v}$ and $\boldsymbol{w}$, their tensor product $\boldsymbol{v} \otimes \boldsymbol{w}$ is a contravariant tensor of rank 2 defined as

$$(\boldsymbol{v} \otimes \boldsymbol{w})(\alpha, \beta) := \boldsymbol{v}(\alpha)\ \boldsymbol{w}(\beta) = \alpha(\boldsymbol{v})\ \beta(\boldsymbol{w}) = v^i w^j \alpha_i \beta_j.$$

In component form,

$$\boldsymbol{v} \otimes \boldsymbol{w} = (\boldsymbol{v} \otimes \boldsymbol{w})^{ij} \frac{\partial}{\partial x^i} \otimes \frac{\partial}{\partial x^j},$$

where $(\boldsymbol{v} \otimes \boldsymbol{w})^{ij} = \boldsymbol{v} \otimes \boldsymbol{w}(dx^i, dx^j) = v^i w^j$.

Mixed Tensors

A *mixed tensor* of rank (s, r), s times contravariant and r times covariant, is a real multilinear function

$$T : \underbrace{T_p^*M \times T_p^*M \times \cdots \times T_p^*M}_{s \text{ times}} \times \underbrace{T_pM \times T_pM \times \cdots \times T_pM}_{r \text{ times}} \to \mathbb{R}$$

on s-tuples of covectors and r-tuples of vectors. We have

$$T(\alpha_1, \ldots,\ \alpha_s,\ \boldsymbol{v}_1, \ldots,\ \boldsymbol{v}_r) := \alpha_{1\ i_1} \ldots\ \alpha_{s\ i_s} T^{i_1\ \cdots\ i_s}{}_{j_1\ \ldots\ j_r} v_1^{j_1} \ldots\ v_r^{j_r},$$

where $T^{i_1\ \cdots\ i_s}{}_{j_1\ \ldots\ j_r} := T(dx^{i_1}, \ldots,\ \partial/\partial x^{j_r})$. Note that covariant and contravariant tensors are special cases obtained when $s = 0$ and $r = 0$ respectively. For example, a mixed tensor of rank (1,1) is given by

$$T(\alpha, \boldsymbol{w}) = \alpha_i T^i_j w^j.$$

The tensor product $\boldsymbol{v} \otimes \alpha$ of a vector and a covector is a mixed tensor of rank (1,1) defined as

$$(\boldsymbol{v} \otimes \alpha)(\beta, \boldsymbol{w}) := \alpha(\boldsymbol{w})\ \beta(\boldsymbol{v}).$$

Vector Valued 1-Forms

Let A be a mixed tensor of rank $(1, 1)$, that is, once contravariant and once covariant. Locally, A can be expressed as

$$A = A^i{}_j\ \frac{\partial}{\partial x^i} \otimes dx^j = \frac{\partial}{\partial x^i} \otimes A^i{}_j\ dx^j = \frac{\partial}{\partial x^i} \otimes \alpha^i,$$

where $\alpha^i = A^i{}_j\ dx^j$. Thus, to A we can associate a *vector-valued 1-form* $\boldsymbol{\alpha}$, that is, a 1-form that acts on vectors to give vectors rather than scalars,

$$\boldsymbol{\alpha}(\boldsymbol{v}) := \alpha^i(\boldsymbol{v}) \frac{\partial}{\partial x^i} = (A^i{}_j v^j) \frac{\partial}{\partial x^i}.$$

We make no distinction between the tensor A and its associated vector-valued 1-form $\boldsymbol{\alpha}$. Thus, the coordinate representation of $\boldsymbol{\alpha}$ is the matrix $A^i{}_j$; a vector-valued 1-form is represented by a matrix.

Appendix B

The Potential Energy Matching Condition

The upper term of equation (4.48) requires that

$$0 = \left(A_{\alpha\gamma} + (\mathcal{A}^d_\alpha + \tau^d_\alpha)\rho_{de}\tau^e_\gamma\right) B^{\gamma\beta}\,(-V_{,\beta}) - \left(A_{\alpha\gamma}B^{\gamma\delta}\mathcal{A}^b_\delta - (\mathcal{A}^c_\alpha + \tau^c_\alpha)\rho_{cd}D^{db}\right)\left(u^{\mathrm{p}}_b - V_{,b}\right) + V'_{,\alpha}\,. \tag{B.1}$$

Noting that

$$A_{\alpha\gamma}B^{\gamma\beta} = \delta^\beta_\alpha + \tau^c_\alpha\sigma_{cd}\tau^d_\gamma B^{\gamma\beta}, \tag{B.2}$$

from the definition (4.27) of $A_{\alpha\beta}$, we may rewrite (B.1) as

$$\begin{aligned} 0 = (-V_{,\alpha}) &+ \left(\tau^c_\alpha\sigma_{cd}\rho^{de} + (\mathcal{A}^e_\alpha + \tau^e_\alpha)\right)\left(\rho_{ef}\tau^f_\gamma B^{\gamma\beta}\right)(-V_{,\beta}) \\ &- \left(A_{\alpha\gamma}B^{\gamma\delta}\mathcal{A}^b_\delta - (\mathcal{A}^c_\alpha + \tau^c_\alpha)\rho_{cd}D^{db}\right)\left(u^{\mathrm{p}}_b - V_{,b}\right) + V'_{,\alpha}\,. \end{aligned} \tag{B.3}$$

Using (4.51) in (B.3) gives

$$\begin{aligned}
0 &= \tilde{V}_{,\alpha} + \left(\tau^c_\alpha \sigma_{cd}\rho^{de} + (\mathcal{A}^e_\alpha + \tau^e_\alpha)\right)\left(-\rho_{ac}D^{cb}\left(u^{\mathrm{p}}_b - V_{,b}\right) - V'_{,a}\right) \\
&\qquad - \left(A_{\alpha\gamma}B^{\gamma\delta}\mathcal{A}^b_\delta - (\mathcal{A}^c_\alpha + \tau^c_\alpha)\rho_{cd}D^{db}\right)\left(u^{\mathrm{p}}_b - V_{,b}\right) \\
&= \tilde{V}_{,\alpha} - \tau^c_\alpha\sigma_{cd}\left(D^{db}\left(u^{\mathrm{p}}_b - V_{,b}\right) - \rho^{db}V'_{,b}\right) - (\mathcal{A}^c_\alpha + \tau^c_\alpha)V'_{,c} - A_{\alpha\gamma}B^{\gamma\delta}\mathcal{A}^b_\delta\left(u^{\mathrm{p}}_b - V_{,b}\right) \\
&= \tilde{V}_{,\alpha} - \left(\tau^c_\alpha\sigma_{cd}D^{db} + A_{\alpha\gamma}B^{\gamma\delta}\mathcal{A}^b_\delta\right)\left(u^{\mathrm{p}}_b - V_{,b}\right) - \left(\tau^c_\alpha\sigma_{cd}\rho^{db} + \mathcal{A}^b_\alpha + \tau^b_\alpha\right)V'_{,b}
\end{aligned} \tag{B.4}$$

Using the definition (4.50) of D^{ab} and the identity (B.2), equation (B.4) simplifies to

$$0 = \tilde{V}_{,\alpha} - \left(\tau^c_\alpha\sigma_{cd}g^{db} + \mathcal{A}^b_\alpha\right)\left(u^{\mathrm{p}}_b - V_{,b}\right) - \left(\tau^c_\alpha\sigma_{cd}\rho^{db} + \mathcal{A}^b_\alpha + \tau^b_\alpha\right)V'_{,b}. \tag{B.5}$$

Substituting the potential shaping portion of the control law

$$u^{\mathrm{p}}_a = V_{,a} + D_{ac}\left(\tau^c_\gamma B^{\gamma\beta}V_{,\beta} - \rho^{cb}V'_{,b}\right)$$

from equation (4.52) gives

$$0 = \tilde{V}_{,\alpha} - \left(\tau^c_\alpha\sigma_{cd}g^{db} + \mathcal{A}^b_\alpha\right)D_{be}\left(\tau^e_\gamma B^{\gamma\beta}V_{,\beta} - \rho^{ef}V'_{,f}\right) - \left(\tau^c_\alpha\sigma_{cd}\rho^{db} + \mathcal{A}^b_\alpha + \mathcal{A}^b_\alpha\right)V'_{,b}. \tag{B.6}$$

Collecting coefficients of the partial derivatives of V' gives the potential matching condition (4.53).

Appendix C

Proof of Proposition 5.1.2

Consider any compact, positively invariant set $\Omega \subset W$, where W is given in (5.9), and let E be the set of all points in Ω at which $\dot{E}_{\tau,\sigma,\rho} = 0$:

$$E = \{(\phi, s, \dot{\phi}, \dot{s}) \in \Omega \mid 3\dot{\phi} + \dot{s}\cos\phi = 0\}.$$

LaSalle's invariance principle asserts that every trajectory starting in Ω approaches the largest invariant set $\mathcal{M}$ contained in E as $T \to \infty$. If the set $\mathcal{M}$ contains only the equilibrium at the origin, it follows that the equilibrium is asymptotically stable. The set Ω provides an estimate of the region of attraction.

By definition, $E_{\tau,\sigma,\rho}$ is constant along trajectories contained in $\mathcal{M}$. Also, since

$$\begin{aligned}\frac{d}{dT}\varphi(\phi, s) &= \frac{d}{dT}\left(s + 6\,\text{arctanh}\left(\tan\left(\frac{\phi}{2}\right)\right)\right) \\ &= \sec\phi\left(3\dot{\phi} + \dot{s}\cos\phi\right),\end{aligned}$$

$\varphi(\phi, s)$ is constant along trajectories contained in $\mathcal{M}$. Noting that ς, given in (5.7), is zero within

the set $\mathcal{M}$, the Euler-Lagrange equations restricted to this set are

$$\frac{d}{dT}\frac{\partial L_{\tau,\sigma,\rho}}{\partial \dot{\phi}} = -\left(2\tan\phi\sec^2\phi + 3\kappa\varphi\sec\phi\right) \tag{C.1}$$

$$\frac{d}{dT}\frac{\partial L_{\tau,\sigma,\rho}}{\partial \dot{s}} = -\kappa\varphi. \tag{C.2}$$

Because φ is constant, (C.2) implies that

$$\frac{\partial L_{\tau,\sigma,\rho}}{\partial \dot{s}} = c_1 T + c_2$$

where $c_1 = -\kappa\varphi$ and c_2 are constants. But, because the equilibrium is stable, trajectories in Ω are bounded. This implies that $c_1 = 0$ and $c_2 = 0$. Thus, $\varphi(\phi, s) = 0$ and

$$\frac{\partial L_{\tau,\sigma,\rho}}{\partial \dot{s}} = 0. \tag{C.3}$$

Restricted to the set $\mathcal{M}$, the momenta conjugate to ϕ and s are

$$\frac{\partial L_{\tau,\sigma,\rho}}{\partial \dot{\phi}} = \frac{2}{3}\sec^2\phi\dot{s} \tag{C.4}$$

$$\frac{\partial L_{\tau,\sigma,\rho}}{\partial \dot{s}} = \frac{2}{3}\sec\phi\dot{s}. \tag{C.5}$$

It follows from (C.3) that $\dot{s} = 0$, since $\sec\phi \neq 0$ in W. From (C.4), we see that

$$\frac{\partial L_{\tau,\sigma,\rho}}{\partial \dot{\phi}} = 0.$$

From (C.1), it follows that $\phi = 0$. Finally, since $\varphi(\phi, s) = 0$ and $\phi = 0$, it follows that $s = 0$ as well. Thus, for any $\Omega \subset W$, the set $\mathcal{M}$ contains only the origin. Asymptotic stability within the set W follows from LaSalle's invariance principle.

Appendix D

Explicit Matching Conditions for $Q = SO(2) \times \mathbb{R}$

Consider a mechanical system whose configuration space is $Q = G \times S = SO(2) \times \mathbb{R}$. The spinning disk example studied in § 6.4 is such a system. Let the Lagrangian $L : TQ \to \mathbb{R}$ be invariant under the action of $G = SO(2)$. The invariance induces a reduced Lagrangian $l : \mathfrak{so}(2) \times T\mathbb{R} \to \mathbb{R} : \quad (\omega, x, \dot{x}) \mapsto \mathbb{R}$, where $\omega \in \mathfrak{so}(2)$ is the angular velocity and $(x, \dot{x}) \in T\mathbb{R}$. Let a control u be applied in the x direction. The reduced Euler-Lagrange equations (see § 6.2.1) are

$$\begin{aligned} \frac{d}{dt}\frac{\partial l}{\partial \omega} &= 0 \\ \frac{d}{dt}\frac{\partial l}{\partial \dot{x}} - \frac{\partial l}{\partial x} &= u. \end{aligned} \tag{D.1}$$

Assuming no potential energy ($V = 0$), the general form of the reduced Lagrangian l is

$$l = \frac{1}{2}\begin{pmatrix} \omega \\ \dot{x} \end{pmatrix}^T \begin{pmatrix} a(x) & b(x) \\ b(x) & c(x) \end{pmatrix} \begin{pmatrix} \omega \\ \dot{x} \end{pmatrix} = \frac{1}{2}\boldsymbol{\psi}^T \boldsymbol{M}(x)\boldsymbol{\psi}, \tag{D.2}$$

where $\boldsymbol{\psi} = [\omega,\ \dot{x}]^T$. The reduced Euler-Lagrange equations (D.1) become

$$\boldsymbol{M}\dot{\boldsymbol{\psi}} + \boldsymbol{C}\boldsymbol{\psi} = \boldsymbol{G}u, \tag{D.3}$$

where

$$\boldsymbol{C} = \begin{pmatrix} \frac{1}{2}a'\dot{x} & \frac{1}{2}a'\omega + b'\dot{x} \\ -\frac{1}{2}a'\omega & \frac{1}{2}c'\dot{x} \end{pmatrix}, \quad \boldsymbol{G} = \begin{pmatrix} 0 \\ 1 \end{pmatrix}, \quad \text{and} \quad (\,)' = \frac{\partial(\,)}{\partial x}.$$

Let the closed-loop Lagrangian be

$$l_c = \frac{1}{2}\begin{pmatrix} \omega \\ \dot{x} \end{pmatrix}^T \begin{pmatrix} a_c(x) & b_c(x) \\ b_c(x) & c_c(x) \end{pmatrix} \begin{pmatrix} \omega \\ \dot{x} \end{pmatrix} = \frac{1}{2}\boldsymbol{\psi}^T \boldsymbol{M}_c(x)\boldsymbol{\psi}, \tag{D.4}$$

and the closed-loop reduced Euler-Lagrange equations be

$$\boldsymbol{M}_c\dot{\boldsymbol{\psi}} + \boldsymbol{C}_c\boldsymbol{\psi} = \boldsymbol{\mathcal{S}}_c\boldsymbol{\psi}, \tag{D.5}$$

where

$$\boldsymbol{C}_c = \begin{pmatrix} \frac{1}{2}a_c'\dot{x} & \frac{1}{2}a_c'\omega + b_c'\dot{x} \\ -\frac{1}{2}a_c'\omega & \frac{1}{2}c_c'\dot{x} \end{pmatrix} \quad \text{and} \quad \boldsymbol{\mathcal{S}}_c = \begin{pmatrix} 0 & s_1(x)\omega + s_2(x)\dot{x} \\ -s_1(x)\omega - s_2(x)\dot{x} & 0 \end{pmatrix}.$$

Comparing the open-loop (D.3) and closed-loop (D.5) equations, we get the matching condition (see § 4.4) as

$$\boldsymbol{G}^\perp \left[\boldsymbol{M}\boldsymbol{M}_c^{-1}(\boldsymbol{\mathcal{S}}_c\boldsymbol{\psi} - \boldsymbol{C}_c\boldsymbol{\psi}) + \boldsymbol{C}\psi\right] = 0, \tag{D.6}$$

where $\boldsymbol{G}^\perp = (1 \;\; 0)$. Let

$$\boldsymbol{\lambda} = \begin{pmatrix} \lambda_{11} & \lambda_{12} \\ \lambda_{21} & \lambda_{22} \end{pmatrix} = \boldsymbol{M}\boldsymbol{M}_c^{-1}.$$

The matching condition (D.6) is a scalar equation given by

$$\lambda_{12}(a_c' - 2s_1)\omega^2 + (\lambda_{11}(s_1 - a_c') - \lambda_{12}s_2 + a')\omega\dot{x} + (2\lambda_{11}(s_2 - b_c') + 2b' - \lambda_{12}c_c')\dot{x}^2 = 0 \tag{D.7}$$

Since (D.7) has to hold for all ω and $\dot{x}$, we set the coefficients of the velocity terms to zero to yield sufficient matching conditions:

$$\lambda_{12}(a_c' - 2s_1) = 0, \tag{D.8}$$

$$\lambda_{11}(s_1 - a_c') - \lambda_{12}s_2 + a' = 0, \tag{D.9}$$

$$2\lambda_{11}(s_2 - b_c') + 2b' - \lambda_{12}c_c' = 0. \tag{D.10}$$

Bibliography

[1] R. Abraham and J. E. Marsden. *Foundations of Mechanics*. Addison-Wesley, Reading, MA, 2nd edition, 1987.

[2] R. Abraham, J. E. Marsden, and T. S. Ratiu. *Manifolds, Tensor Analysis and Applications*. Springer-Verlag, New York, NY, 2nd edition, 1988.

[3] J. Á. Acosta, R. Ortega, and A. Astolfi. Interconnection and damping assignment passivity based control of mechanical systems with underactuated degree one. In *Proc. IEEE Conf. Decision and Control*, pages 3029–3032, Boston, MA, 2004.

[4] V. I. Arnold. *Mathematical Methods of Classical Mechanics*. Springer-Verlag, New York, NY, 2nd edition, 1989.

[5] D. Auckly and L. Kapitanski. On the λ-equations for matching control laws. *SIAM Journal of Control and Optimization*, 41(5):1372–1388, 2002.

[6] D. Auckly, L. Kapitanski, and W. White. Control of nonlinear underactuated systems. *Comm. Pure Applied Mathematics*, 53:354–369, 2000.

[7] B. E. Bishop and M. W. Spong. Control of redundant manipulators using logic-based switching. In *Proc. IEEE Conf. Decision and Control*, Tampa, Florida, 1998.

[8] G. Blankenstein, R. Ortega, and A. J. van der Schaft. The matching conditions of controlled Lagrangians and the IDA-PBC. *International Journal of Control*, 75(9):645–665, 2002.

[9] A. M. Bloch. *Nonholonomic Mechanics and Control*. Springer-Verlag, New York, NY, 2003.

[10] A. M. Bloch, D. E. Chang, N. E. Leonard, and J. E. Marsden. Controlled Lagrangians and the stabilization of mechanical systems II: Potential shaping. *IEEE Trans. Automatic Control*, 46(10):1556–1571, 2001.

[11] A. M. Bloch, P. S. Krishnaprasad, J. E. Marsden, and G. Sánchez de Alvarez. Stabilization of rigid body dynamics by internal and external torques. *Automatica*, 28(4):745–756, 1992.

[12] A. M. Bloch, P. S. Krishnaprasad, J. E. Marsden, and T. S. Ratiu. Dissipation induced instabilities. *Ann. Inst. H. Poincaré, Analyse Nonlinéaire*, 11:37–90, 1994.

[13] A. M. Bloch, N. E. Leonard, and J. E. Marsden. Stabilization of mechanical systems using controlled Lagrangians. In *Proc. IEEE Conf. Decision and Control*, pages 2356–2361, San Diego, CA, 1997.

[14] A. M. Bloch, N. E. Leonard, and J. E. Marsden. Matching and stabilization by the method of controlled Lagrangians. In *Proc. IEEE Conf. Decision and Control*, pages 1446–1451, Tampa, FL, 1998.

[15] A. M. Bloch, N. E. Leonard, and J. E. Marsden. Potential shaping and the method of controlled Lagrangians. In *Proc. IEEE Conf. Decision and Control*, pages 1653–1657, Phoenix, AR, 1999.

[16] A. M. Bloch, N. E. Leonard, and J. E. Marsden. Stabilization of the pendulum on a rotor arm by the method of controlled Lagrangians. In *Proc. Int. Conf. Robotics and Automation*, pages 500–505, Detroit, MI, 1999.

[17] A. M. Bloch, N. E. Leonard, and J. E. Marsden. Controlled Lagrangians and the stabilization of mechanical systems I: The first matching theorem. *IEEE Transactions on Automatic Control*, 45(12):2253–2270, 2000.

[18] A. M. Bloch, N. E. Leonard, and J. E. Marsden. Controlled Lagrangians and the stabilization of Euler-Poincaré mechanical systems. *Int. Journal of Robust and Nonlinear Control (Special Issue on Control of Oscillatory Systems)*, 11(3):191–214, 2001.

[19] W. M. Boothby. *Introduction to Differential Manifolds and Reimannian Geometry*. Academic Press, 2nd edition, 1986.

[20] M. S. Branicky. Multiple lyapunov functions and other analysis tools for switched and hybrid systems. *IEEE Transactions of Automatic Control*, 43(4):475–482, 1998.

[21] R. W. Brockett. Control theory and analytical mechanics. In R. W. Brockett, R. S. Millman, and H. J. Sussmann, editors, *Lie Groups: History, Frontiers and Applications*, volume VII, pages 1–49, Brookline, MA, 1976. Math Sci. Press.

[22] D. E. Chang. *Controlled Lagrangian and Hamiltonian Systems*. PhD thesis, California Institute of Technology, 2002.

[23] D. E. Chang, A. M. Bloch, N. E. Leonard, J. E. Marsden, and C. A. Woolsey. The equivalence of controlled Lagrangian and controlled Hamiltonian systems for simple mechanical systems. *ESAIM: Control, Optimisation, and Calculus of Variations (Special Issue Dedicated to J. L. Lions)*, 8:393–422, 2002.

[24] M. Crampin and F. A. E. Pirani. *Applicable Differential Geometry*. London Mathematical Society Lecture Note Series No. 59. Cambridge University Press, 1986.

[25] P. E. Crouch and A. J. van der Schaft. *Variational and Hamiltonian Control Systems*. Lecture Notes in Control and Information Sciences, 101. Springer-Verlag, Berlin, 2000.

[26] G. Sánchez de Alvarez. *Geometric methods of classical mechanics applied to control theory*. PhD thesis, University of California, Berkeley, 1986.

[27] C. C. Eriksen, T. J. Osse, R. D. Light, T. Wen, T. W. Lehman, P. L. Sabin, J. W. Ballard, and A. M. Chiodi. Seaglider: A long-range autonomous underwater vehicle for oceanographic research. *Journal of Oceanic Engineering*, 26(4):424–436, 2001. Special Issue on Autonomous Ocean-Sampling Networks.

[28] T. Frankel. *The geometry of physics: an introduction*. Cambridge University Press, New York, NY, 2004.

[29] F. Gómez-Estern and A. J. van der Schaft. Physical damping in interconnection and damping assignment and passivity based controlled underactuated mechanical systems. *European Journal of Control*, 10(5):451–468, 2004.

[30] J. Hamberg. General matching conditions in the theory of controlled Lagrangians. In *Proc. IEEE Conf. Decision and Control*, pages 2519–2523, Phoenix, AR, 1999.

[31] J. Hamberg. Controlled Lagrangians, symmetries and conditions for strong matching. In N.E. Leonard and R. Ortega, editors, *Proc. IFAC Workshop on Lagrangian and Hamiltonian Methods for Nonlinear Control*, pages 62–67. Pergamon, 2000.

[32] R. H. Hansen and H. J. van de Molengraft. Friction induced hunting limit cycles: an event mapping approach. In *Proc. American Control Conference*, pages 2267–2272, Alaska, USA, 2002.

[33] D. Husemoller. *Fibre Bundles*. Graduate Texts in Mathematics Vol. 20. Springer-Verlag, 1994.

[34] R. D. Robinett III, B. R. Sturgis, and S. A. Kerr. Moving-mass roll control system for fixed-trim re-entry vehicle. *AIAA Journal of Guidance, Control, and Dynamics*, 19(5):1064–1070, 1996.

[35] Quanser Consulting Inc. *IPO2 Self Erecting Inverted Pendulum User's Guide*, 1996. Available at www.quanser.com.

[36] C. J. Isham. *Modern differential geometry for physicists*. Lecture Notes in Physics Vol. 32. World Scientific, 1989.

[37] A. Isidori. *Nonlinear Control Systems*. Springer-Verlag, New York, NY, 2nd edition, 1989.

[38] S. M. Jalnapurkar and J. E. Marsden. Stabilization of relative equilibria II. *Regular and Chaotic Dynamics*, 3:161–179, 1999.

[39] M. H. Kaplan. *Modern Spacecraft Dynamics and Control*. John Wiley, New York, NY, 1976.

[40] H. Khalil. *Nonlinear Systems*. Prentice Hall, Upper Saddle River, NJ, 2nd edition, 1996.

[41] S. Kobayashi and K. Nomizu. *Foundations of Differential Geometry*, volume 1. Interscience Publishers, 1963.

[42] J. L. Lagrange. *Mécanique Analytique*. Chez la Veuve Desaint, 1788.

[43] N. E. Leonard and J. G. Graver. Model-based feedback control of autonomous underwater gliders. *Journal of Oceanic Engineering*, 26(4):633–645, 2001. Special Issue on Autonomous Ocean-Sampling Networks.

[44] D. Liberzon. *Switching in Systems and Control*. Birkhauser, Boston, MA, 2003.

[45] J. E. Marsden. *Lectures in Mechanics*. Cambridge University Press, New York, NY, 1992.

[46] J. E. Marsden and T. S. Ratiu. *Introduction to Symmetry and Mechanics*. Springer-Verlag, New York, NY, 1994.

[47] J. E. Marsden and J. Scheurle. Lagrangian reduction and the double spherical pendulum. *ZAMP*, 44:17–43, 1993.

[48] J. E. Marsden and J. Scheurle. The reduced Euler-Lagrange equations. *Fields Institute Communications*, 1:139–164, 1993.

[49] J. R. Munkres. *Topology: A first course*. Prentice Hall, New Jersey, 1975.

[50] R. M. Murray, Z. Li, and S. S. Sastry. *A Mathematical Introduction to Robotic Manipulation*. CRC Press, Boca Raton, FL, 1994.

[51] A. H. Nayfeh and B. Balachandran. *Applied Nonlinear Dynamics: Analytical, Computational, and Experimental Methods*. Wiley, New York, NY, 1995.

[52] H. Nijmeijer and A. van der Schaft. *Nonlinear Dynamics Control Systems*. Springer-Verlag, New York, NY, 1990.

[53] R. Olfati-Saber. *Nonlinear Control of Underactuated Mechanical Systems with Application to Robotics and Aerospace Vehicles*. PhD thesis, MIT, Boston, 2001.

[54] R. Ortega, A. Loria, P. Nicklasson, and H. Sira-Ramirez. *Passivity based Control of Euler-Lagrange Systems*. Communication and Control Engineering Series. Springer-Verlag, 1998.

[55] R. Ortega, M. W. Spong, F. Gómez-Estern, and G. Blankenstein. Stabilization of a class of underactuated mechanical systems via interconnection and damping assignment. *IEEE Transactions of Automatic Control*, 47(8):1218–1233, 2002.

[56] J. P. Ostrowski. *The mechanics and control of undulatory robotic locomotion.* PhD thesis, California Institute of Technology, 1995.

[57] J. P. Ostrowski. Computing reduced equations for robotic systems with constraints and symmetries. *IEEE Transactions on Robotics and Automation*, 15:111–123, 1999.

[58] T. Petsopoulos, F. J. Regan, and J. Barlow. Moving-mass roll control system for fixed-trim re-entry vehicle. *Journal of Spacecraft and Rockets*, 33(1):54–60, 1996.

[59] H. Poincaré. Sur une forme nouvelle des équations de la méchanique. *C. R. Acad. Sci.*, 132:369–371, 1901.

[60] C. K. Reddy, W. W. Whitacre, and C. A. Woolsey. Controlled Lagrangians with gyroscopic forcing : an experimental application. In *Proc. American Control Conference*, pages 511–516, Boston, MA, 2004.

[61] M. Reyhanoglu, A. J. van der Schaft, N. H. McClamroch, and I. Kolmanovsky. Dynamics and control of a class of underactuated mechanical systems. *IEEE Transactions of Automatic Control*, 44(9):1663–1671, 1999.

[62] I. M. Ross. Mechanism for precision orbit control with applications to formation flying. *AIAA Journal of Guidance, Control, and Dynamics*, 25(4):818–820, 2002.

[63] B. F. Schutz. *Geometrical Methods of Mathematical Physics*. Cambridge University Press, 1980.

[64] J. Sherman, R. E. Davis, W. B. Owens, and J. Valdes. The autonomous underwater glider "Spray". *Journal of Oceanic Engineering*, 26(4):437–446, 2001. Special Issue on Autonomous Ocean-Sampling Networks.

[65] S. Smale. Topology and mechanics. *Inv. Math*, 10:305–331, 1970.

[66] M. Spivak. *A Comprehensive introduction to Differential Geometry*. Publish or Perish, 1976.

[67] M. W. Spong. Underactuated mechanical systems. In B. Silicians and K. P. Valavanis, editors, *Control Problems in Robotics and Automation*, Lecture Notes in Control and Information Sciences, 230. Springer-Verlag, 1997.

[68] M. W. Spong. Energy based control of a class of underactuated mechanical systems. In *Proc. IFAC World Congress*, July 1996.

[69] N. E. Steenrod. *The topology of fibre bundles*. Princeton University Press, 1951.

[70] A. Takegaki and S. Arimoto. A new feedback method for dynamic control of manipulators. *ASME J. Dyn. Syst. Mech. Contr.*, 103:119–125, 1981.

[71] A. J. van der Schaft. Hamiltonian dynamics with external forces and observations. *Mathematical Systems Theory*, 15:145–168, 1982.

[72] A. J. van der Schaft. Stabilization of hamiltonian systems. *Nonlinear Analysis, Theory, Methods and Applications*, 10:1021–1035, 1986.

[73] A. J. van der Schaft. *L_2-Gain and Passivity Techniques in Nonlinear Control*. Communication and Control Engineering Series. Springer-Verlag, 2000.

[74] L. S. Wang and P. S. Krishnaprasad. Gyroscopic control and stabilization. *Journal of Nonlinear Science*, 2:367–415, 1992.

[75] F. W. Warner. *Foundations of differential manifolds and Lie Groups*. Springer-Verlag, 1983.

[76] D. C. Webb and P. J. Simonetti. The SLOCUM AUV: An environmentally propelled underwater glider. In *Proc. 11th International Symposium on Unmanned Untethered Submersible Technology*, pages 75–85, Durham, N.H, August, 1999.

[77] D. C. Webb, P. J. Simonetti, and C. P. Jones. SLOCUM: An underwater glider propelled by environmental energy. *Journal of Oceanic Engineering*, 26(4):447–452, 2001. Special Issue on Autonomous Ocean-Sampling Networks.

[78] J. E. White and R. D. Robinett III. Principal axis misalignment control for deconing of spinning spacecraft. *Journal of Guidance, Control and Dynamics*, 17(4):823–830, 1996.

[79] C. A. Woolsey. *Energy Shaping and Dissipation: Underwater Vehicle Stabilization using Internal Rotors*. PhD thesis, Princeton University, 2001.

[80] C. A. Woolsey. Reduced Hamiltonian dynamics for a rigid body coupled to a moving mass particle. *AIAA Journal of Guidance, Control, and Dynamics*, 28(1):131–138, 2005.

[81] C. A. Woolsey, A. M. Bloch, N. E. Leonard, and J. E. Marsden. Dissipation and controlled Euler-Poincaré systems. In *Proc. IEEE Conf. Decision and Control*, pages 3378–3383, Orlando, FL, 2001.

[82] C. A. Woolsey, A. M. Bloch, N. E. Leonard, and J. E. Marsden. Physical dissipation and the method of controlled Lagrangians. In *Proc. European Control Conf.*, pages 2570–2575, Porto, Portugal, 2001.

[83] C. A. Woolsey, C. K. Reddy, A. M. Bloch, D. E. Chang, N. E. Leonard, and J. E. Marsden. Controlled Lagrangian systems with gyroscopic forcing and dissipation. *European Journal of Control*, 10(5):478–496, 2004.

[84] D. V. Zenkov, A. M. Bloch, N. E. Leonard, and J. E. Marsden. Matching and stabilization of low-dimensional nonholonomic systems. In *Proc. IEEE Conf. Decision and Control*, pages 1289–1295, Sydney, Australia, 2000.

[85] D. V. Zenkov, A. M. Bloch, and J. E. Marsden. Flat nonholonomic systems. In *Proc. American Control Conference*, pages 2812–2817, Alaska, USA, 2002.

Vita

Konda Reddy Chevva was born on December 14, 1974 in the city of Nandyal in India. In June of 1996, Konda graduated from the Walchand College of Engineering, Sangli, India with a Bachelor's degree in Mechanical Engineering. He spent the next year working as a graduate trainee engineer at Tata Motors (formerly called TELCO), Pune, India. Soon after, Konda joined the Indian Institute of Science (IISc), Bangalore, India for graduate studies. Konda graduated with a Master of Science degree in Mechanical Engineering in May, 2000. His Master's thesis "Lossless Collisions and Complex Behavior in Simple Impacting Systems" was adjudged the best thesis in Mechanical Engineering for the year 2000. In Fall 2000, Konda began a new phase of his academic life when he joined the department of Engineering Science and Mechanics at Virginia Polytechnic Institute and State University (Virginia Tech), Blacksburg, Virginia for his PhD. On August 23, 2005, Konda successfully defended his dissertation to receive a PhD in Engineering Science and Mechanics. In October 2005, Konda will join the University of California, San Diego for post-doctoral research.